uOttawa

L'Université canadienne
Canada's university

FACULTÉ DES ÉTUDES SUPÉRIEURES ET POSTOCTORALES

uOttawa

L'Université canadienne
Canada's university

FACULTY OF GRADUATE AND POSDOCTORAL STUDIES

Özgür Ekici

AUTEUR DE LA THÈSE / AUTHOR OF THESIS

Ph.D. (Electrical Engineering)

GRADE / DEGREE

School of Information Technology and Engineering

FACULTÉ, ÉCOLE, DÉPARTEMENT / FACULTY, SCHOOL, DEPARTMENT

Improvements and Performance Analysis of IEEE 802.11 Medium Access Protocols

TITRE DE LA THÈSE / TITLE OF THESIS

Abbas Yongacoglu

DIRECTEUR (DIRECTRICE) DE LA THÈSE / THESIS SUPERVISOR

CO-DIRECTEUR (CO-DIRECTRICE) DE LA THÈSE / THESIS CO-SUPERVISOR

EXAMINATEURS (EXAMINATRICES) DE LA THÈSE / THESIS EXAMINERS

Yongyi Mao

Hussein Mouftah

Mustafa Mehmet Ali

Halim Yanikomeroglu

Gary W. Slater

Le Doyen de la Faculté des études supérieures et postdoctorales / Dean of the Faculty of Graduate and Postdoctoral Studies

Ph. D. Thesis

Improvements and Performance Analysis of IEEE 802.11 Medium Access Protocols

by

Özgür Ekici

Ottawa-Carleton Institute for Electrical and Computer Engineering
School of Information Technology and Engineering
Faculty of Engineering
University of Ottawa

Your file Votre référence
ISBN: 978-0-494-59547-3
Our file Notre référence
ISBN: 978-0-494-59547-3

Abstract

In IEEE 802.11 standard development process, new physical and medium access layer techniques for higher throughput (IEEE 802.11n) and quality of service (IEEE 802.11e) enhancements are being designed on solid foundation of the distributed coordination function. None of these recently developed enhancements are immune to hidden node and hot-spot (congestion) problems. On the contrary, the increased operational bandwith of the higher throughput implementation makes them more prone to interference in limited number of IEEE 802.11 channels.

Distributed coordination function is and will be the primary contention resolution algorithm of IEEE 802.11 systems. Identification and formulation of the common problems this channel access technique is facing in practical networks would give us a better understanding in terms of its limitations. In this work, we introduce a methodology to estimate the throughput performance of distributed coordination in unsaturated and hidden communication environments. Then by applying this methodology, we analytically estimate the abnormality in its fairness performance. The secondary channel access scheme of IEEE 802.11 is point coordination function, which does not suffer from hidden node and collision problems. We show that point coordination function in its current form has a poor throughput performance due to ignoring of the multi-rate transmission capability of users. We propose a new indexing algorithm for polling that increases the performance of point coordiation function significantly.

In this thesis, we extend the performance analysis of the distributed coordination function to enterprise networks configurations where networks are typically comprised of multiple access points. We propose an intelligent association algorithm that provides consistent higher throughput and better network-wide fairness independent of user load distribution within the network in comparison to the standard association algorithm.

I would like to dedicate this work to my family Ziya, Fatma, Deniz, Meltem Ekici and my wife April Sorenson for their continuous support and also to my professor Abbas Yongacoglu.....

Dr. Özgür Ekici

Contents

List of Tables

List of Figures

Abbreviations

Abbr.	Meaning
ACK	Acknowledgement
AID	Association ID
AIFS	Arbitrary InterFrame Space
AP	Access Point
ARF	Auto Rate Fallback
BER	Bit Error Rate
BPSK	Binary Phase Shift Keying
BSA	Basic Service Area
BSS	Basic Service Set
CCA	Clear Channel Assessment
CDF	Cumulative Distribution Function
CDMA	Code Division Multiple Access
CF	Contention Free
CFP	Contention Free Period
CS	Carrier Sense
CSMA/CA	Carrier Sense Multiple Access-Collision Avoidance
CTS	Clear To Send
CW	Contention Window
DATA	Data Frame Transmission Duration
dB	Decibel
dBm	Measured power referenced to one milliwatt
DCF	Distributed Coordination Function
DIFS	DCF InterFrame Space
DS	Distribution System
ED	Energy Detection
EIFS	Extended InterFrame Space
ESA	Extended Service Area
ESS	Extended Service Set
ETSI	European Telecommunications Standard Institute
FCC	Federal Communications Commision
FCS	Frame Check Sequence

Continued on next page

Abbr.	Meaning
GHz	Gigahertz
HCCA	HCF Controlled Channel Access
HCF	Hybrid Coordination Function
HS	Hot-Spot
IEEE	Institute of Electrical and Electronics Engineers
ISM	Industrial, Scientific and Medical
ITU	International Telecommunications Union
LAN	Local Area Networks
LLF	Least Loaded First association algorithm
LLC	Logical Link Control
MAC	Medium Access Control layer
MCS	Modulation and Coding Scheme
Mbps	Mega bits per second
MIMO	Multiple input, multiple output
MPDU	MAC Protocol Data Unit
MSDU	MAC Service Datta Unit
MT	Mobile Terminal
mW	miliwatt
NAV	Network Allocation Vector
NF	Noise Figure
NS	Network Simulator
OFDM	Orthogonal Frequency Division Multiplexing
QAM	Quadrature Amplitude Modulation
QoS	Quality of Service
PAA	Predictive Association Algorithm
PC	Point Coordinator
PCF	Point Coordination Function
PER	Packet Error Rate
PHY	Physical layer
PIFS	PCF InterFrame Space
PLCP	Physical Layer Convergence Protocol

Continued on next page

Abbr.	**Meaning**
PMD	PHY Medium Dependent
POLL	Poll frame
PPDU	PLCP Protocol Data Unit
PSDU	PLCP Service Data Unit
RF	Radio Frequency
RPO	Received Power Ordering
RRM	Radio Resource Management
RSSI	Received Signal Strength Indicator
RTS	Request To Send
serv	SERVICE field in frame
SIFS	Short InterFrame Space
SNR	Signal to Noise Power ratio
SNIR	Signal to Noise and Interference Ratio
SSF	Strongest Signal First association algorithm
STA	Station
tb	Tail bits
TDD	Time Division Duplex
TPC	Transmit Power Control
UD	Uniformly Distributed
U-NII	Unlicenced National Information Infrastructure
VoIP	Voice over Internet Protocol
wi-fi	Wireless-fidelity
WLAN	Wireless Local Area Networks

Nomenclature

Symbol	Meaning
A	Set of APs in the communication environment
c	Number of contending stations
c_k	Number of contending stations in G_k
cw_{max}	Maximum back-off window size
cw_{min}	Minimum back-off window size
d	The distance between transmitter and receiver
$d_{AP-x,STA-y}$	The distance between AP-x and STA-y
$d_{STA-x,STA-y}$	The distance between STA-x and STA-y
d_{CS}	Carrier sense distance
d_{tx}	Terminal transmission distance
$\mathfrak{E}_{a,s}$	Average effective data rate between AP a and STA s
$\overrightarrow{\mathfrak{E}_s}$	Effective data vector
$E[P]$	Average payload size (in bits)
g_k	Number of users in G_k
G_k	Fairness group k
$G(A, E)$	Interference graph defined by vertex A and edge E
h	Number of hidden users
$h_{k,l}$	Number of hidden users in G_l affecting users in G_k
$I_{a1,b1}$	Interference power of MT a1 affecting MT b1
$\overline{I}^{d}_{ax,b1}$	Average downlink interference of MT a-x on MT b-1
$\overline{I}^{u}_{ax,b1}$	Average uplink interference of MT a-x on MT b-1
$\overline{I}^{t}_{ax,b1}$	Average total interference of MT a-x on MT b-1
$\overline{I}^{d}_{b1}$	Total average interference power affecting MT b-1 on downlink
$\overline{I}^{u}_{b1}$	Total average interference power affecting MT b-1 on uplink
k	Generic slot decrements in $2T_s$ duration
k^{rts}	Generic slot decrements in $2T_{rts}$ duration
K	Maximum amount of time-slots available in CFP
$\mathfrak{l}_{a,s}$	The load induced by STA s on AP a
$\mathfrak{L}_a$	Total load of AP a
L	System loss
m	Number of APs in the communication environment

Continued on next page

Symbol	Meaning
M	Maximum back-off stage number
mac_h	MAC header
$mac_{payload}$	MAC payload
n	Number of STAs in the communication environment
N	Total number of fairness groups
N_{dbps}	Data bits per OFDM symbol
p	Conditional collision probability
$P(x)$	Probability of event x
$P_r(d)$	Received power level at distance d
P_s	Probability of successful frame transmission
P_{sk}	Probability of successful frame transmission in G_k
P_{tr}	Probability of there is at least one frame transmission in the channel
P_t	Transmitted power level
q	Probability that there is a packet waiting in a STA's buffer
R_{data}	Data rate (Mbit/sec)
R_{man}	Mandatory rate (Mbit/sec)
$\mathfrak{R}_{a,s}$	Average communication rate between AP a and STA s
$\mathfrak{R}^d_{a,s}$	Downlink communication rate between AP a and STA s
$\mathfrak{R}^u_{a,s}$	Uplink communication rate between AP a and STA s
S	Set of STAs in the communication environment
S_a	Set of STAs associated to AP a
t^d_a	Downlink frame transmission duration of MT a
t^t_a	Total (uplink and downlink) frame transmission duration of MT a
t^u_a	Uplink frame transmission duration of MT a
$\overline{t^t_a}$	Average transmission duration per connection
$\lvert\overline{t^t_a}\rvert$	Normalized average transmission duration per connection
t	Inter arrival time
t_A	Total utilization time of AP-A
t^{MSDU}_{AP-tot}	Total time for an AP to serve one MSDU frame to all its associated STAs
t^{MSDU}_{sta-1}	STA-1 MSDU transmission duration
t_{sta-x},	The network arrival time of STA-x

Continued on next page

Symbol	Meaning
t_{sta-x}^{Re-1}	First reassociation time of STA-x
T	Generic slot time
T_0	Equivalent noise temperature
T_{ack}	ACK frame transmission duration
T_c	Duration spent in frame collision
T_c^{rts}	Duration spent in frame collision in RTS/CTS
T_{cts}	CTS frame transmission duration
T_{data}	DATA frame transmission duration
T_{difs}	DIFS duration
T_{eifs}	EIFS duration
T_{pre}	PLCP preamble time
T_{rts}	RTS frame transmission duration
T_s	Successful frame transmission duration
T_s^{rts}	Successful frame transmission duration in RTS/CTS
T_{sifs}	SIFS duration
T_{sig}	SIGNAL OFDM SYM time
T_{slot}	PHY specific slot duration
T_{sym}	OFDM SYM interval
Thr^{sys}	System throughput
$\mathfrak{U}_\mathfrak{r}$	Uplink to total link communication ratio
W_0	Minimum contention window size
$\mathfrak{x}_{a,s}$	AP and STA association indicator
X	Random variable
$\overline{X}$	Average value of random variable X
α	Average slot decrements in a successful frame transmission duration
β	Average slot decrements in a duration of packet collision
$\mathfrak{B}$	Access point load balance index
Δ^{min}	Minimum delta effective data rate ratio threshold
$\overrightarrow{\Delta_s}$	Delta effective data rate vector
$\mathfrak{F}$	Fairness index
κ	Number of colliding frames in a collision scenario

Continued on next page

Symbol	**Meaning**
λ	Average packet arrival rate
$\mathfrak{S}_i$	Throughput of STA i
τ	Frame transmission probability of individual MT
τ_{ch}	Propagation duration

Chapter 1

Introduction and Motivations

Deployment of wireless local area networks (WLANs) becomes more and more common in corporate environments including university campuses, airports, because of its inherent features (*i.e.*, flexibility, mobility, ease of use, low deployment cost). However, the expectation to have similar connection speed and reliability as the wired local area networks (LANs) is quite high. Increasing number of wi-fi (wireless fidelity) capable devices along with increased network load in corporate environments and advanced multimedia applications fuel the growing demand for more bandwidth and higher data rates in businesses. WLANs operate in unlicensed frequency spectrums (IEEE 802.11b & g operate at 2.4 GHz industrial, scientific and medical [ISM] band and IEEE 802.11a operates at 5 GHz unlicensed national information infrastructure [U-NII] band [1, 2]) that have limited non-interfering frequencies to operate. This limitation requires an efficient radio resource management technique in large network deployments to compensate for this constraint. At the same time, considering the fact that future IEEE 802.11 implementations proposing to increase bandwidth as a way to boost the data rate (IEEE 802.11n), having an efficient radio resource management becomes a necessity rather than a luxury. In a typical enterprise WLAN deployment, the network is made up of multiple access points (APs) and usually APs have overlapping coverage areas [3, 4]. However, the medium access control (MAC) protocol that underpins all IEEE 802.11 enabled devices was designed for residential and small office applications where it is supposed to operate stand alone with limited amount of users. The operation of the same MAC design in widescale high load multi-AP environments along with non-uniform user distributions comes with consequences [5].

1.1 Problem Formulation

Operation of IEEE 802.11 MAC on multi-AP environments with high data rates and challenging load variations have some chronic problems that are listed in this section.

1.1.1 Non-uniform network load in multi-AP environments

In IEEE 802.11 WLANs, an AP has a serving area defined by its transmission power and channel condition. An AP can accept an association request from any station (STA) in its range. A STA, which is often in an overlapped coverage area of multiple APs, can associate with any AP it receives with a sufficient signal strength. However, according to IEEE 802.11 standard, STAs must associate with the AP that has the highest received signal strength indicator (RSSI) at the receiver [6]. In practice, user load is often unevenly distributed among APs; *e.g.*, flight gates at airports, classrooms in schools, meeting rooms in corporate companies, seminar rooms in conference centres, creating *hot-spots* [7]. Because of the time multiplexing nature of the IEEE 802.11 coordination functions, the serving capability of an AP decreases as more and more STAs associate with it. In the current WLAN implementation, STAs are not informed about AP loadings and standards do not specify an upper limit on the number of users that can be associated with an AP [6]. Therefore in a network configuration, there might be some APs having excessive loads (with longer delays and poor throughput performance), whereas some having just a few STAs associated causing uneven system resource allocation.

1.1.2 High MAC overhead in Distributed Coordination Function

IEEE 802.11 orthogonal frequency division multiplexing (OFDM) physical layer (PHY) can provide connection speeds up to 48 or 54 Mbps [8]. The numbers given are the top speeds a STA might communicate with in low layers of the protocol stack (*i.e.*, PHY). But, those numbers make WLANs sound much faster than they actually are. The inherent overhead structure of the default random-access technique of IEEE 802.11 standard (Carrier Sense Multiple Access, Collision Avoidance [CSMA/CA]) of the primary contention resolution scheme (distributed coordination function [DCF]) causes throughput performance to drop to ~26 Mbps on MAC level. In addition to this fact, 54 Mbps on PHY is possible if the considered STA is the only mobile node connected to the serving AP (no time sharing of the frequency band with other STAs). The scenario might be

even more dramatic (*i.e.*, less throughput) if we consider multiple APs utilizing the same operational band and frequency channel causing additional contention to each other. It is well known that point coordination function (PCF) which is the secondary medium access algorithm of IEEE 802.11 MAC defined in the first draft of the standards gives a better throughput performance than the default access mechanism of DCF [9] (*i.e.*, no performance loss due to collisions or hidden node and less overhead).

1.1.3 Collision and hidden-node problem in DCF

An AP and the STAs it serves share a certain frequency channel on the considered operational band. When the traffic of certain amount of users increases or when more users join the AP service, increased number of collisions and retransmission attempts occur; resulting in longer packet delays and poor throughput performance. Collisions are part of IEEE 802.11 MAC operation and dealt with accordingly, *e.g.*, by increasing contention window size in a single AP environment, waiting an additional time in case of collision (*i.e.*, extended inter-frame space). It is highly desirable for a WLAN equipment to include provisions to mitigate this increased latency and reduced throughput problem.

As the number of users in the network increases and different propagation environments (*i.e.*, factory, university campuses, office environments) are considered due to the popularity of this technology, *hidden node* problems become more of an issue. A hidden node is defined as a STA whose transmissions cannot be detected using carrier sense by a second STA, but whose transmissions interfere with the transmissions from the second STA to a third STA*. Non-centralized structure of IEEE 802.11 MAC is not able to cope with hidden-node problem which causes considerable performance drop of a network under operation. In the initial standard development process, this problem was considered and an alternative contention resolution scheme aimed to reduce the packet collision due to hidden node is designed. In the technique called request-to-send (RTS)/clear-to-send (CTS), both the transmitter and receiver notify the users in their carrier sense region for the packet transmission, in a sense clearing the channel before the data transmission to avoid packet collision. The transmitter reserves the channel with RTS control packet, whereas the receiver performs the same operation with CTS packet. With this RTS/CTS scheme, the latency over the packet transmission is further increased, causing severe throughput reductions.

*An example of hidden node scenario will be given in Chapter 3

1.1.4 Suboptimal polling list creation algorithm of PCF

Point coordination function channel access algorithm is remarkably efficient due to its inherent features like: *i)* reduced time interval between channel access, *ii)* piggy-packing of control packets onto data packets and *iii)* no collisions due to central controller. PCF operation is based on polling the STA for packet transmission. However, the current implementation of PCF does not achieve its full potential. The standard polling list creation method does not consider the multi-rate capability of the STAs in the communication environment. On the link from AP to STA (downlink), AP can target two STAs at once (with a single packet). In such a scenario, AP has to choose the minimum communication rate of the two to be able to guarantee the packet delivery to both STAs. A polling list creation method that does not consider the multi-rate capability of the STAs may suffer considerable performance loss.

1.2 Contributions

In this dissertation, we have addressed the problems inherent to primary contention resolution algorithm of WLANs (*e.g.*, DCF overhead, hidden node effect) as well as the problems due to resource handling in multi-AP environments (*e.g.*, non-uniform user distributions, suboptimal association algorithm). The recent upgrades to the standard (*i.e.*, IEEE 802.11e, IEEE 802.11n) do not offer any novel solutions to the problems of hidden node and association control. IEEE 802.11e made an improvement on the channel access for time sensitive applications with prioritization in the channel contention [10] whereas IEEE 802.11n [11] is proposing throughput performance increase with mainly multiple antenna and channel bandwidth expansion. This channel expansion technique of IEEE 802.11n will bring additional constraints on the already limited number of channels and will make radio resource efficiency a requirement.

The main contributions of this dissertation are:

- **Developing analytical estimation of hidden node problem on network throughput:** Hidden node is a common problem for the large scale WLAN deployments. As the number of such deployments and wi-fi capable devices increase, hidden node will be a bottle-neck for attainable network throughput with high data rate capable devices (*e.g.*, devices with IEEE 802.11n interface.)

  In this thesis, the fairness and throughput performance of wireless local area network environments considering multiple hidden nodes and unsaturated traffic con-

dition are studied. Analytic performance of IEEE 802.11 primary medium access algorithm (distributed coordination function) is presented for practical network conditions. It has been analytically proven that the presence of hidden nodes barely affects the per user network fair share in low traffic conditions, but it causes considerable performance loss in moderate-to-high traffic scenarios. It has also been shown that per user performance highly depends on user location in the network. In the analysis, two types of network configurations are presented:

1. **Symmetric networks:** In such a network set-up, each user in the network experiences the same amount of difficulty to access the channel (*i.e.*, in terms of collision, latency). This network configuration can be visualized if every user in the network has the same number of users that are hidden (outside the carrier sense region) and users it has to contend with (inside the carrier sense region). For instance, the requirement of a symmetric network will be fulfilled if each user has b number of hidden users and c number of contending users in the network. In this thesis, it has been shown that in a network where initially there are no hidden nodes the introduction of the first hidden node has the most decremental effect compared to the subsequent hidden node arrivals.
2. **Asymmetric networks:** In such network configurations, each user might have different levels of difficulty to access the channel (*i.e.*, packet collision probability). This difference is due to that fact that each user might have different number of contending and hidden users affecting its own transmission (*e.g.*, STA1 could have b number of hidden nodes and c number of contending nodes, whereas STA2 can experience d number of hidden and e number of contending nodes while communicating through the same AP). It is not hard to see that the most common practical network configurations tend to have asymmetric network configurations. In this thesis, we show that in an asymmetric network configuration, increasing traffic increases per user throughput up to a certain point, depending on overall network orientation. Further increase of traffic causes starvation of unfavourable users who encounter a larger number of hidden nodes during channel contention.

- **Proposing a new polling list indexing scheme for point coordination function:** Point coordination function (PCF) is an important access mechanism of IEEE 802.11 MAC, which is resurrected as Hybrid Coordination Function (HCF) Controlled Channel Access in the recent standards [10]. Scheduled access in WLANs

promises certain QoS and high throughput as well as immunity from hidden-node problem and collisions, which are especially critical for popular real time systems. Current IEEE 802.11 applications implement auto rate fallback (ARF) algorithm in order to increase transmission efficiency in changing wireless channel environments. However, standard scheduled access algorithms do not take into account the multirate capability of the mobile stations in populating contention free polling list. In this thesis, a novel polling list creation method is designed. We illustrate that by utilizing the proposed technique, a throughput gain more than 20% can be obtained with moderate payload sizes, comparison to standard scheduled access. It is shown that for typical communication links requiring high download ratios, the proposed indexing algorithm significantly increases the throughput performance without any need of major change in the MAC or PHY layer of current IEEE 802.11 standard.

- **Novel association algorithm for IEEE 802.11 extended service sets:** In this thesis, a novel association algorithm taking into account not only the received signal strength of the APs at STAs, but also AP loadings, STA transmission rate and interference is proposed. The proposed algorithm is *online** and *distributed* †. The network fairness index is also calculated in performance evaluations. The proposed algorithm consistently provides fair access to its associated users, whereas with the standard association algorithm the network fairness becomes a function of user-density in hot-spots. We evaluated the performance gains of the proposed association algorithm under many different scenarios:

  1. **Interference:** An interference calculation method in a multi-AP communication environment is developed. The designed method takes into account users' location, downlink-uplink communication ratio, transmit power level, radio propagation, time share of the channel and association status (*i.e.*, which AP and therefore the operational frequency channel is being used.). Different frequency reuse clusters are considered. We show that the proposed algorithm consistently provides performance increase in both limited (IEEE 802.11g) and partially unlimited (IEEE 802.11a) frequency channel configurations.

*STAs re-evaluate their association decision upon a change in system conditions like slow channel fading or load.

†The association algorithm is located in the STA avoiding central association algorithm and minimizing the complexity and implementation.

2. **User Distribution:** We illustrate the decremental effect of the hot-spots on the network throughput and fairness performance. Different hot-spot configurations are considered (*i.e.*, size of the hot-spot cells, user density in the hot-spot areas.) We show that the current association algorithm of IEEE 802.11 is not fair in hot-spot scenarios, which is generally the case in practical networks. The proposed algorithm provides fair access to the channel in spite of the hot-spot existence.
3. **User Traffic:** In the previous configurations, the users are assumed to be greedy, where they constantly have a packet to send in their buffer. It was also our desire to evaluate the effect of user traffic in a given network and number of users. One should notice that having a certain amount of users in the network and increasing their traffic would not have the same effect as increasing the number of users with a given traffic. Each method would lead to saturation of the channel. However, the network resources wasted due to collision would be higher in a network configuration that has higher number of users. The increased collision is due to the fact that each STA has an independent MAC and discrete time backoff mechanism. Therefore, in a network configuration where channel capacity is 54 Mbps (all the STAs are in close proximity of the AP), a STA with generated traffic rate more than 54 Mbps would have higher throughput than 4 STAs each having a traffic rate more than 13.5 Mbps. We quantify the performance of the proposed and standard association algorithms under different traffic conditions in multi-AP environments. We show that in hot-spot scenarios, the proposed algorithm proposes a considerable throughput performance increase compared to the standard association algorithm.

1.3 Outline

The rest of this dissertation is organized as follows. In Chapter 2, the network architecture is summarized. The targeted network configurations and parameters are given. An overview of IEEE 802.11 MAC&PHY and background information regarding IEEE 802.11 specific channel coordination functions are also presented.

In Chapter 3, an analytic performance formulation of distributed coordination function is presented for practical network environments. In this chapter, the DCF analytic formulation is extended to cover the hidden-node scenarios with OFDM PHY. *Fairness*

classes are defined, indicating a set of users experiencing similar packet collision probabilities in the considered network configuration. Experimental results are displayed providing the support for the consistency of the analytically derived results.

Considering the limitation of the DCF in congested and hidden-node environments, PCF throughput performance with developed polling list indexing scheme is presented in Chapter 4. Simulation results are presented showing the relative performance improvement of the offered indexing method in comparison to both standard indexing in PCF and DCF performance. The inferior throughput performance of DCF due to excessive overhead is also illustrated.

The congestion problem in multi-AP communication environments is considered in Chapter 5. AP load calculation method to be used in the proposed association algorithm is defined. An interference calculation method considering IEEE 802.11 PHY&MAC is introduced for extended service sets. The fairness performances of the proposed and standard association algorithms are estimated. Simulation results are presented for various network scenarios to prove that the developed method is not only applicable to a specific scenario but applicable in general. The obtained results show the improved network fairness and throughput performance with the proposed association algorithm.

In Chapter 6, conclusions and suggestions for future work are given.

The propagation channel model and noise calculation method used to generate results are presented in Appendix-A. The additional information regarding IEEE 802.11 OFDM frame structure and vertical packet flow over MAC and PHY layers and overhead framework are given in Appendix-B. Finally, the list of papers published in conferences and journals are given in Appendix-C.

Chapter 2

IEEE 802.11 Network Architecture and Nomenclature

The aim of this thesis is to model the inherent problems of IEEE 802.11 networks and to offer performance improvements to the current implementation defined by IEEE 802.11 standards [6]. Therefore, before going into modeling and performance analysis details in the following chapters, we start by giving definitions of the network components and explanation of features which are used throughout the dissertation. In this chapter, the basic structure of IEEE 802.11 wireless networks is presented. The definitions of major network components are given. IEEE 802.11 PHY and MAC features of the IEEE 802.11 networks are reviewed and the specific network configuration targeted by this thesis is explained.

2.1 IEEE 802.11 Wireless Local Area Network Overview

IEEE 802.11 WLAN architecture and major components of the network are illustrated in Fig. 2.1. The wireless networks designed according to IEEE 802.11 standards include three major components [6]:

Station (STA) : Networks are built to transfer data to and from STAs. STAs are computing devices that contain an IEEE 802.11-conformant MAC and PHY interface to the wireless medium. Typically STAs are battery-operated laptop (portable) or cell phones (mobile). However, it might as well be personal desktop computers (fixed).

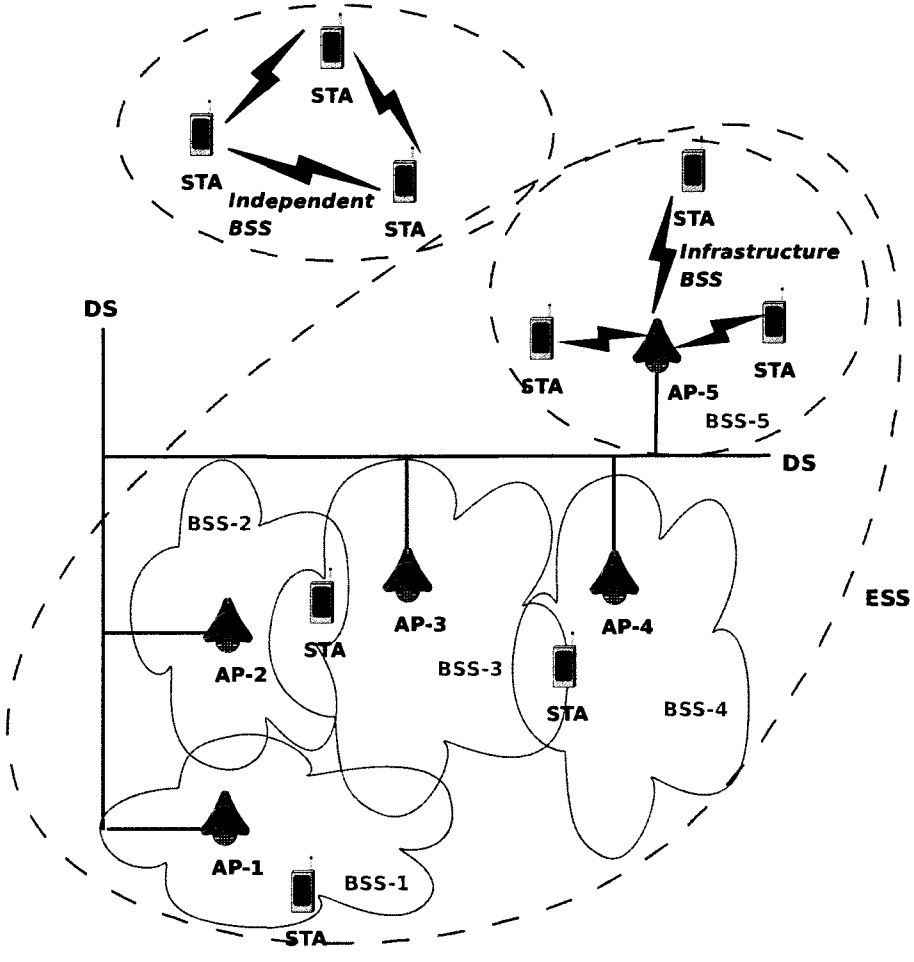

Figure 2.1: IEEE 802.11 architecture overview. Configurations for independent basic service set (STAs communicating with each other), infrastructure basic service set (STAs communicating through an AP) and extended service set (made up of overlapping or disjoint basic service sets) are illustrated.

Access Point (AP) : In IEEE 802.11 networks APs perform the wireless-to-wired bridging function. Basically, it is an entity that has STA functionality along with features to provide access to its associated STAs with the wired networks. Only one type of AP and its functionality is defined in the standards [6]. However, in practice one can name two types of APs: *i)* Thin APs* and *ii)* AP controllers.† [12]

Distribution system (DS) : DS is a system used to interconnect a set of STAs and integrated LANs. Basically it is the logical component of IEEE 802.11 used to relay the frames to their destinations. IEEE 802.11 standards do not specify any particular technology for it, but generally Ethernet is used as the backbone network technology [13].

The fundamental building block of an IEEE 802.11 network is the basic service set (BSS), which is simply a group of STAs (optionally with an AP) that either communicate or contend with each other. In a BSS, communication takes place in a wireless medium called basic service area (BSA), which is defined by the propagation characteristic of the radio frequency (RF) channel. BSSs come in two breeds:

Independent BSS : Independent BSSs are also referred to as *ad-hoc* networks since they can exist whereever two or more STAs come together to form a wireless network. The communication is carried out directly between STAs with no reliance on any fixed or wired network (*i.e.* AP).

Infrastructure BSS : Infrastructure networks are distinguished by the use of the APs. In infrastructure BSSs, all the communication between STAs is tunnelled through an AP. In such a configuration, STAs must associate with an AP to obtain network services. IEEE 802.11 standard places no limit on the number of STAs that an AP may serve. [6].

BSSs can create enough coverage for personal spaces (*i.e.* homes, small offices), but they can not provide network coverage to larger areas. However, IEEE 802.11 allows wireless networks of arbitrarily large size to be created by chaining infrastructure BSSs into an extended service set (ESS). The connectivity is provided with a common backbone. A sample ESS is illustrated in Fig. 2.1. In the figure, the ESS is made up of AP-1, AP-2,

*APs whose several core functionalities like association, load balancing are moved to central controller.

†A central control unit that rules thin APs to improve radio resource efficiency.

AP-3, AP-4 and AP-5. The area within which members of an ESS may communicate is defined as extended service area (ESA). As expected, an ESA is larger than or equal to a BSA and may involve several BSSs in overlapping, disjointed, or both configurations. In this dissertation, infrastructure basic service sets are considered for performance evaluation.

2.2 IEEE 802.11 WLAN Features

During the course of the development process, multiple PHY capabilities as well as MAC features are defined for IEEE 802.11 WLANs. In this section, a brief overview of the PHY and MAC specifications of IEEE 802.11 WLANs that are considered in this dissertation are given. An introductory summary of the IEEE 802.11 MAC coordination functions is also presented.

2.2.1 Physical Layer (PHY) Overview

The initial IEEE 802.11 standard supported three different physical layers in 2.4 GHz Industrial Scientific & Medical (ISM) band. These were the Infrared, Frequency Hopping and Direct Sequence Spread Spectrum. Further standards have been developed offering higher data rates up to 54Mbps. Namely, IEEE 802.11a/g [8] implements high-speed OFDM PHY that operates in the 5 GHz Unlicensed National Information Infrastructure (U-NII) (802.11a) and 2.4 GHz ISM (802.11g) bands. OFDM PHY offers multi-rate transmission capability [14] with eight different rates ranging from 6 Mbps up to 54 Mbps. Among these offered data rates, a STA has liberty to choose a suitable rate considering the propagation environment. Typically an auto rate fallback (ARF) algorithm, where data rate of the STA is decreased in case of deteriorating channel condition, is implemented in STAs. De-facto implementation of this algorithm tunes the communication rate relative to experienced signal-to-noise power ratio (SNR). When SNR is high (*i.e.*, good channel condition), low demand for error correction capability and an efficient modulation scheme enable high transmission rates. On the other hand, when the SNR is low, high bit error rates (BER) can be prevented by using a robust modulation scheme and powerful error correcting codes, which results in a low data transmission rate.

For performance evaluation of any wireless system, an accurate wireless channel model is vital for proper estimation of received signal power level and to find out the communication rate of a STA in a BSS. For indoor propagation channel characterization, the

Table 2.1: Different OFDM PHY modulation and coding scheme properties. SNR and communication range is calculated considering the channel model given in (Appendix-A).

Rate	Min. Sensitivity	Modulation	Coding Rate	SNR	Range
54 Mbps	-65 dBm	64-QAM	3/4	26.76 dB	33 m
48 Mbps	-66 dBm	64-QAM	2/3	25.76 dB	36 m
36 Mbps	-70 dBm	16-QAM	3/4	21.76 dB	48 m
24 Mbps	-74 dBm	16-QAM	1/2	17.76 dB	64 m
18 Mbps	-77 dBm	QPSK	3/4	14.76 dB	80 m
12 Mbps	-79 dBm	QPSK	1/2	12.76 dB	93 m
9 Mbps	-81 dBm	BPSK	3/4	10.76 dB	107 m
6 Mbps	-82 dBm	BPSK	1/2	9.76 dB	116 m

pathloss model (in dB) that International Telecommunications Union (ITU) has recommended in the 5 GHz band (IEEE 802.11a) is used in this work [15]. The details of the propagation model can be found in Appendix-A. Table 2.1 illustrates the minimum required received power levels for each data rate along with modulation and coding techniques. In the table, the pathloss model presented in Appendix-A is used. It is assumed that terminals* transmitting with 200 mW (23 dBm) power (maximum power allowed in 802.11a networks [8]). As it can be seen from the table, a STA within a radius of 30 m to an AP can communicate with 54 Mbps, whereas a STA with the distance of 110 m to AP must choose the rate 6 Mbps in order to close the link. To represent real network environments, shadowing effect should also be considered in the propagation model. See Appendix-A for details. One should also pay attention to the fact that the communication rates presented in Table 2.1 are the rates in PHY. If we take into account PHY and MAC overhead on each transmitted packet, we see that the attainable data rate on MAC is considerably less (less than half) than what is being actually advertised. Noticing this deceiving publicity, IEEE 802.11 standards moved the data rate requirement one

*Throughout the thesis the ***terminal*** term is used to represent any AP or STAs in the communication environment.

layer up to MAC from PHY for the next generation protocols (*i.e.* IEEE 802.11n) [16]. Another detail that should be considered in performance evaluations is, the fact that a terminal choosing a certain data rate for communication does not necessarily mean that all the outgoing packets of the considered terminal is being transmitted by the chosen data rate. In IEEE 802.11 systems, the control frames are required to be transmitted with the *mandatory rates*. These are the list of data rates that must be supported by any station wishing to join the network. Stations must be able to receive data at all the rates listed in the set. The mandatory rates for OFDM PHY are defined as 6 Mbps, 12 Mbps and 24 Mbps. As an example, if a STA is very close to its serving AP securing a data rate of 54 Mbps, it must still transmit control packets like acknowledgement, request-to-send, clear-to-send with the mandatory rate of 24 Mbps.

2.2.2 Medium Access Control (MAC) Layer Overview

In IEEE 802.11 systems, terminals use a peculiar mechanism called Carrier Sensing Multiple Access/Collision Avoidance (CSMA/CA) for channel access. Before any information is transmitted over the wireless medium, a terminal will first *sense* the carrier (*i.e.* channel) to ensure that no other devices are using it. Two types of carrier-sensing functions in IEEE 802.11 control this process: *i)* physical carrier sensing (and/or energy detection) and *ii)* virtual carrier sensing (*i.e.* network allocation vector [NAV]). If either carrier-sensing function indicates that the carrier is busy, the terminal postpones the data transmission on the channel.

Physical carrier-sensing functions (provided by PHY) depend on the PHY scheme (*e.g.* OFDM) being used. In such a carrier-sensing function, PHY reports binary (true or false) clear channel assessment results to MAC layer after measuring the carrier energy (for non-IEEE 802.11 signals) or detecting an OFDM signal with proper IEEE 802.11 PHY preamble. Virtual carrier sensing is provided by the network allocation vector (NAV). IEEE 802.11 frames carrying a duration field (data frames, request-to-send, clear-to-send control frames *etc.*) can be utilized to reserve the channel for a limited amount of time for data transaction. The NAV is a timer that indicates the amount of time (in microseconds) transmission onto the wireless medium will not be initiated by the STA. The virtual carrier-sensing function will indicate the medium as idle if the NAV counts down to zero, busy otherwise.

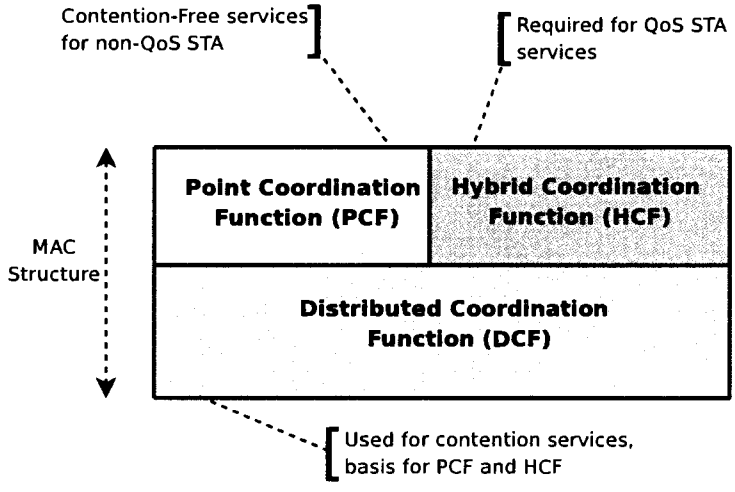

Figure 2.2: IEEE 802.11 MAC architecture. DCF is the fundamental access mechanism implementing CSMA/CA. PCF and HCF are designed on top of DCF, claiming channel access through DCF.

2.2.3 MAC Coordination Functions

In IEEE 802.11 networks, the access to the channel is controlled by coordination functions. The typical access scheme of CSMA/CA is provided by distributed coordination function (DCF). For time sensitive services, contention free access is delivered by point coordination function (PCF). PCF is build on top of DCF, meaning that initial channel access for contention free period is executed through DCF. Among two extreme access methods (DCF providing channel contention for all users and PCF where channel is accessible only by a single user), hybrid coordination function (HCF) is defined for QoS-STAs*. IEEE 802.11 MAC architecture is illustrated in Fig. 2.2. As it can be seen, PCF and HCF claim channel access through DCF contention scheme. A brief overview of the coordination functions are given as follows:

DCF : DCF forms the basis for CSMA/CA. A STA utilizing DCF will ensure that the communication medium is idle for a minimum specified duration (DCF inter frame space [DIFS]) before attempting to transmit. If the medium is busy, the STA will defer until the end of the current transmission. After this deferral period, the STA will select a random backoff interval. When this backoff timer expires,

*STAs supporting IEEE 802.11e MAC implementation

provided the medium is still idle, the STA may begin transmission. Every successful frame transmission is acknowledged after a duration of short interframe space (SIFS) which depends on the PHY being used. DCF may also use request-to-send (RTS)/clear-to-send (CTS) scheme for additional protection against packet collision. In RTS/CTS mode, the channel is reserved on both transmitter and receiver side to avoid any collision during packet transmission. In such a scheme, a single data frame transmission requires three control frames, introducing further latency to already overhead overloaded DCF mechanism. More details and performance analysis of this coordination function are presented in Chapter 3.

PCF : PCF is only used in contention free operation in an infrastructure BSS. This access method uses a PC (Point Coordinator), which operates in an AP, to determine which STA currently has the right to transmit. This method of operation can be considered as *polling*, where the PC acting in the role of polling master. PC uses DCF to grab the channel control but, waiting a shorter duration (PCF inter frame space [PIFS]) than a regular STA that enables easier channel access. Further details and performance analysis of this coordination function are presented in Chapter 4.

HCF : Hybrid coordination function permits QoS-STAs to have a priority in DCF contention scheme for time sensitive applications by defining shorter backoff windows and inter-frame spaces (arbitrary interframe space [AIFS]). It also defines access classes (*i.e.* voice, background) and multiple service queues within STA MAC for various applications. In other words, HCF combines the functionalities of PCF and DCF for channel access.

The illustration of the interframe spaces mentioned in the coordination function definitions along with CSMA/CA channel access mechanism are illustrated in Fig.2.3. As it can be seen in the figure, if the medium is busy according to virtual or PHY carrier sense mechanism, the STA defers the packet transmission. A non-QoS STA, after DIFS duration, picks a random backoff and decrements the backoff count one slot duration at a time as long as the carrier is sensed idle. Upon expiry of the backoff counter, the STA initiates packet transmission on the channel.

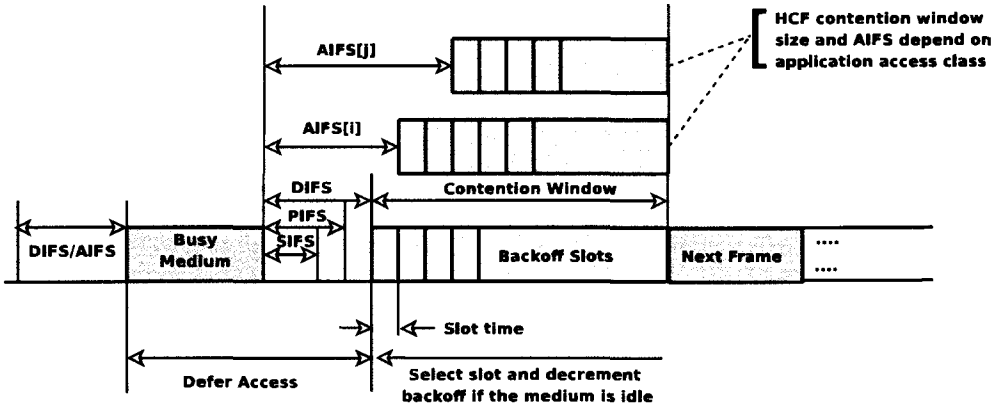

Figure 2.3: Illustration of channel access with CSMA/CA and interframe space relations. A discrete time scale is used in IEEE 802.11 networks, slot being the unit time, Inter frame time to defer the channel access after busy medium indication depends on terminal characteristics. An AP in contention period uses PIFS. A QoS-STA can use AIFS. A non-QoS STA has to wait for a duration of DIFS. SIFS on the other hand is typically used for acknowledgement frame transmission after data frame reception.

2.3 Conclusions

In this chapter, the definitions of the important network components are given. An overview of IEEE 802.11 PHY and MAC capabilities are presented. We have also reviewed various MAC coordination functions that allow channel access for terminals. In the network performance evaluations presented in this thesis, we assumed that all the STAs have the same channel access priority (non-QoS STAs) in order to evaluate the fairness and the overall network performance. Considering the following facts:

- HCF combines the functionalities of PCF and DCF for channel access.
- DCF is the primary and the most commonly utilized coordination function.
- PCF provides high throughput with less overhead in the overall network.
- RTS/CTS is used to avoid hidden terminals causing packet collisions, but it has excessive overhead causing additional latency in the network.

The rest of this dissertation primarily focuses on:

- Throughput and fairness performance of DCF.

- The challenges the primary coordination function (DCF) faces (*i.e.* hidden node problem, congestion, uneven load distribution in multi-AP environments.)
- The attainable throughput performance of PCF and possible performance improvements on this scheduled access scheme

The modelling of DCF coordination function, along with the performance estimations in various network configurations and the decremental effects of hidden nodes are presented next (Chapter 3).

Chapter 3

Throughput and Fairness Performance of DCF

DCF is a best effort, primary contention resolution algorithm that is widely used in WLAN market. It provides a distributed channel access mechanism to terminals in communication environments that might have single or multiple APs. DCF defines a basic access mechanism (two-way hand shake) and an optional RTS/CTS mechanism (four-way hand shake) for STAs to claim channel usage. RTS/CTS mechanism is designed especially to overcome *hidden node problem*. In a wireless network hidden nodes refer to nodes that are out of RF range of each other while sharing a common paired partner (typically an AP) for data transfer. RTS/CTS method introduces excessive overhead in the data transfer that degrades network throughput. It has been shown that the throughput loss of 30% is expected for systems using 54 Mbps communication rate and 1500 byte packets in OFDM PHY [17]. In this transmission procedure, for each packet to be transmitted, the channel has to be reserved with two control frames (RTS and CTS) and the packet transmission has to be acknowledged with the third control frame (acknowledgement [ACK]). Therefore unless very long frames are being exchanged in a highly congested network with moderate-to-high data rates, the benefits of RTS/CTS are very limited. Detailed overhead analysis of RTS/CTS scheme is presented in [18] along with possible solutions like concatenation and piggy-packing. Considering that RTS/CTS scheme improves the performance in hidden node environments and unnecessary activation of this feature costs network resources, multiple analysises are presented to detect the hidden node in the environment to activate the RTS/CTS scheme [19],[20]. On the other hand, in highly congested networks or hidden node environments RTS

frame transmission is also prone to hidden node problem [21]. An illustration of packet transmission with RTS/CTS scheme is given in Fig. 3.2.

In this chapter throughput and fairness performance of DCF access mechanism is evaluated. Initially, a brief explanation of DCF procedure is given in Section 3.1. Details of the analytical formulation of DCF scheme are presented in Section 3.2. The performance of DCF under different traffic conditions, hidden node scenarios and channel access schemes is evaluated in Section 3.3. The impact of cell loading on DCF is considered later in Section 3.3.1. The effect of hidden-node on DCF operation is evaluated in Section 3.3.2. In hidden node configurations, the benefits of RTS/CTS channel access scheme are also estimated and the results are compared to DCF channel access performance. Finally the conclusions are given in Section 3.4.

3.1 DCF Contention Resolution Scheme Overview

STA behaviour with DCF access mechanism which is mentioned briefly in Chapter 2 is explained in this section. A STA that has a frame to transmit monitors the channel activities. If there is an ongoing transmission, the STA defers its packet transmission until an idle period which equals to a DIFS is detected. After sensing channel idle for a duration of DIFS, the station waits for a random back-off interval before commencing a packet transmission. The backoff time counter is decremented in terms of slot time (T_{slot}) as long as the channel is sensed idle. The counter is frozen if a transmission is detected on the channel, and reactivated when the channel is sensed idle again for a duration of DIFS or more. The STA transmits its frame when the backoff time reaches zero. Packet transmission fundamentals with DCF are illustrated in Fig. 3.1. At each transmission opportunity, the backoff time is uniformly chosen in the range of zero to current contention window (CW) size. At the very first transmission attempt, CW equals the minimum backoff window size (cw_{min}). After each unsuccessful transmission, CW size is increased exponentially until a maximum backoff contention window size (cw_{max}) is reached. If the destination STA successfully receives the frame, it transmits an acknowledgement (*ack*) frame following a short inter-frame space (T_{sifs}). If the transmitting STA does not receive the *ack* within a specified duration of *ack* timeout, or if it detects the transmission of a different frame on the channel, it concludes that the transmitted packet is lost and reschedules the frame retransmission.

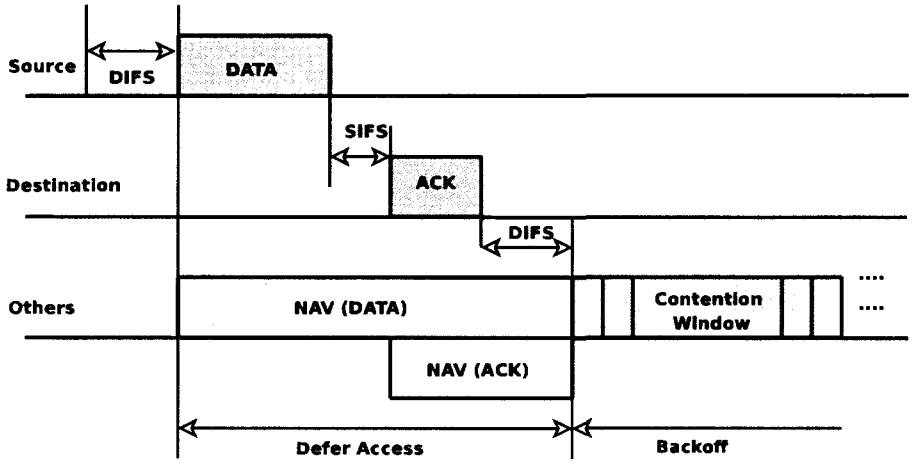

Figure 3.1: Basic channel access in DCF contention resolution scheme. Every transmitted packet needs to be acknowledged. Other STAs adjust their network allocation vector (virtual carrier sense) to avoid interfering with the ongoing packet transmission.

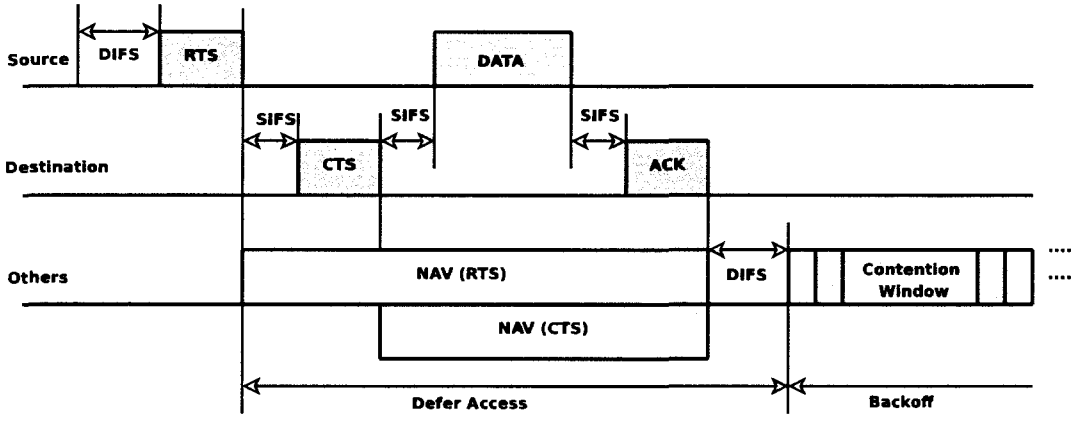

Figure 3.2: The channel access with RTS/CTS in DCF contention resolution scheme. The source and the destination terminals clear the channel before commencing packet transmission. The other STAs in the communication environment update their network allocation vector (NAV) upon receiving RTS and CTS messages. As it can be seen, in this access scheme, a single packet transfer requires exchange of three control packets, introducing further latency and overhead on the system.

3.2 Modelling DCF

Analytical formulation of DCF performance considering *non-saturated traffic* * conditions will be summarized in this section. The theoretical results will be used to illustrate the decremental effect of congestion on DCF functioning. It will be explicitly shown that in congested APs, the STAs are actually getting a fraction of the throughput values that is usually being advertised (54 Mbps).

3.2.1 Modelling IEEE 802.11 MAC

In DCF of IEEE 802.11 MAC, as the number of contending STAs increases, the probability of successful frame transmission decreases. By considering the DCF state transitions as discrete-state Markov process and with certain assumptions (*e.g.* saturated channel condition, *perfect propagation channel*†, the frame transmission probability with DCF contention resolution scheme is calculated initially in [22]. The algorithm later applied to several different scenarios: Adapting it to different back-off schemes [23, 24], deriving saturation delay [25], taking into account finite retransmission attempts [26], considering multiple traffic classes [27], taking into account propagation channel errors [28] *etc.*. The chief postulate that enables the analysis in [22] is the assumption of constant and independent collision probability of a frame transmitted by each station. The considered assumption is proven to be extremely accurate by simulation results. In the model, a MAC state is represented by two variables: *i*) The current retransmission stage and *ii*) remaining backoff time. A frame is transmitted when the backoff time counts to zero. The frame transmission suffers collisions with probability p, and it is assumed to be successful with probability $1 - p$. In case of a collision, the STA's retransmission stage is incremented by one and a new backoff time is uniformly chosen from the new contention window range. The algorithm presented in [22] is further improved for non-saturated traffic condition in [29]. By denoting $1 - q$ as the probability that there are no packets waiting in a STA's buffer, the packet transmission probability τ in a generic slot time can be estimated as follows [29]:

$$\tau = \eta \left(\frac{q^2 W_0}{(1-p)(1-q)(1-(1-q)^{W_0})} - \frac{q^2(1-p)}{(1-q)} \right) \tag{3.1}$$

*where the users can have idle periods where no packet is scheduled in the transmitter buffer; *i.e.* non-greedy users.

†All users are in carrier sense range of each other and the propagation channel is assumed to be errorless.

where W_0 is the minimum window size and η is:

$$\begin{aligned}
&\frac{1}{\eta} = (1-q) + \frac{q^2 W_0(W_0+1)}{2(1-((1-q))^{W_0})} + \dots \\
&\frac{q(W_0+1)}{2(1-q)} \left(\frac{q^2 W_0}{1-(1-q)^{W_0}} + p(1-q) - q(1-p)^2 \right) \frac{pq^2}{2(1-q)(1-p)} \dots \\
&\left(\frac{W_0}{1-(1-q)^{W_0}} - (1-p(1-p)) \right) \left(2W_0 \frac{(1-p) - p(2p)^{M-1}}{1-2p} + 1 \right)
\end{aligned} \tag{3.2}$$

where M is the maximum back-off stage. Given q, the probability that there is a pending frame to be transmitted in the buffer, and constants W_0, M; τ would still depend on p, which is unknown as well. The value of p can be calculated by noting that the probability of a transmitted packet encounters a collision, is the probability that, in a time slot, at least one of the other STAs transmit. The fundamental independence assumption implies that each transmission *sees* the system in the same state. Considering that there are n contending STAs and each STA transmits with τ probability, p can be calculated as:

$$p = 1 - (1-\tau)^{n-1} \tag{3.3}$$

Other than conditional collision probability (p), Markov Chain model also gives us the probability measures of the events possible in a slot time. Basically a slot can be: *i)* Idle, *ii)* used for successful packet transmission or *iii)* in a collision. Transition from Markov Chain model's stationary probabilities to real-time can be accomplished by taking into account how much time is spent in each slot time. Then, the network throughput can be calculated by the number of bits transmitted during an average slot time:

$$Thr^{sys} = (P_s P_{tr} E[P])/T \tag{3.4}$$

where $E[P]$ is the average payload size (in bits); P_{tr} is the probability that there is at least one frame transmission in the channel ($P_{tr} = 1-(1-\tau)^n$); P_s is the probability of successful frame transmission ($P_s = (n\tau(1-\tau)^{(n-1)})/P_{tr}$) in a communication environment with n contending users and T is the average slot time (or average occupation time in a markov state). Considering the events possible in a slot time and their durations, the average slot time T can be calculated as:

$$T = (1-P_{tr})T_{slot} + P_{tr}\left[P_s T_s + (1-P_s)T_c\right] \tag{3.5}$$

where T_{slot} is the slot duration, T_s and T_c are the expected durations for successful packet transmission and packet collision respectively which can be calculated as follows:

$$\begin{aligned}
T_s &= T_{data} + T_{sifs} + 2\tau_{ch} + T_{ack} + T_{difs} \\
T_c &= max(T^1_{data}, \dots, T^\kappa_{data}) + \tau_{ch} + T_{eifs}
\end{aligned} \tag{3.6}$$

Table 3.1: IEEE 802.11a MAC and PHY characteristics.

Parameter	**Definition**	**Value**	**Layer**
T_{slot}	Slot time	$9\,\mu s$	MAC
T_{sifs}	SIFS time	$16\,\mu s$	MAC
T_{difs}	DIFS time	$34\,\mu s$	MAC
T_{eifs}	EIFS time	$94\,\mu s$	MAC
mac_h	MAC header	$24 - 30\,oct$	MAC
$mac_{payload}$	MAC payload	$0 - 2312\,oct$	MAC
fcs	Frame control seq.	$4\,oct$	MAC
ack	ACK frame size	$14\,oct$	MAC
cw_{min}	Min CW	$16\,slots$	MAC
cw_{max}	Max CW	$1024\,slots$	MAC
serv	SERVICE field	$16\,bits$	MAC
tb	Tail bits	$6\,bits$	MAC
T_{pre}	PLCP preamble	$16\,\mu s$	PHY
T_{sig}	SIGNAL field	$4\,\mu s$	PHY
T_{sym}	SYM interval	$4\,\mu s$	PHY
τ_{ch}	Propagation delay	$1\,\mu s$	PHY
R_{data}	Data rate (Mbit/sec)	$6, 9, 12, 18, 24, 36, 48, 54$	PHY
R_{man}	Mandatory rate (Mbit/sec)	$6, 12, 24$	PHY
N_{dbps}	Data bits per OFDM SYM	$24, 36, 48, 72, 96, 144, 192, 216$	PHY

where κ is the number of colliding frames in a collision scenario; τ_{ch} is the propagation duration; T_{data} packet frame transmission duration and T_{ack} ACK frame transmission time; T_{sifs}, T_{difs} and T_{eifs} are PHY specific inter-frame spaces given in Table 3.1. All the parameters utilized in (3.6) can either be found explicitly in [8] or can easily be estimated (*i.e.* T_{data} and T_{ack}) considering vertical data flow across IEEE 802.11 MAC and PHY layers (Appendix-B). Data and acknowledgement frame transmission durations can be calculated as follows:

$$\begin{aligned} T_{data} &= T_{pre} + T_{sig} + T_{sym}\left\lceil \frac{sevr + tb + 8(mac_{(h+payload)} + fcs)}{N_{dbps}} \right\rceil \\ T_{ack} &= T_{pre} + T_{sig} + T_{sym}\left\lceil \frac{serv + tb + 8ack}{N_{dbps}} \right\rceil \end{aligned} \tag{3.7}$$

where N_{dbps} is a modulation dependent parameter indicating data bits per OFDM symbol. All the IEEE 802.11 OFDM PHY and MAC parameters related to our study are presented in Table 3.1 for convenience. If we consider the parameters presented in Table 3.1, we can easily obtain the numerical value for (3.7) as follows:

$$\begin{aligned} T_{data} &= 20\,\mu sec + 4\,\mu sec * \left\lceil \frac{16 + 6 + 8 * (24 + mac_{Payload} + 4)}{N_{dbps}} \right\rceil \\ T_{ack} &= 20\,\mu sec + 4\,\mu sec * \left\lceil \frac{16 + 6 + 8 * 14}{N_{dbps}} \right\rceil \end{aligned} \tag{3.8}$$

3.2.2 Modelling User Traffic

So far in the model the offered network load is represented by parameter q, the probability that a packet becomes available to the MAC buffer in a given slot time. For the verification of the analysis with simulation results, it is vital to correlate the parameter q with the actual STA load (*i.e.* 4 Mbps). Considering exponentially distributed independent and identically distributed inter-arrival times t of rate λ between packets, the probability that no packets arrive during an average slot time can easily be calculated as $1 - q = P(t > T) = e^{-\lambda T}$. Different traffic conditions in the analysis can be met by modifying the packet arrival rate. The estimated q value can be used in (3.1). Finally, the analytical network throughput then can be calculated by solving (3.1), (3.3) and (3.4) jointly for a range of q values.

3.3 DCF Performance

DCF contention resolution algorithm is designed in 1999 considering residential and small office applications where STAs are supposed to operate stand alone in a low traffic and contention conditions. During the course of technology evolution, the usage of WLANs expanded to businesses that deal with large coverage areas (*i.e.* airports, conference centres, university campuses). These communication environments involving high traffic and user populations scattered in a large area with possible obstacles between them had negative effect on the DCF performance due to two apparent reasons: *i)* Elevated traffic load, where a single AP serves large number of users and *ii)* hidden nodes, where the users utilizing a common AP for communication unintentionally interfere with each other due to spatial separation.

3.3.1 The Impact of Cell Loading

Congestion has a decremental effect on DCF throughput performance. It can hamper the DCF throughput performance in two different ways:

1. Considering the fact that the capacity of an operating channel is fixed in a given propagation environment and transmission power, individual user throughput is inversely proportional to the number of users sharing the common resources.

2. In case of congestion, IEEE 802.11 networks naturally increase the contention window size to decrease the probability of packet collision. This has a negative effect of increased latency in the packet transmission. Considering a fixed contention window size (*i.e.* 1023 [Max in IEEE 802.11a]), the probability of a transmitted packet being in a collision increases as the number of contending users in the channel increases. This is due to the fact that each user has its own backoff counter and start transmission as this counter reaches to zero. The increased collision probability leads to a high fraction of the network time being wasted for packet collision and recovery algorithm; eventually ending up with low network throughput.

Since the current interest is on the impact of congestion on the DCF throughput performance, it is important to evaluate the DCF performance in single user environment for comparison reasons. Figure 3.3 illustrates the throughput performance of a single user with different modulation and coding schemes along with different packet sizes. As it can be seen, ~26 Mbps is possible if a single user with transmit packet size of 1000

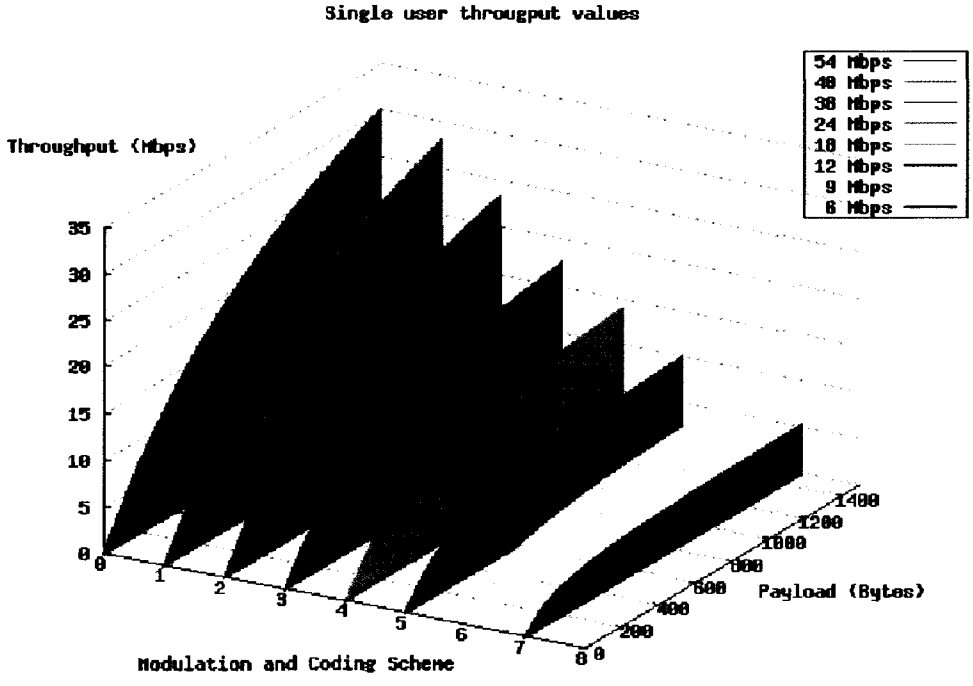

Figure 3.3: DCF performance in single-user environment with multirate transmission. Different modulation and coding schemes are illustrated for comparison purposes. The STA throughputs is calculated on MAC layer considering PHY and MAC overhead.

bytes utilizes the whole capacity of the serving AP. As mentioned in Section 2.2.1 of Chapter 2, this is due to the fact that the data rate figures stated by IEEE 802.11 manufacturers consider the data rate on PHY level, whereas we calculate the throughput on MAC layer with (3.4). Finally, the throughput performance results for overall network as well as individual STAs are illustrated in Fig. 3.4 for a range of contending number of users. IEEE 802.11a OFDM MAC & PHY frame structure, modulation and coding scheme, frame control overhead and control packets presented are taken into account in the results. In the figure, per user packet arrival rates are chosen high enough to satisfy saturated channel condition. It can be seen that there is only a slight degradation on network throughput as the number of contending users increase. The slight decrease on the throughput performance is due to increased contention-window size. It is clearly seen that per user throughput is inversely proportional to the number of users in the network.

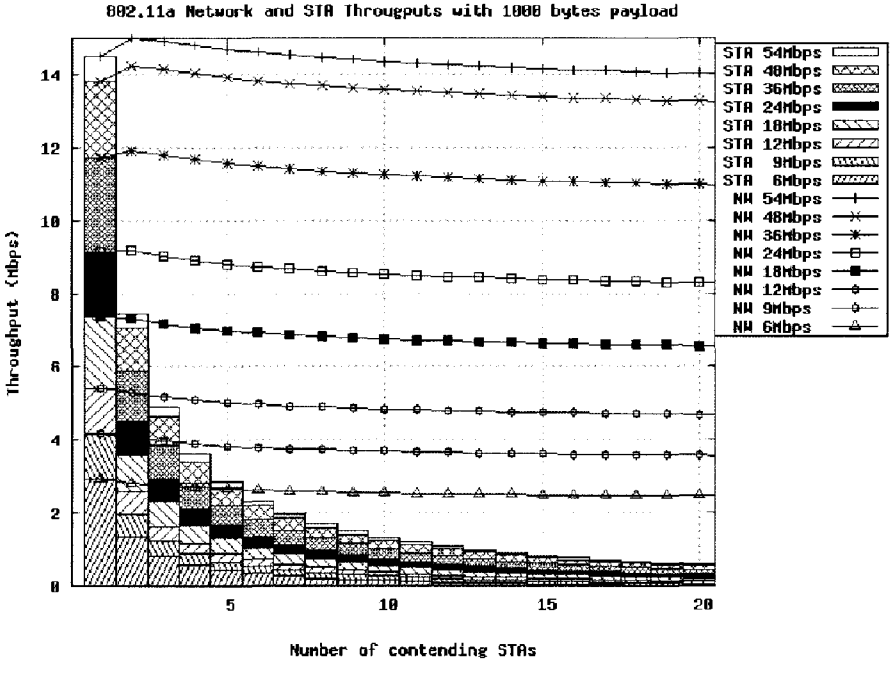

Figure 3.4: DCF performance in multi-user environment. The number of contending users (STAs are in the carrier sense range of each other) is changed from 2 to 20. 1000 byte frame length is considered with different data rate configurations. A single AP serving its users is simulated.

Fig. 3.4 points out possible performance issues in hot-spots and the importance of the load balance algorithm. The figure suggests that the network load sharing is critical to have better network throughput performance and the STAs that suffer the most are usually the ones associated to highly congested APs. In Chapter 5, the techniques to alleviate this problem are explained in detail.

3.3.2 The Impact of Hidden Nodes

Hidden nodes in a basic service set refer to STAs that are out of range of each other but still sharing the same AP for backhaul connectivity. A hidden node scenario is illustrated in Fig. 3.5. If we consider a network with a single AP with many nodes surrounding it in a circular fashion, each node will be within communication range of the AP. However, not each node can hear the transmitted packets of every other node tunnelled through the common AP. The problem arises when the hidden nodes start to send packets simultaneously to the common AP. Since the nodes can not hear each other due to spatial separation, *the collision avoidance* mechanism of IEEE 802.11 can not handle this situation and the collision becomes unavoidable. The hidden node problem is commonly observed in widespread WLAN setups (airports, conference centres *etc.*) where communicating node can have obstacles between them that hinders their line of sight signal strength and impairs their carrier sense mechanism [30, 31, 32].

3.3.2.1 Hidden Node Effect

DCF employs a discrete-time backoff scale where a STA that has a pending frame waits for the channel availability. In contention resolution, the time following an idle DIFS is slotted, and a STA is allowed to transmit only at the beginning of each slot time [6]. The assumption of perfect carrier sense by every STA in [29] and [22] implies that a collision may occur only when two or more packets are transmitted within the same slot time. For hidden node considerations, we need to extend this collision probability period to whole packet transmission duration of the considered STA (that will extend multiple slot durations). Considering a certain collision probability, τ does not depend on the access mechanism but the MAC structure. Therefore consideration of hidden node problem has no effect on the derivation of τ. p needs to be reworked to include hidden user interactions. In a hidden node scenario, all the users in the communication environment might have the same number of contending and hidden users (*i.e.* symmetric networks). The common assumption of papers [22] and [29] (where all the users are contending) is

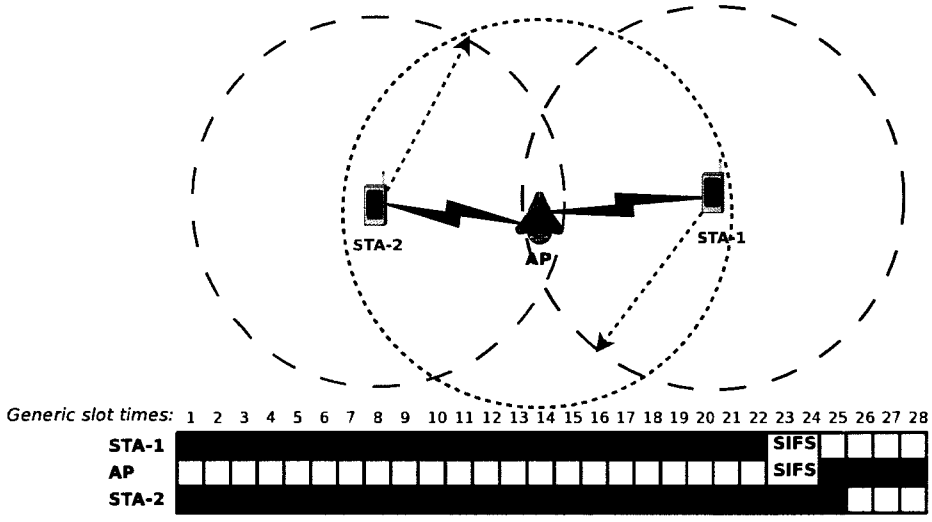

(a) **Hidden node scenario.** STA-2 can not detect the uplink transmission (from STA to AP) of STA-1. Therefore it could initiate an uplink data transfer any time during STA-1's packet transmission. The generic slot times in which STA-2 could start transmission are illustrated as X in the figure. Collision prone period spans from beginning of the packet transmission until the ACK packet transmission from AP. The same scenario is valid for from STA-1 perspective (*i.e.* symmetric network).

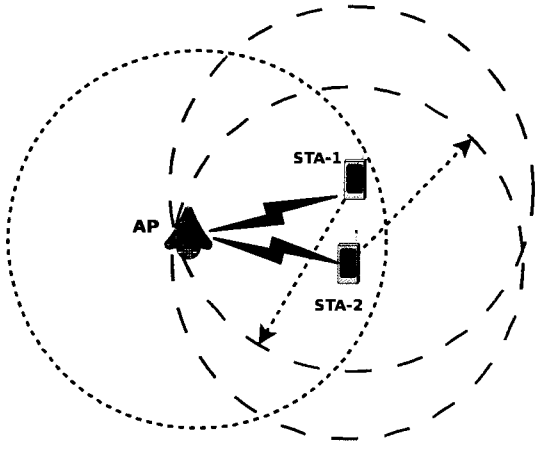

(b) **Contending node scenario.** STAs are in the carrier sense region of each other. Therefore STA-2 defers its packet transmission until STA-1 completes its packet delivery. The only time a packet collision is possible in this scenario is if the STAs have a frame to send in their buffers and choose the same slot to start the frame transmission. Possible packet collision in this scenarios is illustrated as X in the figure.

Figure 3.5: Hidden and contending user scenario illustrations in a network with 2 STAs communicating with a common AP.

a subset of the symmetric networks. In practical networks however, it is more likely to see users having different number of hidden and contending stations (*i.e.* asymmetric networks). Analytical formulation of the user performances differ for these two scenarios and therefore will be handled in two different subsections.

3.3.2.2 Symmetric Networks

In a wireless network, if users experience the same number of terminals inside the carrier sense region as well as outside, then such a network configuration is called symmetric (*e.g.* each STA in the network has d number of users in their carrier sense region and e number of users outside). In a considered network, we use S to denote the set of mobile users that reside in the network coverage area and let $n = |S|$ denote the total number of STAs in S. In a symmetric network, from the considered STA point of view, n number of users can be categorized as contending (c) if the STAs are in the carrier sense of the considered STA or hidden (h) if they are not (*i.e.* $n = c + h$). Considering the hidden node network setup, a STA would have a successfull frame transmission if:

1. In a generic slot time*, none of the contending STAs transmit. The probability of such condition can be expressed as: $(1-\tau)^{c-1}$
2. During the duration of packet delivery (*i.e.* DATA + SIFS + T_{slot}), none of the hidden STAs has interfering transmission and vice-versa (*i.e.* the considered user does not interfere with an ongoing hidden node transmission). This probability can be calculated by: $[(1-\tau)^h]^k$

where k indicates approximate number of generic slot decrements in $2T_s$ duration:

$$k = 2T_s/T \tag{3.9}$$

In symmetric networks, all the users have the same contention characteristics (*e.g.* each user in the network has 2 contending users [in carrier sense region] and 1 hidden [outside of the carrier sense region] user affecting own transmission). Therefore they share the same packet transmission, τ, and conditional collision, p, probabilities. Considering the fact that a STA that has a pending packet is allowed to proceed for transmission only at the beginning of a slot time (once in contending case and k times for hidden node case) the common conditional collision probability can be calculated as:

$$p = 1 - (1-\tau)^{c-1}\left[(1-\tau)^h\right]^k \tag{3.10}$$

*The derivation of the generic slot time, also named as average slot time is given in equation 3.5.

Then, for symmetric hidden node scenario, the common packet transmission probability (P_{tr}) and successful packet transmission probability (P_s) for each STA become:

$$P_{tr} = 1 - (1-\tau)^n, \quad P_s = \frac{n\tau(1-\tau)^{c-1+hk}}{1-(1-\tau)^n} \tag{3.11}$$

In the formulation, the parameter k needs to be expressed in constants and known parameters in order to have a numerical solution. Assuming that successful frame transmission and collision durations can be expressed in slot time (T_{slot})

$$T_s = \alpha T_{slot}, \quad T_c = \beta T_{slot} \tag{3.12}$$

then k can be found by replacing T_s and T_c of (3.12) along with (3.5) in (3.9):

$$k = \frac{2\alpha}{(1-P_{tr}) + P_{tr}\left[P_s\alpha + (1-P_s)\beta\right]} \tag{3.13}$$

Notice $P_s P_{tr} = n\tau(1-p)$ from (3.11) and (3.10) and replacing this in (3.13) would give us:

$$k = \frac{2\alpha}{1 + P_{tr}(\beta - 1) + n\tau(1-p)(\alpha - \beta)} \tag{3.14}$$

Finally we rearrange (3.14) and replace P_{tr} from (3.11) to obtain:

$$k = \frac{2\alpha}{1 + (1-(1-\tau)^n)(\beta - 1) + n\tau(1-p)(\alpha - \beta)} \tag{3.15}$$

The k value given in (3.15) can be substituted to (3.10). A non-linear system represented by (3.1) and (3.10) can be solved using numerical techniques for the two unknowns τ and p. After estimating p along with τ, the average slot durations and finally the system throughput can be calculated by (3.5) and (3.4) sequentially.

The derived equations are put in place in Example 1, demonstrating the performance of possible symmetric hidden node network scenarios up to 4 users (*i.e.* $n = 1, 2, 3, 4$).

EXAMPLE 1: Consider a wireless system of one AP with multiple STAs. The contending and symmetric hidden node network scenarios considered for performance evaluation are illustrated in Fig. 3.6. Fig. 3.6-(a) illustrates the classic contending user case, where STAs are in the carrier sense range of each other. Figs. 3.6-(b),(c) and (d) show the hidden node cases, where each STA is symmetrically hidden from each other. Considering the same amount of traffic per STA, under medium to high user loads we

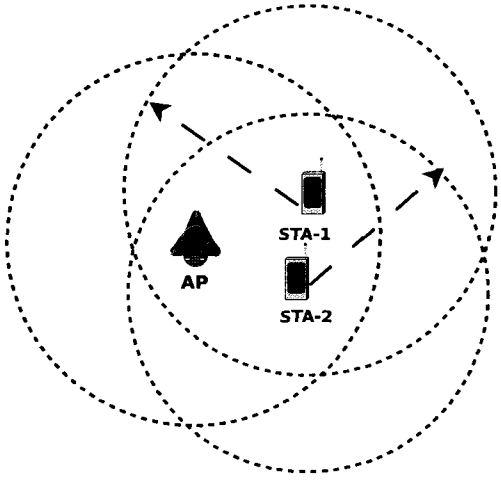

(a) **One contending node scenario.** Considering the communication environment from a considered user perspective, for instance STA-1, there is only one STA (STA-2), that contends with it. Therefore in the simulation results, this scenario is called *one contending node.*

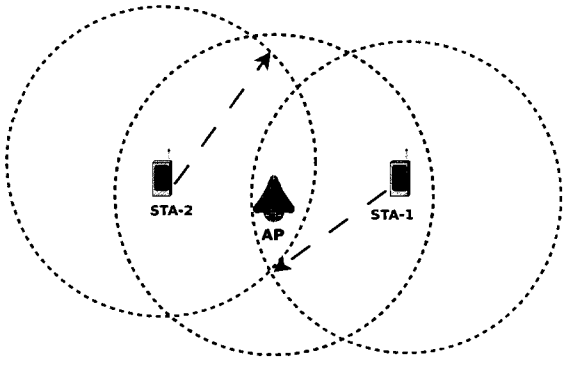

(b) **One hidden node scenario.** Considering the communication environment from a considered user perspective, for instance STA-1, there is only one STA (STA-2), that is hidden to its communication. Therefore in the simulation results, this scenario is called *one hidden node.*

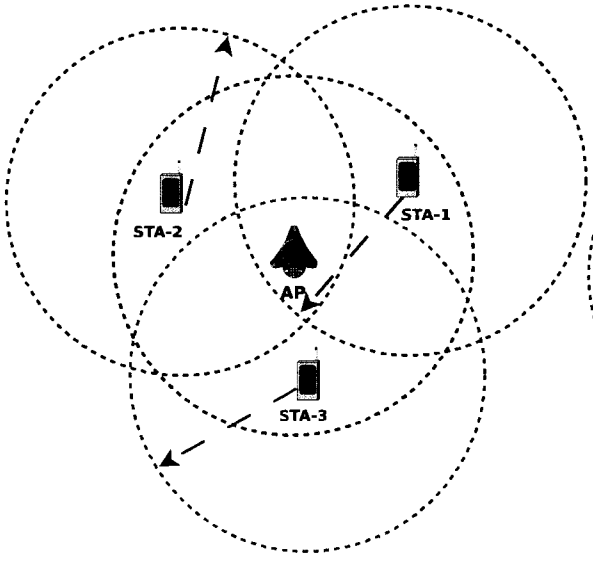

(c) **Two hidden nodes scenario.**

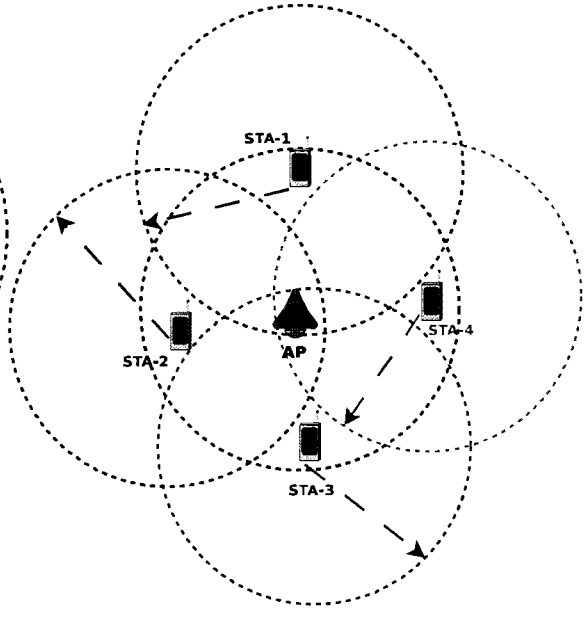

(d) **Three hidden nodes scenario.**

Figure 3.6: Contending and hidden node scenarios in a network with multiple STAs.

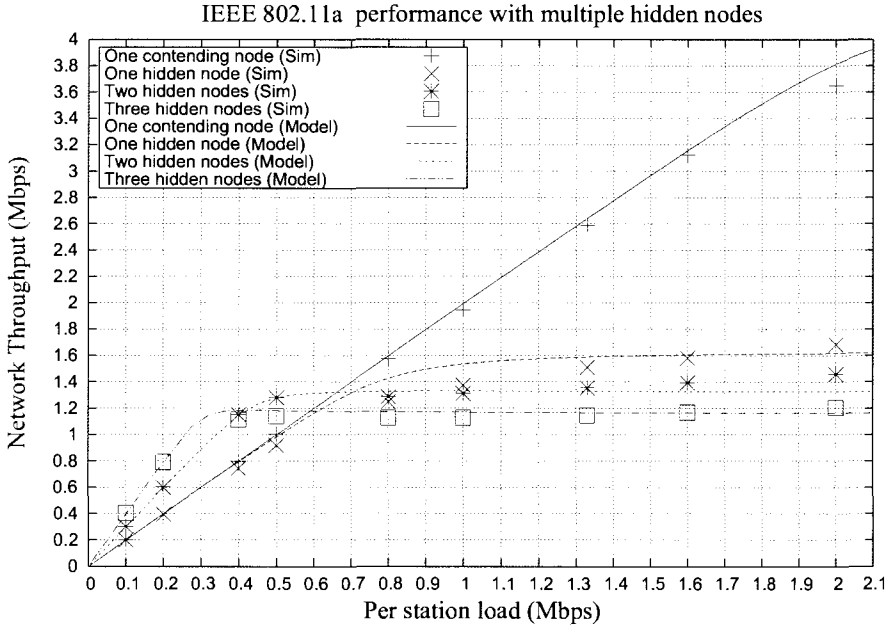

Figure 3.7: Network throughput with different symmetric hidden node network configurations are illustrated. 500 byte frame length is considered. STAs are assumed to be transmitting with 6 Mbps communication rate. IEEE 802.11a MAC and PHY parameters are utilized in the results.

expect the network performance of Fig. 3.6-(d) to be the worst among others due to high number of hidden nodes and increased number of collisions. Network throughput relative to changing traffic condition are presented in Fig. 3.7. As it can be seen, hidden-nodes cause more than 50% capacity loss in medium-to-high traffic conditions compared to no-hidden user case and barely affect the system in low traffic. Contending user results are obtained by modifying throughput equation of [29] for the IEEE 802.11a OFDM PHY characteristics. It should be noticed that there is a significant performance gap between one contending node and one hidden node scenarios. Addition of more hidden users causes slight incremental performance degradation in comparison. The scenarios with high number of users (*i.e.* Figs. 3.6-(c) and (d)) present a better network throughput performance when the STAs are lightly loaded. This is the case when the network is highly unsaturated and the network throughput is increasing linearly with the traffic. In such a scenario, packet collisions occur very seldom due to long idle periods in the unsaturated channel. As the traffic load per user increases, the network experiences more collisions and eventually suffer throughput performance loss. It should be noticed that networks with different number of hidden STAs have different throughput breaking points (when the network reaches to saturation). The more hidden users a network has, the less traffic it requires to reach to this saturation point.

Fig. 3.7 includes not only the model equations but also NS2 simulation results for comparison purposes. In the simulations, the STAs are transmitting packets to a single AP. Along with the hidden user scenarios, one contending user case is also presented to validate the analytic formulation as well as for comparison purposes. NS2 parameters are configured for the IEEE 802.11a OFDM PHY and MAC values as given in Sec 17.5.2 of [8] and partially in Table 3.1 for convenience. In NS2, the carrier sense range of an individual STA is configured and hidden nodes are simulated by tuning *CSThresh_* parameter of wireless PHY. UDP frames are generated according to NS2 exponential on/off distribution. In the simulation campaign, the exponential on/off generator is configured to behave as a *Poisson process* by setting the variable `burst_time_` to 0 and the variable `rate_` to a very large value, making the packet transmission time negligible and setting `idle_time_` parameter as packet inter-arrival time. In NS2 performance figures, the packet payload is assumed to be 500 bytes (*i.e.* `packetSize_` 500). AP and STA transmission power levels are assumed to be constant $200\,mW$ ($23\,dBm$) and located accordingly to simulate hidden or contending user scenarios considering two-ray ground reflection propagation model [33]. As it can be seen, the model developed matches the simulation results perfectly, verifying the model's accuracy.

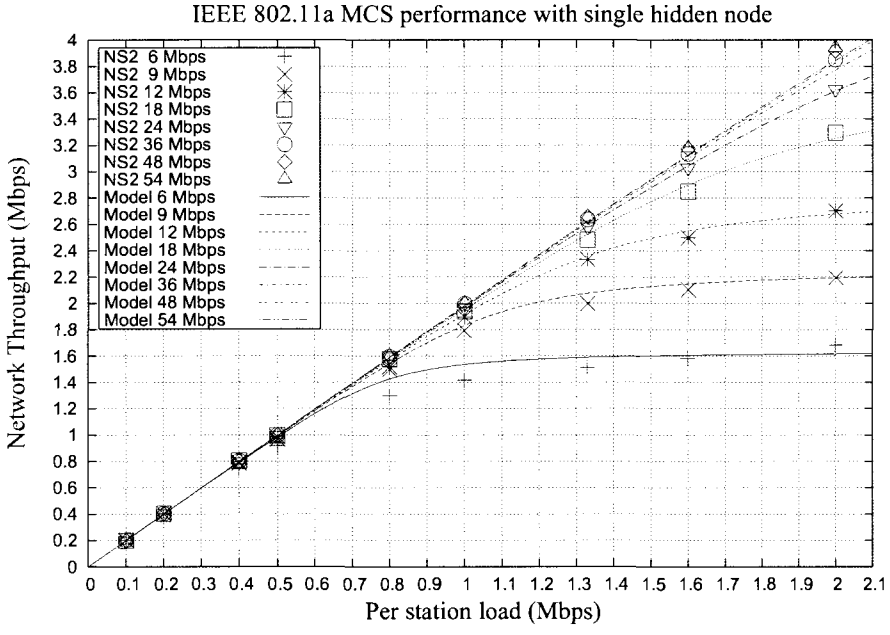

Figure 3.8: Network throughput with different IEEE 802.11a modulation and coding schemes. Single hidden user scenario with 500 byte packet size.

The effect of a hidden node on different modulation and coding schemes (MCSs) are illustrated in Fig. 3.8. In the figure, only single hidden user case is illustrated (Scenario-b of Fig. 3.6). As it can be seen from the illustration, the derived model follows closely the NS2 results confirming the accuracy. The traffic required to saturate the communication channel is an increasing function of the communication rate. It requires 1.3 Mbps per STA load to saturate the channel with data rate of 6 Mbps, whereas it needs more than 2 Mbps for the communication rate of 24 Mbps. Considering a fixed STA load, as the communication rate increases, the time required to transmit a frame (fixed length packet) decreases; this reduces the probability of the hidden STA to interfere with the ongoing packet transmission, increasing the network throughput. From Fig. 3.8, we can see that for 2 Mbps per STA load, the network can have the throughput of 1.6 Mbps with 6 Mbps data rate, whereas 54 Mbps data rate (with 24 Mbps mandatory rate) can supply up to 3.8 Mbps network throughput.

Conditional packet collision probability (p) of single hidden user scenario along with different user traffic load and MCSs is illustrated in Fig. 3.9. As expected, conditional collision probability is an increasing function of user traffic load and decreasing function

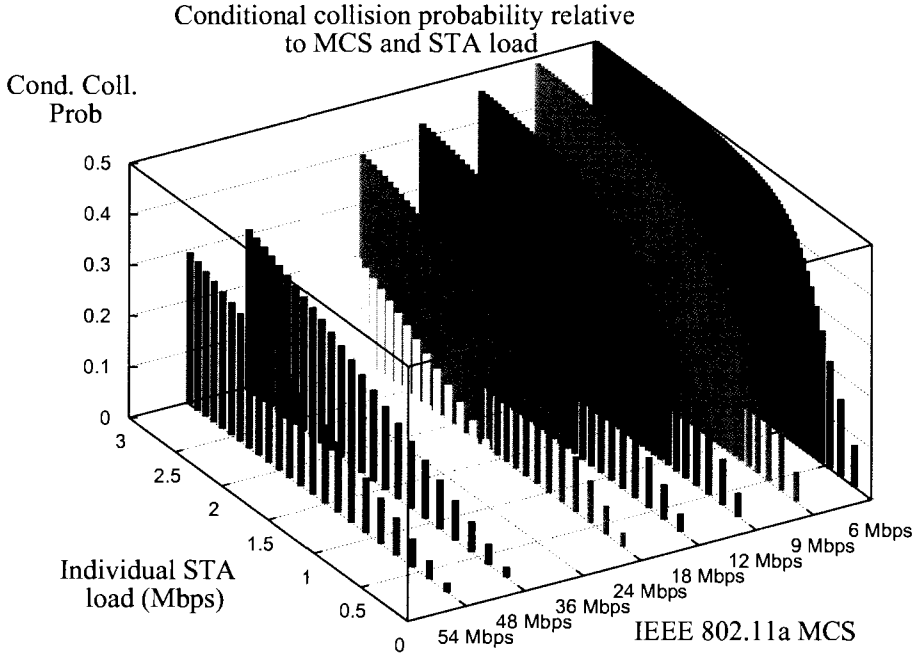

Figure 3.9: Packet conditional collision probability relative to user load and communication rate. Single hidden user scenario with 500 byte packet size is illustrated in the figure.

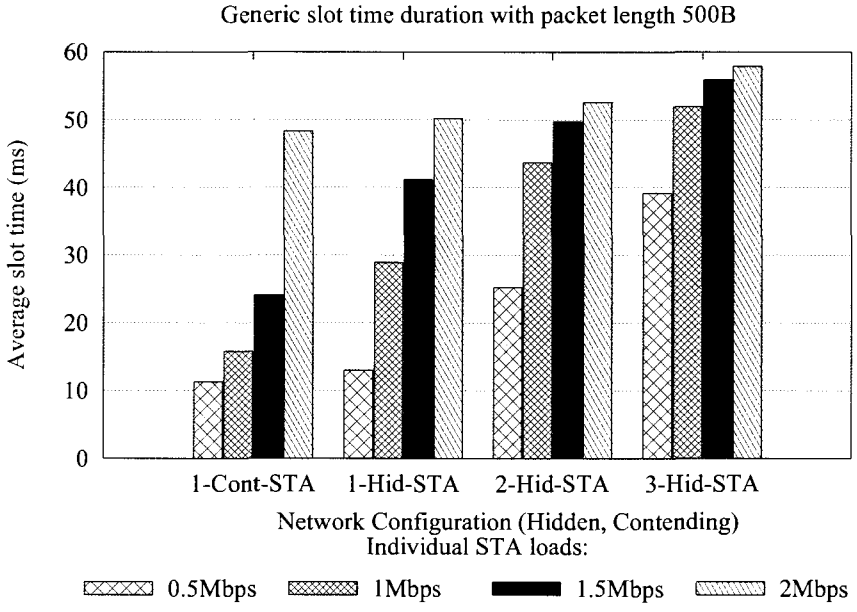

Figure 3.10: Average generic slot duration for different network configurations. Users are transmitting with data rate of 6 Mbps.

of communication speed. This behaviour can be explained as follows: Increased communication speed, providing shorter transmission time, can afford lower k value for the same frame size, which in turn decreases the collision propability presented in (3.10).

The other measure of interest considered in this thesis is the average (generic) slot duration with different traffic loads and network configurations which is given in (3.5). Fig. 3.10 illustrates the average slot durations for hidden user as well as contending user scenarios along with different traffic loadings. Average slot duration is an important indicator for network congestion and performance. As it can be seen, generic slot duration is an increasing function of network traffic as additional traffic amplifies P_{tr} weighing T_s and T_c against T_{slot} in (3.5). For the same traffic conditions, the hidden node scenario has a higher average slot duration comparison to contending users case as collision takes more network time than successful packet transmission (*i.e.* $T_c > T_s$). Comparing 2Mbps data point in the figure, it can be seen that both contending and hidden user scenarios have comparable average slot time values. In the contending user case however, this increased average slot time is due to domination of T_s in (3.5), whereas in hidden user case this is due to the influence of T_c.

3.3.2.3 Asymmetric Networks

In asymmetric networks, the users in the communication environment are naturally clustered into fairness groups, $G_k \subseteq S$. This clustering depends on the users' orientation in the network. In a network, it is possible for a set of users to have a similar contending and hidden node numbers. For instance, if a set of users all have 3 hidden nodes and 2 contending nodes, then they will have similar packet transmission probability (and conditional collision probability), making them members of the same fairness group. In a single AP network environment, the list of groups are mutually exclusive and collectively exhaustive. Considering there are N different fairness groups then

$$G_1 + G_2 + G_3 ... + G_N = S \tag{3.16}$$

Let's denote the number of STAs in each group as $g_k = |G_k|$. The number of contending STAs in G_k is denoted as c_k whereas the number of hidden stations in G_l effecting STAs in group G_k is denoted as $h_{k,l}$. It should be noted, the fact that STAs are in the same fairness group, does not necessarily mean that those STAs are co-located (*i.e.* in the carrier sense of each other). In each group, STAs can be either contending with or hidden to each other, $g_k = c_k + h_{k,k}$. In a network of n users and N fairness groups, it can easily be shown that

$$\forall k \in 1, 2, ..., N : n = c_k + \sum_{i=1}^{N} h_{k,i} \tag{3.17}$$

For calculation of the packet transmission probability, a similar approach presented for symmetric networks will be followed. However, in asymmetric networks, the users in different fairness groups will have different τ as well as p parameters. Let's denote τ_k and p_k as the packet transmission and conditional collision probabilities of users in G_k. For asymmetric case, the network wide probability that there is at least one transmission in the considered slot time, P_{tr} can be found as:

$$P_{tr} = 1 - \prod_{i=1}^{N} (1 - \tau_i)^{g_i} \tag{3.18}$$

Successful frame transmission probability would be different for each fairness group. The probability that a transmission of a user in G_k is successful can be found by calculating the probability that exactly one STA in that fairness group transmits and all the hidden users to the considered user do not interrupt the transmission conditioned on the fact

that there is a packet transmission on the channel:

$$P_{s_k} = g_k \tau_k (1-\tau_k)^{c_k - 1} \left[\prod_{i=1}^{N} (1-\tau_i)^{h_{k,i}} \right]^k \Big/ 1 - \prod_{i=1}^{N} (1-\tau_i)^{g_i} \tag{3.19}$$

The conditional collision probability for a user in G_k can be calculated by taking into account the fact that a packet transmission would be successful if: *i)* None of the contending STAs in the considered fairness group initiate a packet transmission on the same slot time and *ii)* none of the hidden nodes in all fairness groups interfere with the ongoing data transmission:

$$p_k = 1 - \frac{(1-\tau_k)^{c_k - 1} \left[\prod_{i=1}^{N} (1-\tau_i)^{h_{k,i}} \right]^k}{1 - \prod_{i=1}^{N} (1-\tau_i)^{g_i}} \tag{3.20}$$

Finally, the corresponding average slot duration (T) for asymmetric networks can be estimated by calculating the average durations the channel is used for successful packet transmission, packet collision or not used at all (idle channel condition):

$$T = (1 - P_{tr}) T_{slot} + P_{tr} \left[\left(\sum_{i=1}^{N} P_{s_i} \right) T_s + \left(1 - \sum_{i=1}^{N} P_{s_i} \right) T_c \right] \tag{3.21}$$

Calculation of k value becomes more convoluted in asymmetric networks, if the steps of symmetric hidden node scenarios are followed. However, if assume $\alpha = \beta^*$ the formulation of the value of k simplifies to:

$$k = 2\alpha \Big/ \left\{ 1 + (\beta - 1) \left[1 - \prod_{i=1}^{N} (1-\tau_i)^{g_i} \right] \right\} \tag{3.22}$$

In Example 2, the performance analysis of all possible network configurations with 4 users (*i.e.* $n = 4$) are illustrated. In such a configuration (4 STAs communicating with a single AP), one can have three symmetric and two asymmetric hidden node configurations as illustrated in Fig. 3.11.

*This assumption implies $T_c = T_s$. Packet collision duration depends on *ACKTimeout_* if the user is involved in the collision. Considering the fact that *ACKTimeout_* is not defined in the standards, it is possible to tune this parameter relative to expected network load. In this work, it is verified with simulations that this assumption is safe with small-to-medium packet sizes.

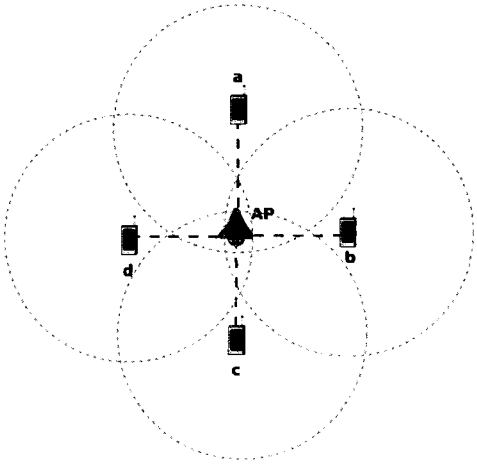

(a) Scenario 1: All hidden.

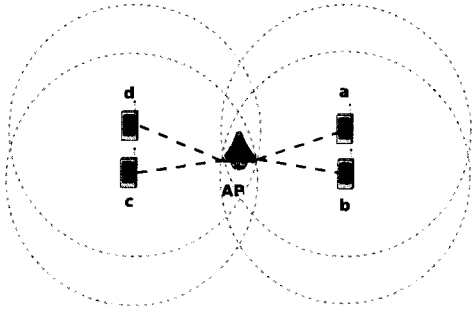

(b) Scenario 2: 2 hid.&1 cont.

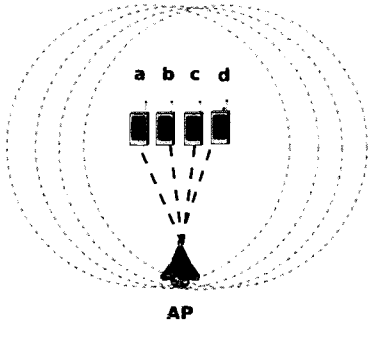

(c) Scenario 3: All contending.

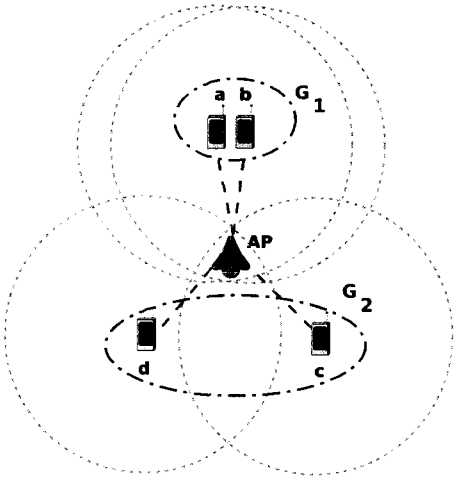

(d) Scenario 4: Fairness group $G1$: 1 cont.&2 hid. Fairness group $G2$: 3 hid.

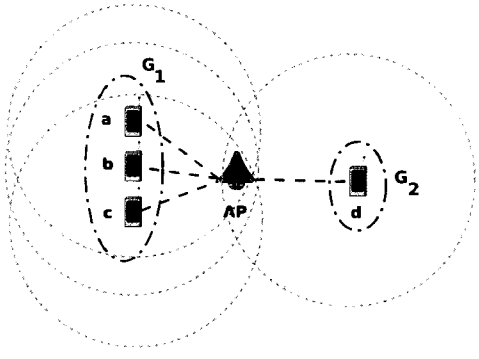

(e) Scenario 5: Fairness group $G1$: 2 cont.&1 hid. Fairness group $G2$: 3 hid.

Figure 3.11: Possible symmetric and asymmetric scenarios in a network with 1 AP and 4 STAs.

EXAMPLE 2: Scenarios (d) and (e) illustrate asymmetric scenarios for a network configuration of 4 STAs and 1 AP given in Fig. 3.11. Different fairness groups in each orientation is also shown in the figure. Let's focus on Scenario 4 to illustrate the formulation parameters. In this spacial setup, there are total of two fairness groups, $N = 2$ as $G_1 = \{a, b\}$ and $G_2 = \{c, d\}$. If we consider the performance of users in G_2; from a considered user perspective there is only one contending STA, $c_2 = 1$ and STAs in G_2 are hidden to each other, $h_{2,2} = 1$. All the users of G_1 are also hidden to users in G_2; therefore, $h_{2,1} = 2$. Intuitively, it is expected that the users of G_2 in both scenarios 4 and 5 (which have higher number of hidden nodes), would have less of a network fair share. Simulated network configurations are illustrated in Fig. 3.12 and Fig. 3.13. Performance of a more elaborate network configuration can be calculated by natural extension of the ideas presented in this work. Similar to the symmetric hidden node network configuration, in the simulated network environment, STAs are transmitting packets to a single AP. In NS-2 performance figures, the packet payload is assumed to be 256 bytes (*i.e.* `packetSize_` 256).

Total network throughput of all the scenarios relative to changing traffic conditions is presented in Fig. 3.12. Mandatory and communication data rate of the users are assumed to be 6 Mbps, and the frame length of 256B is chosen in the simulation. Numerical results obtained from NS-2 show good agreement with the results obtained from analytical expressions. As expected, all contending STAs scenario illustrated in Scenario-3 has the best throughput performance whereas all hidden STAs presented in Scenario-1 has the worst performance. As it can be seen, presence of hidden nodes does not affect the network performance in low traffic conditions. As mentioned in Section 3.3.2.3, users in different fairness groups illustrated in Scenario-4 of Fig. 3.11 are expected to have different network shares. This phenomenon is illustrated in Figs. 3.13 and 3.14. It can be seen that network fairness performance is a function of offered load. In low-traffic conditions, all the users of the network (independent of the number of hidden users affecting the transmission) have their fair share of the network. As the network load increases, users that have less number of hidden-nodes dominate the network, causing starvation of the badly located users. Higher packet transmission probability and lower conditional collision probability of users in fairness group G_1 illustrated in Fig 3.14 clearly indicates that users in this group have an unfair advantage in this network configuration. Similar network fairness abnormality is seen in Scenario 5 illustrated in Fig. 3.11 are presented in Figs. 3.15 and 3.16. As expected, the performance difference of the fairness groups is bigger in this case compared to Scenario 4, because the user in G_2 has three

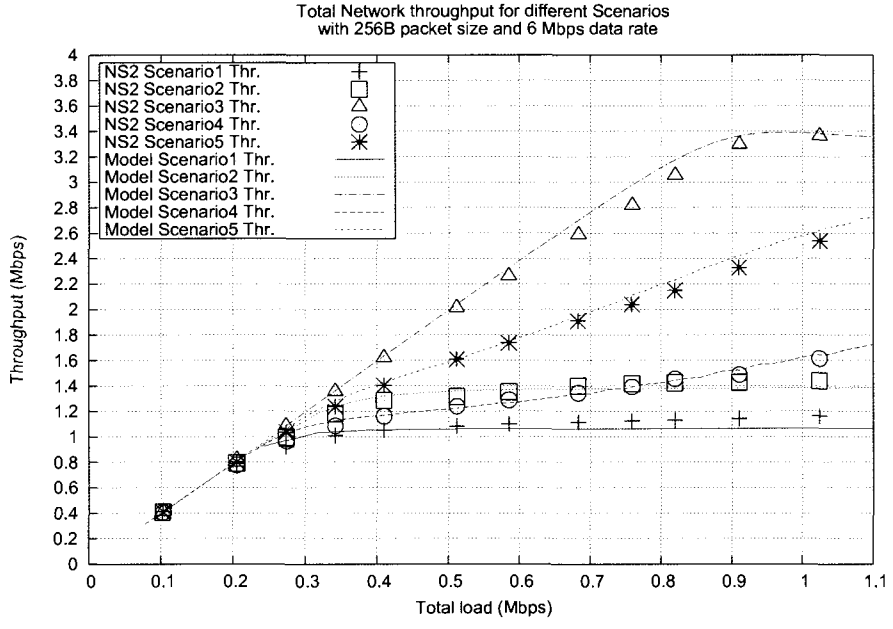

Figure 3.12: Total network throughputs in all the scenarios.

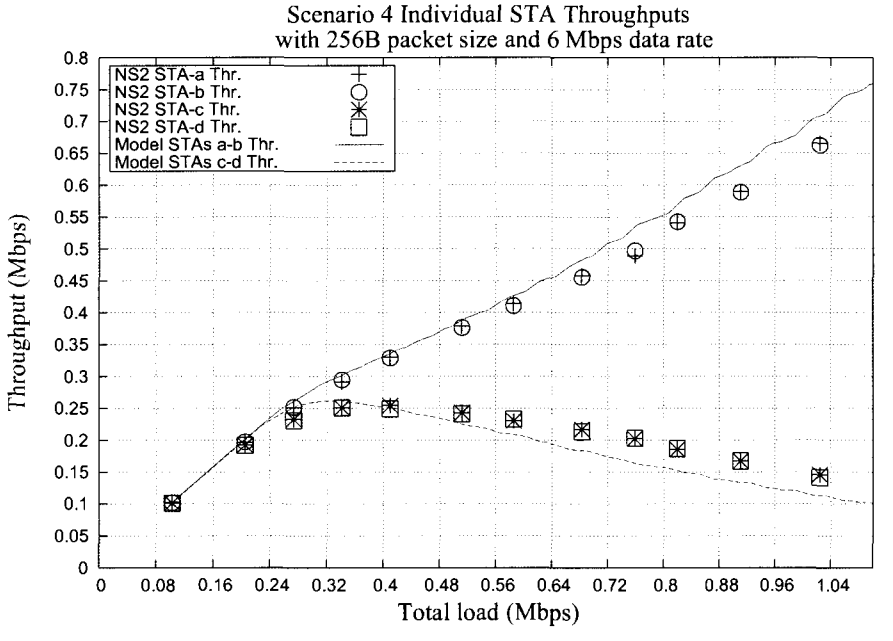

Figure 3.13: Throughputs of different fairness groups in Scenario 4.

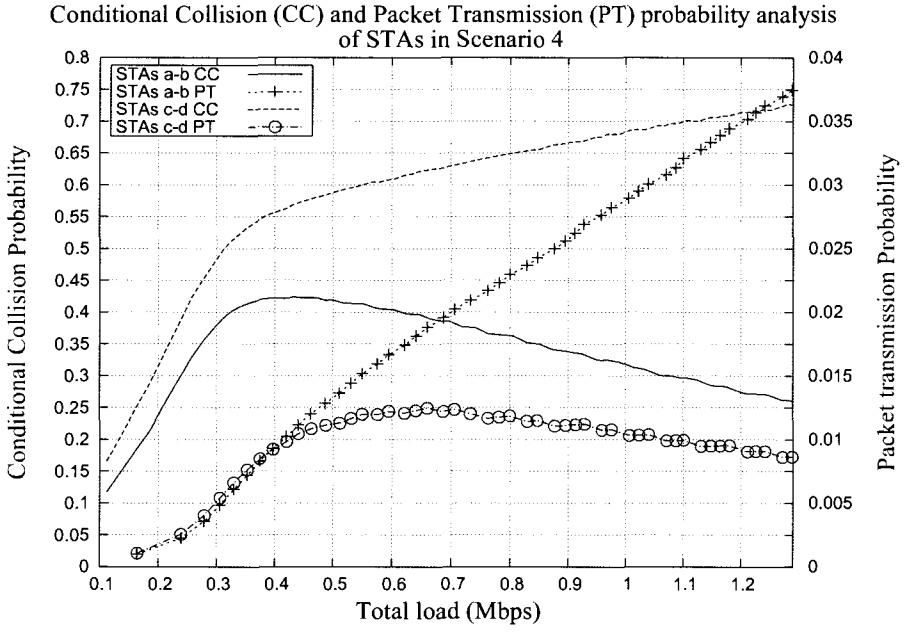

Figure 3.14: Packet transmission and conditional collision probability of different fairness groups in Scenario 4.

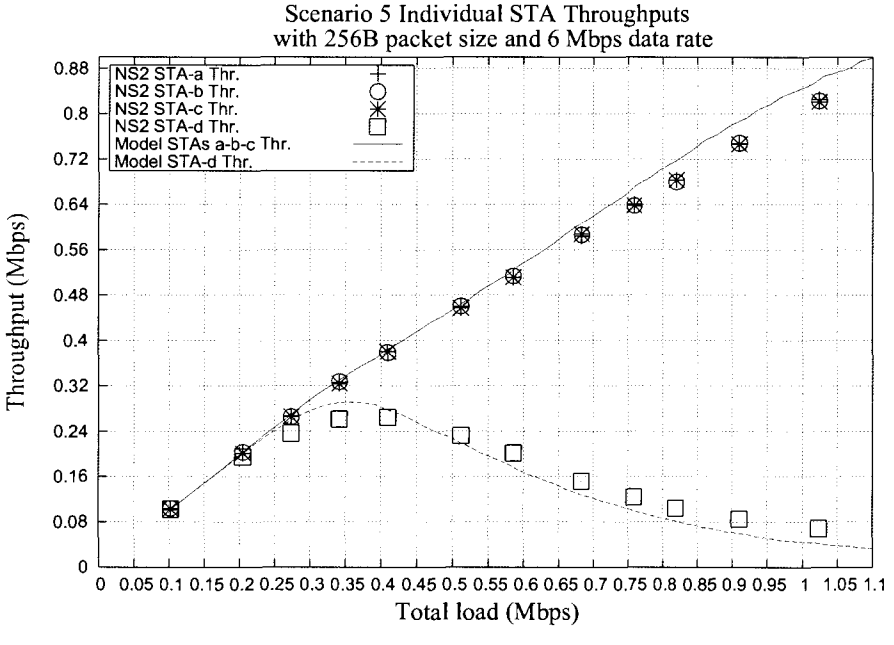

Figure 3.15: Throughputs of different fairness groups in Scenario 5.

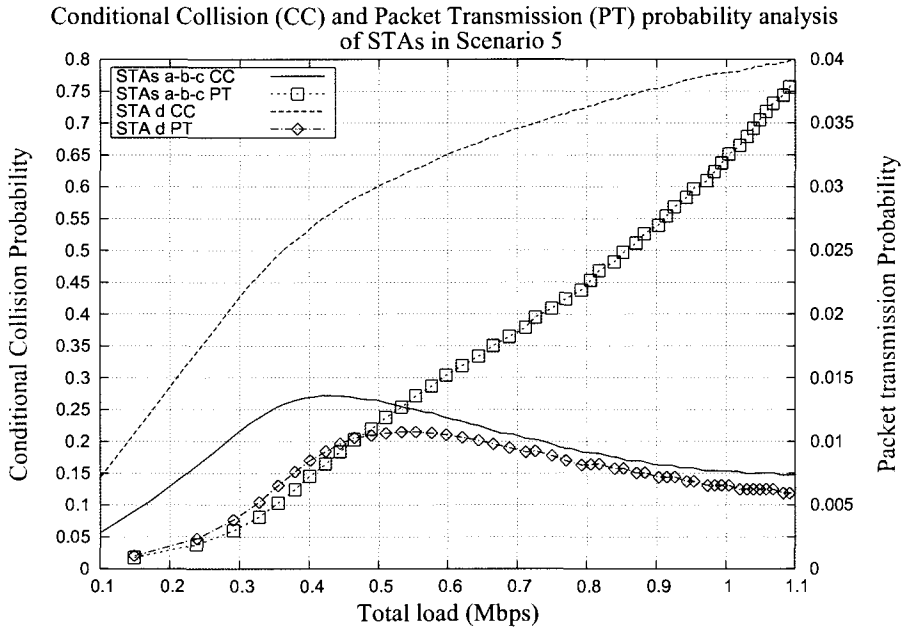

Figure 3.16: Packet transmission and conditional collision probability of different fairness groups in Scenario 5.

hidden users interfering with its transmission whereas users in G_1 have only one. As it can be seen from the illustrations, the derived model follows closely the NS2 results confirming the model accuracy.

The other measure of interest considered in this section, assessing the network fairness performance, is the number of collided packet transmissions per successful transmission. Fig. 3.17 illustrates this performance figure in asymmetric network configurations with different traffic loadings. As it can be seen, average packet collision per successful transmission is an increasing function of network traffic as well as number of hidden users in a network. For the same traffic conditions, users that experience more hidden nodes interfering with their transmissions have higher number of collided packets per successful transmission.

Besides individual STA throughputs, a network fairness index is also calculated and compared in asymmetric scenarios. To quantify the network fair share of the asymmetric network configurations, *the fairness index* (also called The Jain's index) introduced in [34] and [7] is used as a metric. Consider $\mathfrak{S}_i$ as the throughput of STA i in a multi-STA

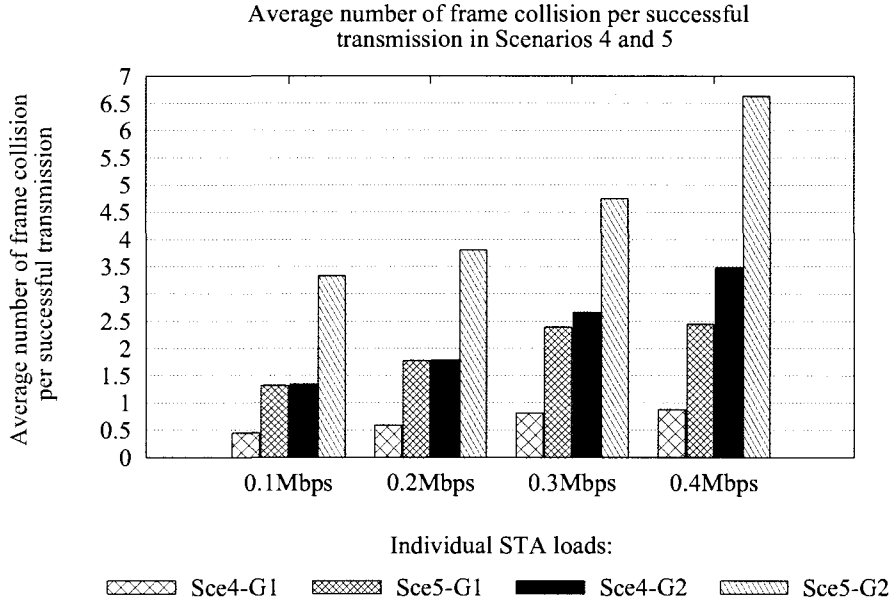

Figure 3.17: Average number of collided transmissions per successfull transmission for fairness classes in Scenario 4 and 5. Data rate is 6 Mbps and frame length is 256B.

network, then the fairness index $\mathfrak{F}$ can be defined as:

$$\mathfrak{F} = \left(\sum_{i=0}^{n} \mathfrak{S}_i\right)^2 \Big/ n \sum_{i=0}^{n} \mathfrak{S}_i^2 \tag{3.23}$$

The fairness index has the property that it is equal to 1 when all STAs have the fair share of the network and it gets closer to $1/n$ ($n = |S|$) when the STA throughputs are distinctly different. Fairness index results of the asymmetric networks relative to offered user load are illustrated in Fig. 3.18. It can be seen that network fairness index is a decreasing function of user load. Considering the same number of users, Scenario 5 scores way lower fairness index comparison to Scenario 4, illustrating worse fairness performance in such setup.

3.3.2.4 RTS/CTS Performance

In IEEE 802.11 standards RTS/CTS channel access scheme is developed as solution to hidden-node problem. However, since the implementation of RTS/CTS scheme is costly from radio resource perspective, its performance evaluation is mostly ignored in

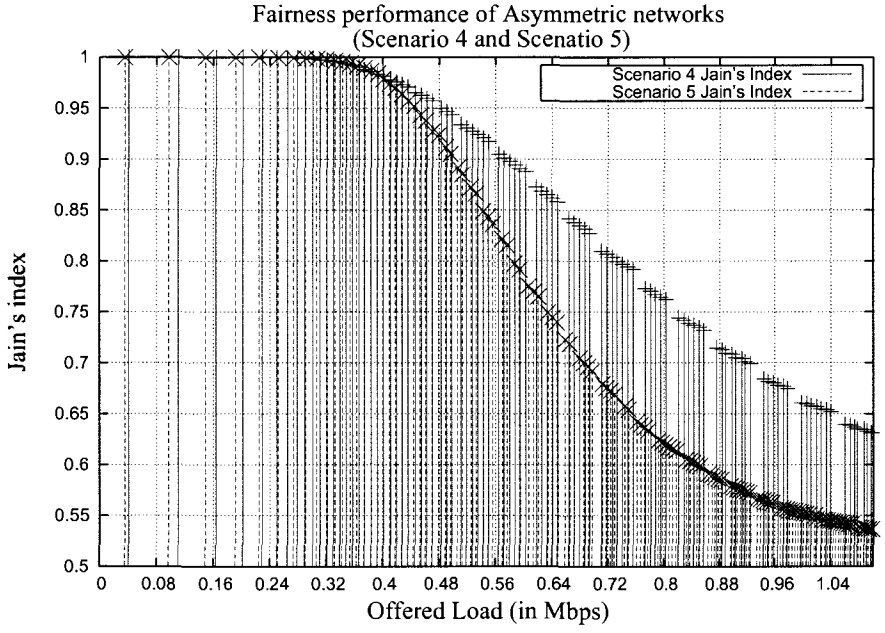

Figure 3.18: Jain's index in asymmetric network Scenarios 4 and 5.

literature. In RTS/CTS mode, the channel is reserved on both transmitter (RTS) and receiver (CTS) side to avoid any collision during packet transmission. In such a scheme, a single data frame transmission requires three control frames (four-way handshake), introducing further latency comparison to DCF mechanism.

The developed model explained in this paper is also applicable to RTS/CTS channel access scheme with a couple of modifications. Initially the expected successful packet transmission and collision durations will be different than the values presented in Section 3.2.1. For RTS/CTS four-way handshake, the successful packet transmission (T_s^{rts}) and packet collision (T_c^{rts}) durations can be calculated as follows:

$$\begin{aligned} T_s^{rts} &= T_{rts} + T_{sifs} + \tau_{ch} + T_{cts} + T_{sifs} + \ldots \\ &\quad \tau_{ch} + T_{data} + T_{sifs} + \tau_{ch} + T_{ack} + T_{difs} + \tau_{ch} \\ T_c^{rts} &= T_{rts} + T_{difs} + \tau_{ch} \end{aligned} \tag{3.24}$$

In (3.24), RTS and CTS frame transmission durations are indicated as T_{rts} and T_{cts}. With the help of the OFDM PHY and MAC parameters, the frame transmission durations

defined for RTS/CTS scheme can be calculated as follows:

$$T_{rts} = T_{pre} + T_{sig} + T_{sym}\left\lceil \frac{serv + tb + 8rts}{N_{dbps}} \right\rceil \tag{3.25}$$
$$T_{cts} = T_{pre} + T_{sig} + T_{sym}\left\lceil \frac{serv + tb + 8cts}{N_{dbps}} \right\rceil$$

The analytic formulation of the RTS/CTS throughput performance in hidden node communication environment is similar to the study presented in Section 3.3.2. However, for hidden node collision cases, we will need to consider only RTS frame transmission duration rather than whole data frame transmission duration which was valid for DCF usage case. Therefore, in a hidden-node communication environment, the considered STA using RTS/CTS scheme would have a successfull frame transmission if:

1. In a generic slot time, none of the contending STAs transmit RTS frame. The probability of such condition can be expressed as: $(1-\tau)^{c-1}$

2. During the duration of a RTS frame transmission (*i.e.* $T_{rts} + T_{sifs} + \tau_{ch}$), none of the hidden STAs has interfering transmission and vice versa. (*i.e.* the considered user does not interfere an ongoing hidden node transmission). This probability can be calculated by: $[(1-\tau)^{h}]^{k^{rts}}$

where k^{rts} indicates approximate number of average slot decrements in $2T_{rts}$:

$$k^{rts} = 2T_{rts}/T \tag{3.26}$$

The throughput performance of the RTS/CTS channel access scheme is given for the scenarios presented in Section 3.3.2.3 and illustrated in Figure 3.11. Total network throughput performance of different channel access schemes (RTS/CTS and DCF) is given in Figure 3.19. As it can be seen from the illustration, the overall throughput variation of RTS/CTS scheme is less comparison to DCF channel access mechanism. The reason for such a behaviour is the reduced network time being wasted during collision even in multiple hidden-node environments. In RTS/CTS channel access, even though both transmitter and receiver reserve channel for further data transmission, we notice overall throughput reduction as the number of hidden nodes increases. This is due to RTS packet collision during channel reservation. RTS packet transmission is not protected against hidden node problem. Therefore as the traffic of individual users increase the probability of transmitted RTS packets increases; which eventually causes throughput loss.

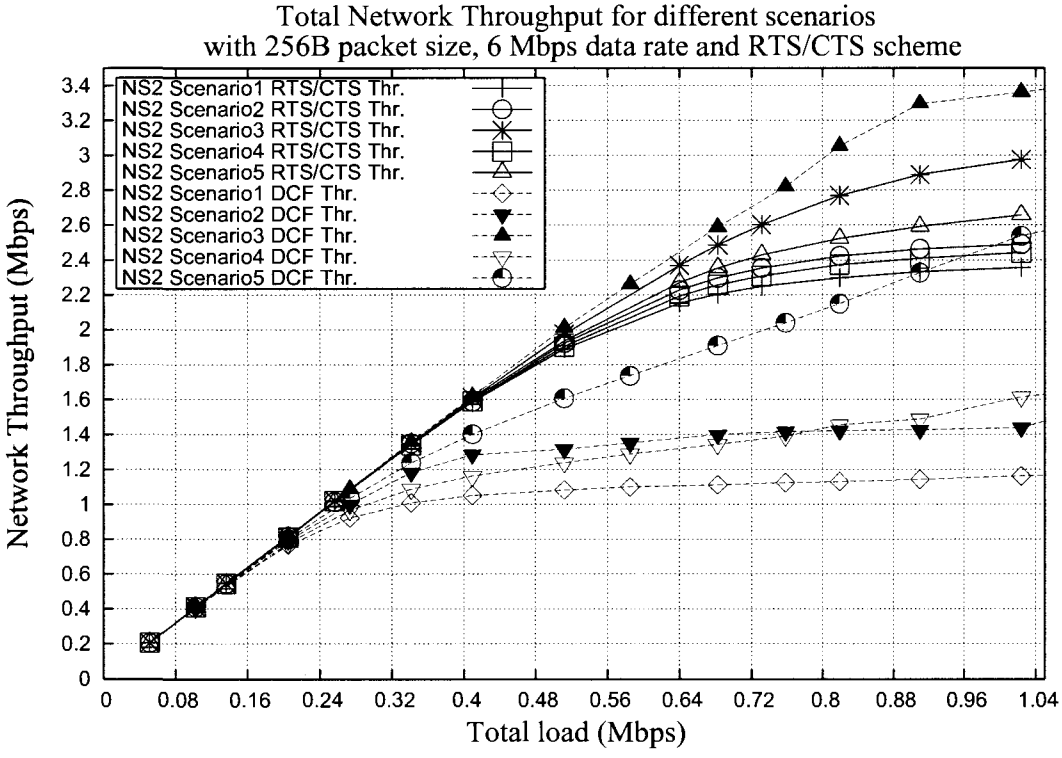

Figure 3.19: Total network throughputs of different scenarios with DCF and RTS/CTS channel access schemes.

Individual STA throughputs of Scenario-4 with RTS/CTS channel access scheme is illustrated in Figures 3.20 and 3.21. As it can be seen, RTS/CTS channel access scheme provides a better fairness performance in terms of throughput allocation in asymmetric network allocations. In higher load regions, RTS packet collision causes throughput performance differences among network users. Similar performance illustration for Scenario-5 is given in Figure 3.23 and 3.22.

3.4 Conclusions

The fairness performance of practical wireless local area network environments considering multiple hidden nodes and unsaturated traffic condition is studied in this Chapter. Analytic performance of IEEE 802.11 primary medium access algorithm (DCF) is presented for both symmetric and asymmetric hidden node networks. It has been shown

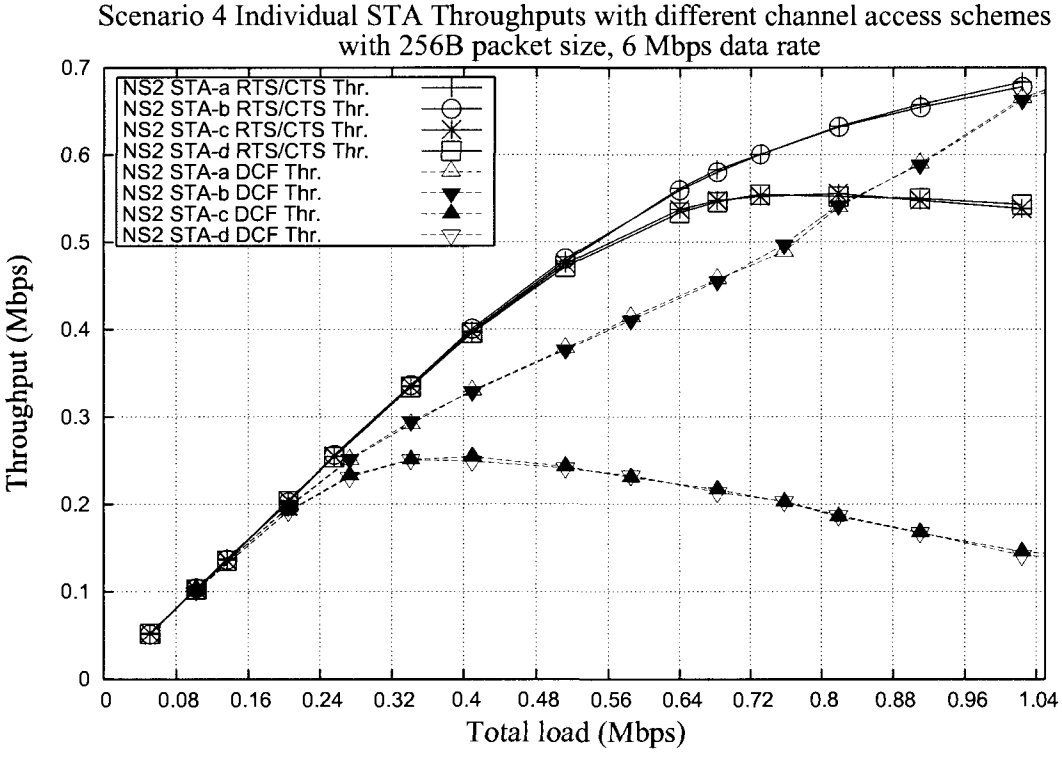

Figure 3.20: Throughput performances of individual users in Scenario-4. RTS/CTS and DCF channel access scheme performances are compared.

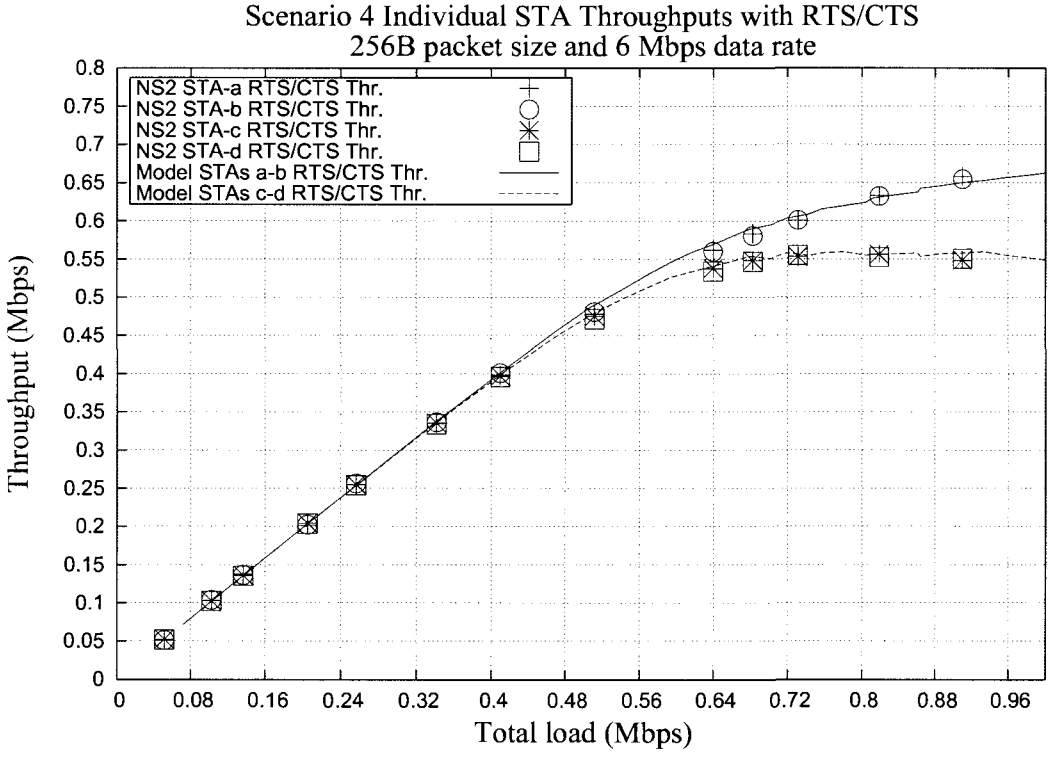

Figure 3.21: Throughputs of different fairness groups in Scenario 4 with RTS/CTS channel access mechanism.

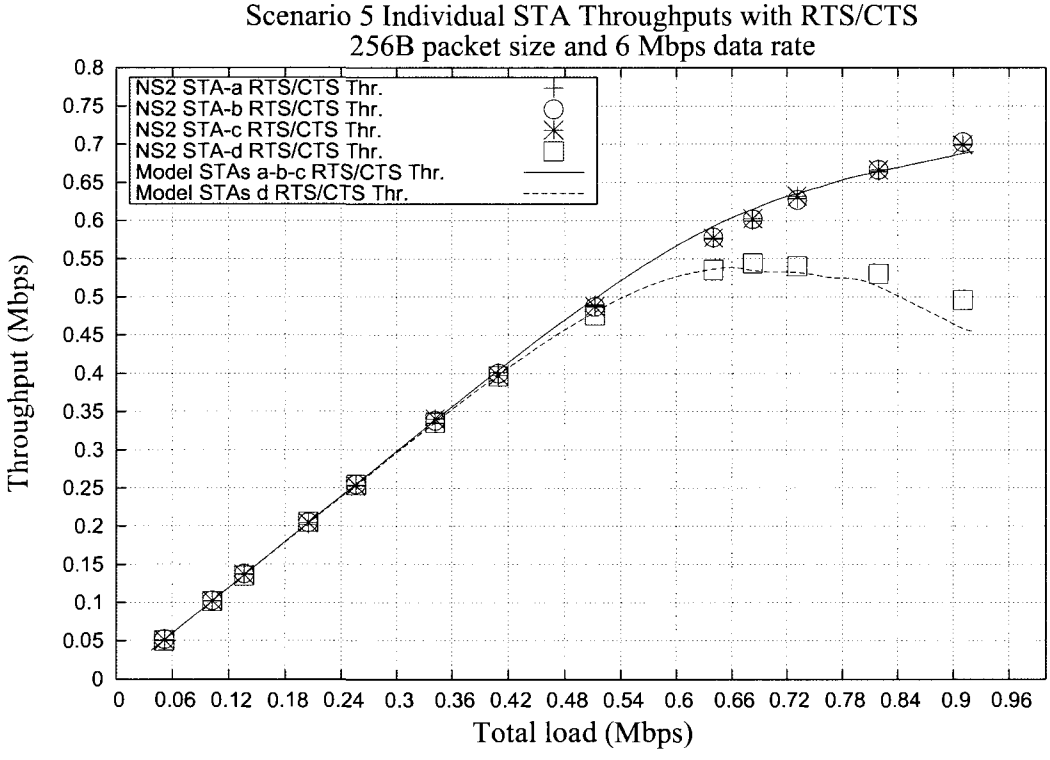

Figure 3.22: Throughputs of different fairness groups in Scenario 5 with RTS/CTS channel access mechanism.

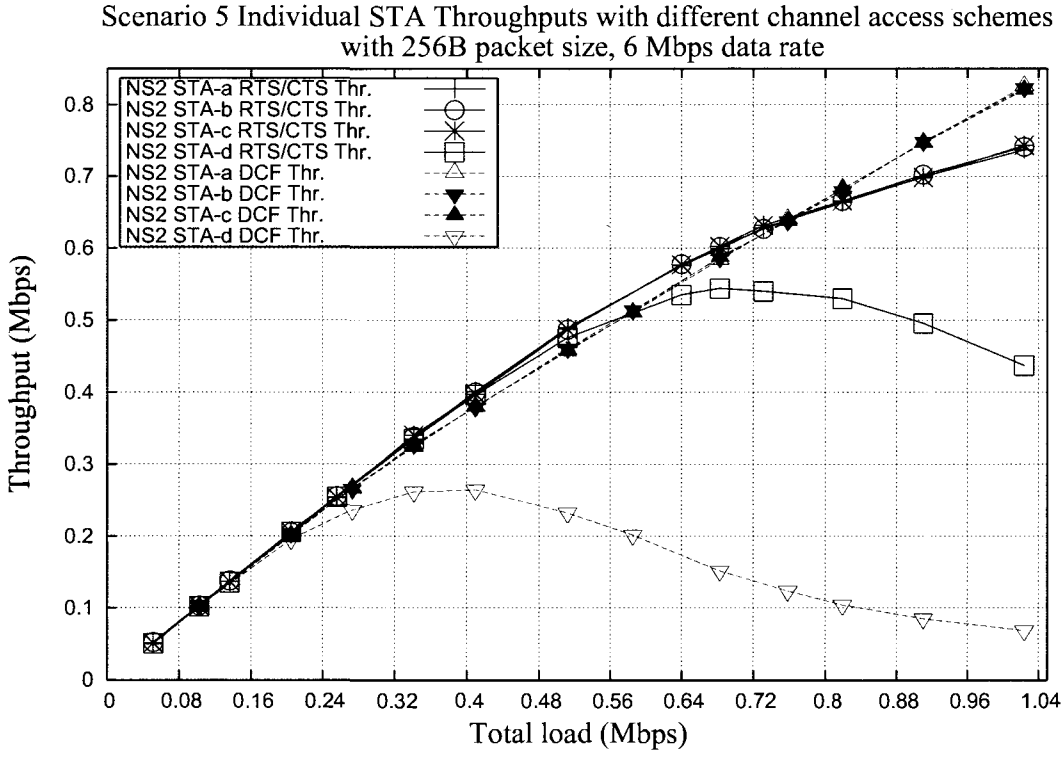

Figure 3.23: Throughput performances of individual users in Scenario4. RTS/CTS and DCF channel access scheme performances are compared.

that the presence of hidden nodes barely affects the per user network fair share in low traffic conditions, but it causes considerable performance loss in moderate-to-high traffic scenarios.

It has also been shown that per user performance highly depends on user location in the network. In an asymmetric network configuration, increasing traffic increases per user throughput up to a certain point, that depends on the overall network orientation. Further increase of traffic causes starvation of badly located users that has more number of hidden nodes. The accuracy of the analytical model presented is illustrated by comparison to simulation results. The throughput performance of RTS/CTS channel access scheme is also presented with NS2 simulations. It is shown that even though, RTS/CTS scheme helps network achieve a better throughput performance, RTS packet collision seen mostly highly loaded environments causes performance drop in hidden node environments.

After evaluating the DCF throughput and fairness performance in practical network configurations, we see that congestion and commonly observed hidden node problem limits DCF performance. Reducing the communication overhead and avoiding excessive collisions (either due to congestion or hidden node) would drastically increase the network throughput. In the next Chapter we show that point coordination function (PCF) provides a superior throughput performance with its reduced overhead, no contention environment and proposed polling indexing scheme.

Chapter 4

PCF Performance with Advanced Indexing Scheme

Communication delay is a limiting factor for any real time, time bounded link. IEEE 802.11 WLANs implement point coordination function (PCF) and hybrid coordination function (HCF) controlled channel access (HCCA) to accommodate real time services with a certain QoS [10]. Scheduled access schemes (PCF and HCCA) allow an IEEE 802.11 network to provide an enforced *fair* access to the medium. In some ways, the access to the channel is scheduled such that only the STA that is being polled is allowed to use the medium where AP is the poll-master (point or hybrid coordinator). Scheduled access has not been widely implemented in commercial products. As a result, most of the performance improvement studies are concentrated on DCF algorithm in the literature, ignoring the basic scheduled access scheme of PCF. Despite the fact that PCF has a better MAC efficiency (less overhead and better piggy-pack implementation) [35, 9] and no loss due to contention, it is mostly neglected in the literature and only limited number of studies are published [36, 37, 38, 39, 40]. This is mainly because DCF is the default access scheme configured with the commercial products and it has more independent and distributed channel access mechanism, not requiring any central controller. Only limited number of enterprise class products have implemented PCF to have the control centralized in the AP. This implementation targeted the hot-spot scenarios aiming to seize the wireless channel control in the presence of greedy herd of stations.

It is possible to increase the efficiency and throughput of the scheduled access even further. Current implementation of scheduled access (HCCA and PCF) in IEEE 802.11 WLANs does not take into account the physical channel information and multi-rate

capability of the STAs in building the STA polling list in contention free period. This usually results in much lower downlink data rates than what can ideally be achieved causing the overall network throughput drops.

In this chapter, the performance of point coordination function is evaluated and compared to distributed coordination function. The shortcoming of the current polling list creation technique in the current scheduled access schemes is illustrated and an efficient polling order scheme with increased throughput performance is proposed for infrastructure basic service sets with multirate transmission capability. Significant throughput performance increase (up to 20%) can be achieved, in a typical communication environment where downlink dominates the overall communication link. Initially the PCF mode of operation is summarized in Section 4.1. Later, the problem of the currently deployed PCF mechanism that is limiting the throughput performance is explained in Section 4.2. The proposed polling list creation method is described in Section 4.3. Finally, simulation results are presented to illustrate the performance increase with the proposed polling list creation method.

4.1 Point Coordination Function of IEEE 802.11

PCF is a deterministic access scheme which eliminates the packet collisions on the wireless communication medium. It is typically used for real-time services requiring a timely delivery of traffic with less error. It should also be noted that the polling based PCF might as well be used for non-real time services. PCF is known to achieve a better throughput performance than the contention based DCF [9], and hence one may want to use the PCF instead of the DCF in order to maximize the system throughput for data traffic. PCF is utilized in infrastructure BSS and it requires a point coordinator (PC) in each BSS that initiates and controls the contention free period (CFP). PC takes control of the wireless medium by sensing the channel for PCF inter frame space (PIFS) duration, which is shorter than DIFS, giving it a priority to grab and hold on to the channel. Once PC has the control of the medium, it may start transmitting downlink (from AP to STA) traffic to STAs. PC starts a CFP by broadcasting a beacon signal. All users in the BSS update their network allocation vector (NAV) duration by this beacon, to avoid contending during the CFP. PC can end the CFP at anytime by sending a CF-END signal. During a CFP, STAs can start data transmission after a poll if: *i)* they have a pending data frame (DATA) and respond to a poll frame (POLL) from the PC and *ii)* they acknowledge a data packet after a short interframe space (SIFS)

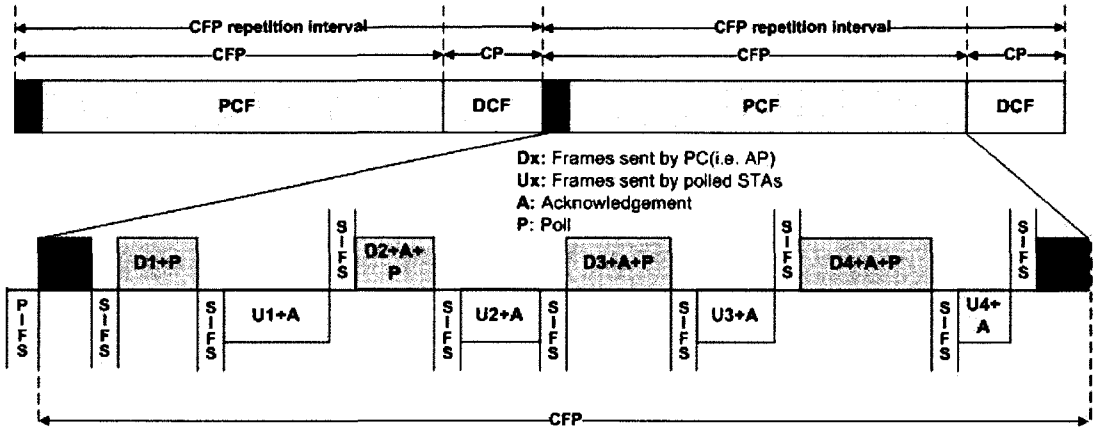

Figure 4.1: Example of PCF frame transfer. Contention free period is initiated with a Beacon (B) frame from point coordinator. Point coordinator has liberty to end contention free period with contention-free-period-end (CFE) frame. In the contention free period, only the STAs polled can transmit uplink data.

interval. In the PCF transmission scheme, it is a common practice to combine POLL and acknowledgement (ACK) frames onto data frame in order to utilize the medium more efficiently.

A sample PCF frame transfer is illustrated in Fig. 4.1. PC takes control of the channel after PIFS of inactivity. PC could start data transmission (on the downlink) a SIFS interval after the beacon frame by sending a POLL, DATA or DATA+POLL frame. If a *CF-aware STA** receives a POLL frame from the PC, STA can respond to PC after a SIFS idle period, with a ACK or a DATA+ACK frame transmission (on the uplink). If PC receives a DATA+ACK frame from a STA, it can send a DATA+ACK+POLL frame to a wireless medium, where the ACK portion of the frame is used to acknowledge the receipt of the previous data frame of a STA and the DATA and POLL is targeted to a different STA. After creating a polling list during the contention period (CP), PC shall issue polls to STAs on the polling list in the order of ascending association ID (AID) value as stated in Section 9.3.4.1 of [6]. Considering the fact that AID is an arbitrary number in the range 1-2007 assigned by the AP to a STA when it associates with a BSS, we can assume that the polling list ordering in IEEE 802.11 standard is done in a random manner. After addressing all the STAs, if there is no further data to send or receive, PC can terminate the CFP by transmitting a CF-END frame.

*A STA that supports contention free transmission.

4.2 Problem Statement

In contention-free period of scheduled access mechanism, every single transmitted frame needs to be acknowledged as in DCF contention resolution method. Additionally, every STA needs to be polled prior to transmission, which would cause a high spectrum inefficiency due to PHY and MAC overhead if every acknowledgement (ACK), poll (POLL) and data frame (DATA) is to be transmitted individually. However, PC can combine polling and ACK frames with data frames in order to improve the throughput efficiency by cutting the extra overhead that might be introduced otherwise [41]. On the downlink communication (*i.e.* from PC to STAs) with the piggy-packed frame format (*e.g.* DATA+ACK+POLL), the frame carries information for two separate STAs that are ordered one after the other in the polling list. Correspondents of the frame are: the STA who is waiting for an ACK for the previously sent data frame and the STA who is the recipient of the DATA (and the POLL if it is included in the frame).

The polling list ordering issue becomes important if we take into account the multi-rate transmission capabilities of the ordered STAs. IEEE 802.11a OFDM PHY has multi-rate transmission rate skill that allows implementations to perform dynamic rate switching with the objective of improving performance. Clause 9.3 of [6] indicates that, on the downlink PC must choose a data rate to send DATA+ACK, DATA+POLL+ACK or POLL+ACK frames that satisfies the communication link conditions of both the STA that is expecting DATA or POLL frame and the STA to which the ACK is directed to. Such an implementation implies that the common communication rate should be the lower of both STAs' data rates in order to guarantee the reliable communication. Adaptive multi-rate transmission enhancement enables STAs to determine their own data rate by the channel condition. Therefore, the STAs targeted by the same frame might have two different connection speeds with the PC. However, the frame directed to those two STAs on the downlink will be transmitted with the lower data rate of the both PC-STA links in order to guarantee the reliable data transmission to both STAs. For example, consider a downlink frame targeting STA1 and STA2 (*i.e.* it is either DATA+ACK or DATA+ACK+POLL). If STA1's channel condition allows the data rate of 54 Mbps with PC, and the STA2's channel condition barely guarantees the data rate of 6 Mbps and in the polling list if they are ordered consecutively, then the data rate of the STA1, on the downlink, would be trimmed down to 6 Mbps in order to guarantee the QoS to STA2 [6]. IEEE 802.11 standards indicate that during CFP, the PC shall issue polls to STAs in the polling list in the order of ascending association ID (AID) [6]. Since

AID is assigned to a STA randomly as part of an association without considering the transmission rate capability or the communication link condition of the STAs, it results in reduced system throughput. This problem can be solved by modifying the polling list order generation algorithm at the PC. Instead of ordering the STAs relative to their AIDs, if we build the polling list order relative to descending received signal strength at PC, the negative effect of the trimming data rate on the system throughput would be minimized. The detrimental effect of standard polling list applies to both HCCA and PCF. The performance increase with the proposed solution is illustrated on PCF access scheme in this work. Similar results can also be obtained with HCCA.

4.3 Adaptive Multi-rate Transmission

An efficient communication system can be designed by selecting the data rate according to the channel condition as proposed in [42] and [43]. IEEE 802.11a/g OFDM PHY can serve its clients with high data rates up to 54 Mbps. These high data rates are made possible through advanced modulation and coding techniques that dramatically increase bandwidth efficiency. An adaptive multi-rate transmission algorithm is responsible for selecting the data rate that gives the optimum throughput for the specific channel condition. In order to close the link, different data rates require different received power levels. The receiver minimum input level sensitivity of OFDM PHY is clearly indicated in [8]. Data rate fallback algorithm tunes the communication rate relative to experienced signal-to-noise power ratio (SNR). When SNR is high, STA can afford to use higher order modulation schemes enabling high transmission rates. On the other hand, when the SNR is low, the need for a robust modulation scheme and powerful error correcting codes results in a low data transmission rate.

An illustration of a data rate map relative to receiver-transmitter separation is given in Fig.4.2. Radios for 5 GHz wireless LAN applications could transmit at a power level of 200 mW (23 dBm) or less [8]. The attainable data rate regions of adaptive rate fall back algorithm is estimated with pathloss model presented in Appendix-A. The figure shows the received signal strength regions of an AP transmitting with 200 mW power. As it can be seen, a STA within a radius of 30 m to AP can communicate with 54 Mbps, whereas a STA with the distance of 110 m to AP must utilize autorate fallback to shift the speed down to 6 Mbps in order to close the link.

An example CFP frame exchange with multi-rate transmission enhancement is illustrated in Fig. 4.3. Data rates of four STAs illustrated in CFP data exchange of Fig. 4.3

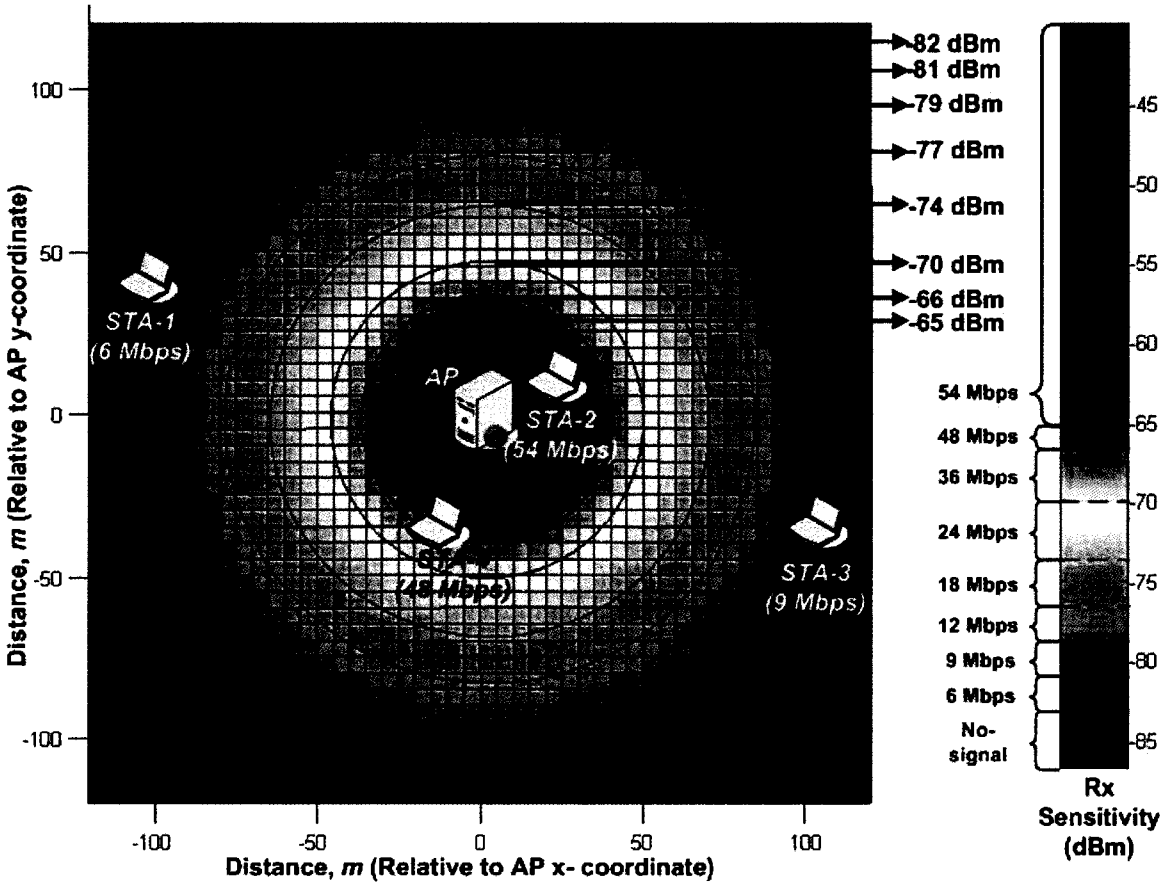

Figure 4.2: IEEE 802.11a coverage and data rate illustration. The deterministic ITU propagation model for 5 GHz U-NII band detailed in Appendix-A is utilized for data rate map. All the STAs and AP are assumed to transmit at max power level possible (200 mW).

are assumed to be the same as STAs' illustrated in Fig. 4.2 for convenience. Taking into account the fact that AIDs are randomly assigned and are in the range of 1-2007, assume that AIDs of four STAs as follows: $AID^{STA1} = 15$, $AID^{STA2} = 59$, $AID^{STA3} = 548$ and finally $AID^{STA4} = 2001$. According to current IEEE 802.11 standards, PC is supposed to order the STAs in the polling list by ascending AID values. Therefore, the polling list of the considered STAs would be like: *"STA1 → STA2 → STA3 → STA4 ⇒ STA1" ... .* The double arrow in the last transition illustrates the round-robin characteristic of the polling order, which polls the first STA after going through all the STAs in the polling list considering all STAs have pending data in their buffers. The data rates of the both AP and STAs are color-coded in Fig. 4.3. The uplink data rates of the STAs are 6 Mbps, 54 Mbps, 9 Mbps and 48 Mbps respectively; whereas the downlink data rates are forced to be 6 Mbps, 6 Mbps, 9 Mbps and 9 Mbps for sequential polling interrupts to accommodate the succeeding transmission rates. The proposed polling order algorithm suggests reconfiguring the polling order relative to received signal strength. Therefore, the suggested polling order would be: *"STA2 → STA4 → STA3 → STA1 ⇒ STA2 ..."* which has the same uplink transmission rates but improved downlink rates; namely 54 Mbps, 48 Mbps, 9 Mbps and 6 Mbps for sequential polling interrupts.

4.4 Throughput Calculation Method

For throughput calculation, we need precise information of IEEE 802.11a MAC and OFDM PHY frame formats and overhead. In Appendix-B MAC and PHY OFDM overhead for IEEE 802.11a systems as well as vertical data flow are explained in detail. A data frame has 34 bytes overhead including the MAC header and FCS field. PHY overhead of OFDM includes fixed PHY preamble delay (T_{pre}) of $16\mu s$, PHY header of $4\mu s$ and variable delay of service (16 bits), tail (6 bits) and pad bits (variable length). The symbol time (T_{sym}) and SIFS time (T_{sifs}) of OFDM PHY is $4\mu s$ and $16\mu s$ respectively with propagation delay $\tau_{ch} << 1\mu s$. All the relevant MAC and OFDM PHY parameters are also presented in Table 3.1, but replicated in this chapter for convenience. For IEEE 802.11a/g systems, the transmission duration of a data frame can be calculated by (4.1) [35, 44].

$$T_{data} = T_{pre} + T_{sig} + T_{sym}\left\lceil \frac{sevr + tb + 8(mac_{(h+payload)} + fcs)}{N_{dbps}} \right\rceil \tag{4.1}$$

Throughput of a basic service set can be found by calculating the ratio of the number of correctly received data bits (excluding control bits) per second. Following assumptions

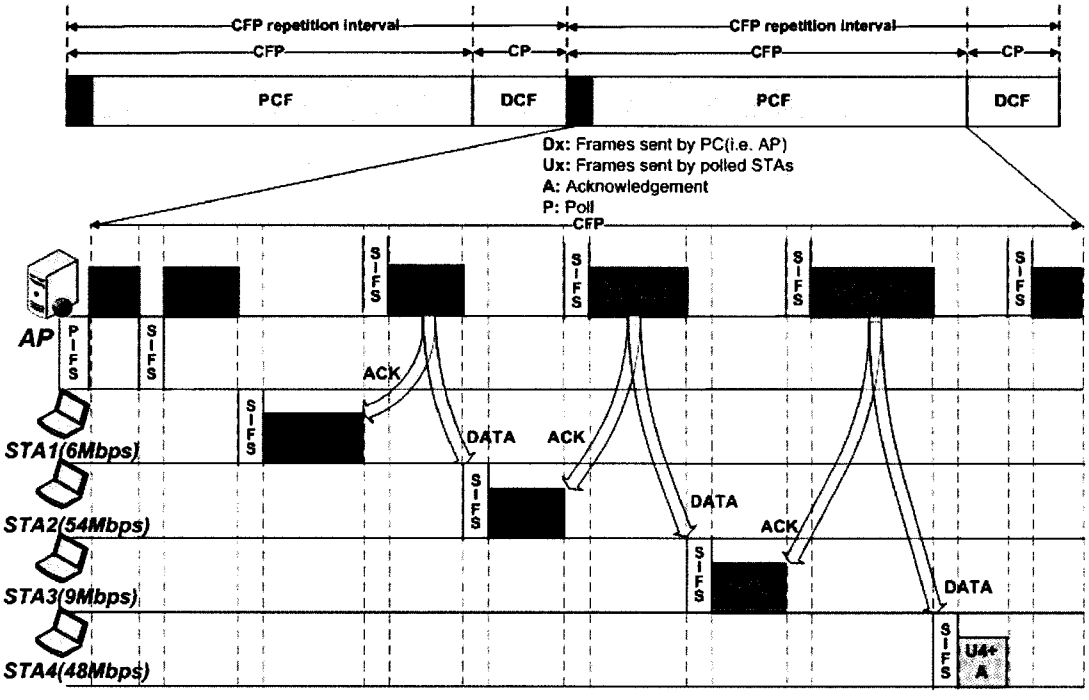

Figure 4.3: CFP data exchange algorithm with multi-rate adaptation. As it can be seen on the downlink, the piggypacked packets target two STAs at a time to increase transmission efficiency. The downlink frames are required to be transmitted with the lower data rate of the two to guarantee packet delivery to both STAs.

are made for throughput estimations: *i)* ideal channel with no communication errors. *ii)* During the CFP downlink all the POLL and ACK frames are piggy-packed on to data frame to reduce excessive overhead. *iii)* All the STAs are in the coverage area of AP. *iv)* The length of the CFP is assumed as the maximum value attainable (*i.e.* CFPMaxDuration). *v)* All the user traffic is greedy. *vi)* All the frame lengths are the same. For each CFP repetition interval, the throughput of the BSS can be found by calculating ratio of total received (uplink and downlink) bits (excluding the PHY and MAC overhead) to the transmission duration of CFPMaxDuration. BSS throughput calculation flow chart is given in Fig. 4.4. The system throughput is expected to be a function of the connection speed of each STA, polling order of the STAs in the polling list and payload size of the frame.

4.5 Simulation Results

In this section, the effect of polling order creation method on IEEE 802.11 PCF throughput performance is evaluated and compared to DCF performance. DCF throughput data points obtained from NS-2 simulations [33]. In the simulations both uplink (STA to AP) and downlink (AP to STA) traffic is simulated. The ratio of the overall traffic is modified and its effect on the throughput gain is illustrated. As mentioned in section 4.3, the proposed indexing algorithm improves the performance on downlink communication. In order to see the effect on the downlink percentage on the gained performance, the throughput performance of proposed received power ordering (RPO) algorithm as well as standard (STD) IEEE 802.11 ordering algorithm are illustrated relative to frame payload size and the downlink communication percentage. We expect the performance margin between two indexing algorithms to be maximum when the communication is dominated by downlink (100% downlink). Figure 4.5 illustrates average PCF throughput performance of 10 STAs relative to different payload sizes and downlink communication ratios with mentioned indexing algorithms. Communication rates of 10 STAs are selected randomly from values described in Table 2.1 of Chapter 2 and the results are averaged over 200 simulations for each data point.

From Fig. 4.5 it can be seen that, for 1000 byte payload size, the proposed indexing algorithm improves the throughput performance almost by 20% for downlink dominated communications which is normally seen in practice. The gain margin decreases as uplink communication eclipses the downlink data transfer. Despite the decreased gain margin, the actual throughput performance of the network increases as uplink communication

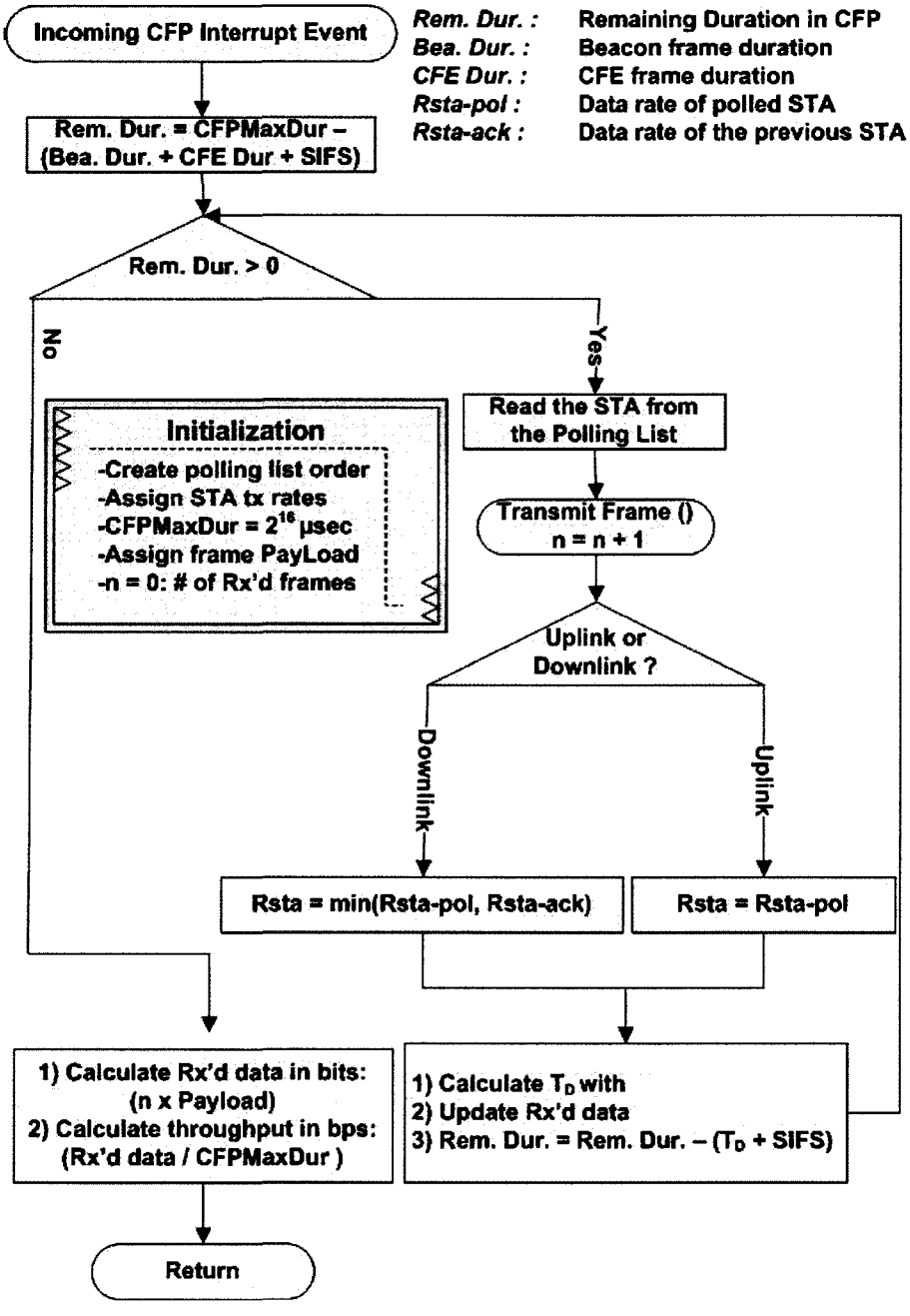

Figure 4.4: Throughput calculation flow chart for a single contention free period.

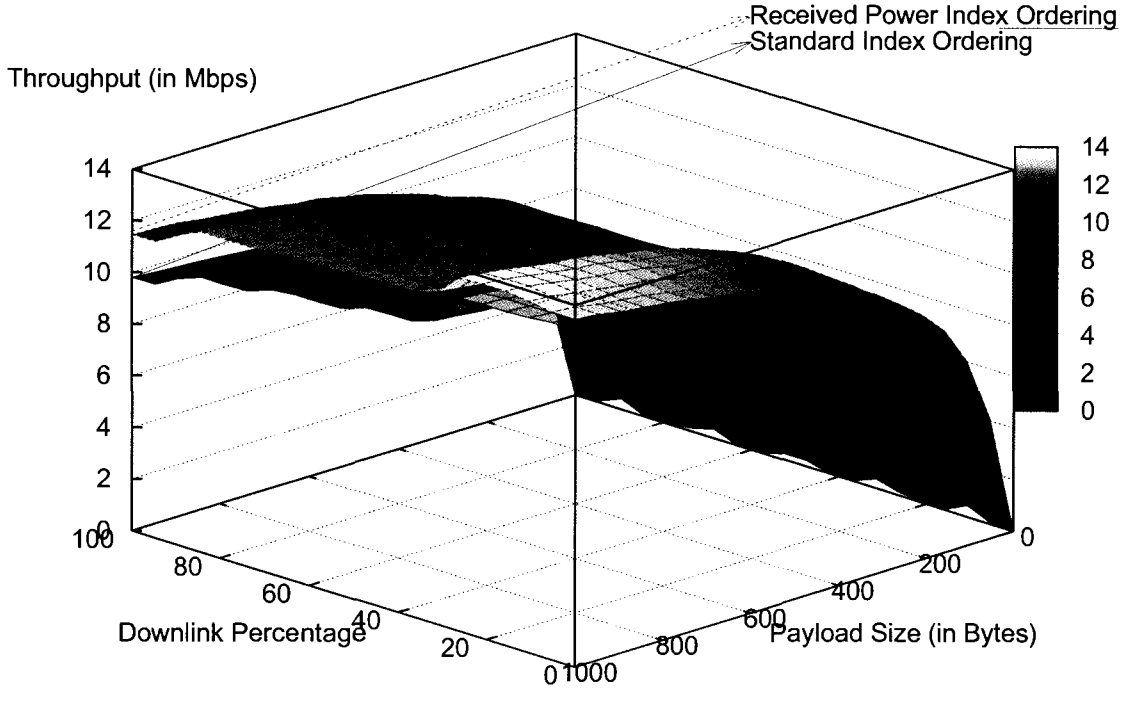

Figure 4.5: Throughput of different data rates of IEEE 802.11a point coordination function. As the downlink communication dominates the overall packet transfer the delta gain provided by the proposed polling indexing algorithm increases. The network throughput is increasing naturally as the data frame size increases.

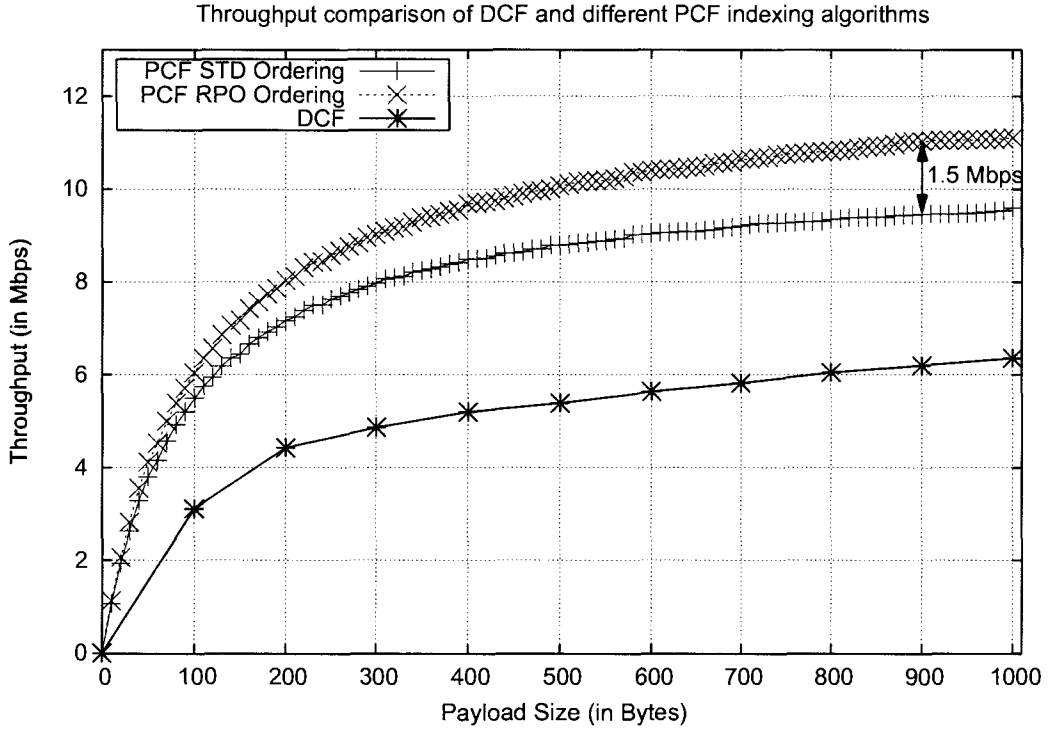

Figure 4.6: IEEE 802.11a PCF performance with different polling order schemes along with comparison to DCF contention resolution technique. 10 STAs are randomly assigned communication rate. The communication rate of a STA is estimated by taking into account STA-AP separation and simulated propagation model (Appendix-A).

overrules the link because contrary to downlink that has to choose the minimum communication rate to deliver ACK and DATA information in a single frame, on the uplink communication STAs are not bounded with that constraint and the probability of a frame being transmitted with a higher communication rate increases.

In order to show the performance improvement of the proposed indexing algorithm with PCF to de facto contention resolution technique DCF, similar assumptions and channel conditions are simulated with NS-2 simulator. 10 STAs are generated in the communication environment with randomly chosen communication rate. Mandatory data rates are chosen relative to the communication rate as specified in the standards [8]. Exponential traffic is simulated for each user. Generated traffic is kept bigger than the link capacity of each and every user to simulate greedy user environment. NS-2 snapshot simulations are repeated 200 times to obtain average throughput value

for each data point. Fig. 4.6 illustrates the throughput performance of PCF indexing algorithms as well as DCF contention resolution technique. The performance of downlink communication is presented in the figure. The performance improvement of the proposed algorithm can be observed by selecting a fixed payload size. For instance, at the payload size of 900 bytes, the proposed algorithm gives a throughput performance increase of almost 1.5 Mbps relative to standard indexing algorithm. This performance gap reaches to 5 Mbps relative to DCF contention algorithm almost doubling the performance. The fact that PCF scheduled access has no hidden-node problem is one of the reasons for the performance gap comparison to DCF contention resolution mechanism.

4.6 Conclusions

PCF is an important access mechanism of IEEE 802.11, which is resurrected as HCCA in the recent standards. Scheduled access in WLANs promises certain QoS and high throughput as well as immunity for packet collision and hidden node issues, which is especially critical for popular real time systems. Current IEEE 802.11 applications implement adaptive rate fallback algorithm in order to increase transmission efficiency in changing wireless channel environments. However, standard scheduled access algorithms do not take into account the multi-rate capability of the mobile stations in populating contention free polling list. It has been illustrated that by carefully designing the polling list ordering method of scheduled access, more than 1.5 Mbps additional throughput can be obtained with moderate payload size of 1000 bytes. It has been shown that for typical communication links requiring high download ratios, the proposed indexing algorithm significantly increases the throughput performance without any need of major change in the MAC or PHY layer of IEEE 802.11 standard.

After estimating the DCF performance and challenges it is facing in Chapter 3 and proving that a better fairness and throughput performance can be obtained with modified PCF in a single AP environment, we want to move to a more challenging communication environment, namely extended service sets. In the next Chapter, the DCF throughput and fairness performance with standard association algorithm are evaluated in extended service sets where multiple APs are operational in the communication environments. After pointing the performance issues with the standard association algorithm, a novel association algorithm is proposed to improve the performance.

Chapter 5

DCF Performance in Extended Service Sets

In literature most of the studies evaluating DCF performance in an extended service set have common assumption of uniformly distributed users in the communication environment. In practice however, STAs are distributed unevenly among APs, causing congested hot-spots and under-utilized APs [45, 46]. Considering a typical network with multiple APs which has some nodes carrying excessive loads degrades not only the considered AP's performance, but also the overall network operation [47]. The system performance can be improved by associating STAs efficiently throughout the network, in a sense sharing the network resources fairly among APs and thus relieving congestion. The association algorithm currently employed in IEEE 802.11 systems, that is specifically designed for residential and small office environments, takes into account signal strength as the only parameter and associates STAs to the closest (in signal strength sense) AP, ignoring its load. Novel user association algorithms are required to solve the problems commonly seen in corporate network environments spanning multiple APs. Such algorithms would improve DCF performance by avoiding congestion and reducing the time wasted during packet collisions.

In this chapter, a distributed (*i.e.* running in individual STAs rather than centralized) and online (*i.e.* adapting to changing network and radio conditions) association algorithm is proposed that demonstrates improved average throughput performance, a balanced load distribution as well as fairness across the network compared to the conventional algorithm. It has also been demonstrated that the developed association algorithm has superior performance in various network conditions *i.e.* different hot-spot configurations,

user loads, frequency reuse clusters.

5.1 Introduction

In IEEE 802.11 WLANs, an AP has a serving area defined by its transmission power and channel conditions. An AP can accept an association request from any STA in its range. In a typical multi-AP deployment (also called extended service set [ESS]) a WLAN is made up of multiple APs and usually APs have overlapping coverage areas. Therefore, a STA in an overlapped area can associate with any AP it receives with a sufficient signal strength. However, according to IEEE 802.11 standard, STAs must associate with the AP that has the highest received signal strength indicator (RSSI) at the receiver [6]. In practice, the network load is often unevenly distributed among APs, *e.g.* flight gates at airports, classrooms in schools, seminar rooms in conference centres, creating *hot-spots* [7]. Because of the time multiplexing nature of the IEEE 802.11 coordination functions, the serving capability of an AP decreases as more and more STAs associate with it. In the current WLAN implementation, STAs are not informed about AP loadings. Therefore in a network configuration, there might be some APs having excessive loads, whereas some having just a few lightly loaded STAs associated with.

From STA point of view, the current association method lets STAs, that are in the communication range of multiple APs, associate themselves with an AP that *promises* the maximum transmission rate. However, being able to communicate with the highest transmission rate (*i.e.* strongest signal) does not necessarily mean that this association would provide the best throughput and delay performance. Association of a STA to a less loaded AP with weaker signal strength might supply a higher *effective data rate* and better overall network performance, especially in networks with hot-spots. *Effective data rate* term indicates the actual data rate share of individual users communicating with a specific AP by taking into account the time division multiple access nature of IEEE 802.11 MAC layer (*i.e.* as more users associate with a specific AP, the less effective data rate they will have).

A novel association algorithm that alleviates this abnormality of IEEE 802.11 MAC is needed. WLANs spanning multiple APs are the most vulnerable to this inefficient way of operation. The proposed algorithm should be able to balance the network load, have a distributed nature and adapt to the changing load fluctuations in the network. By *the load of AP*, the congestion level or the serving capability of an AP is denoted. Association control is the key to adjust the individual AP loadings and network wide

resource sharing as it can be achieved by directing new STAs to less loaded APs.

5.2 Resource Sharing by Association Control

Currently a very simple association algorithm which takes into account only RSSI values is implemented in IEEE 802.11 WLANs. An efficient association algorithm should be able to infer the business level of the APs in the network and adjust to the changing system conditions in the communication environment. In the literature this type of algorithms are called *on-line* association algorithms [48].

Network resource sharing through association control has been considered by both academic community and industry. Advanced association algorithms to balance the network load are already implemented by various WLAN equipment vendors [49], such as least loaded association algorithm which takes into account only the AP loadings and associates the new users to the AP that has the least load. In this chapter, it will be shown that implementation of such an algorithm will have chronic problems like high average network load and therefore fair but overall reduced throughput. An association algorithm which estimates the possible signal to noise plus interference power ratio (SNIR) for each connection is proposed by [50]. The algorithm estimates the available signal to noise and interference power ratio before association and chooses the best offer in a bi-directional link. Although this algorithm is one step ahead of the standard association algorithm in terms of taking interference into account rather than just RSSI at the receiver side, adaptive transmission rate ability of wireless equipment is ignored and AP load or congestion relief are not considered. Another predictive association algorithm is described in [51]. In that study, each STA calculates its own RSSI value and compares it to the average RSSI value of the STAs associated with the considered AP and runs the association algorithm relative to the condition of if STA's own RSSI is less or more than the AP average RSSI. In the association technique of [51], adaptation of the algorithm to the changing traffic condition is not taken into account. An AP based association algorithm is described in [52]. In this scheme, access controller (a central control unit that rules all the *thin* APs* in the communication environment) decides on two thresholds: *i*) overload threshold, *ii*) underload threshold. APs that have the load values higher than the overload threshold force their excessive STAs to associate with the neighboring APs. Another association control algorithm [53] illustrates network-wide fair data rate

*APs whose several core functionalities are moved to access controller from where radio resource control and management can be done centrally in an ESS

allocation among users independent of their locations, while maximizing the fair share of each user. Their fairness concept is called *max-min fairness*, which is a data rate allocation if there is no way to give more data rate to any user without decreasing the allocation of a user with less or equal data rate. In [54], authors define a cost function which takes the average uplink throughput vector (*e.g.* AP throughputs are individual elements of the vector) as a variable and outputs a scalar value and they try to maximize this scalar value by choosing different user associations. The last two algorithms mentioned require to run a central association algorithm to minimize the cost function and allocate data rate fairly which is computationally complex and not suitable for large networks.

5.3 Load Definition

A proper definition of load in WLANs is required for problem formulation. Intuitively, the load of an AP should reflect its inability to serve properly to all its associated users. Assuming that each STA has the same traffic characteristic, a STA that has the highest connection rate among the associated STAs would be the least burden on the AP. Hence a load imposed on an AP by a STA should be inversely proportional to the connection rate that considered STA attains.

In order to formulate the load definition, a description of the considered network setup should be given. We assume a WLAN that comprises a large number of APs and STAs. We use A to denote the set of APs and let m denote their number, *i.e.* $m = |A|$. Each AP has a transmission range limited by its transmission power as well as propagation condition and can only serve STAs in this range. We use S to denote the set of STAs that reside in the network and let $n = |S|$ denote the total number of STAs in the network. For each STA $s \in S$ and each AP $a \in A$, we use $\mathfrak{R}_{a,s}$ to denote data rate they communicate with and $\mathfrak{E}_{a,s}$ refers to the average effective data rate they experience as a result of resource sharing with other STAs in the environment. A distinction between communication ($\mathfrak{R}_{a,s}$) and effective ($\mathfrak{E}_{a,s}$) data rate can easily be made by a simple example. Let's consider a communication environment that comprises of a STA and an AP. Consider that STA communicating with AP with data rate of 54 Mbps. Assuming that STA always has a pending data frame to transmit (*i.e.* greedy user assumption), then its effective and communication data rate would be the same, which is 54 Mbps. However, association of another STA with the same propagation and traffic characteristics to the considered AP would have a communication rate of 54 Mbps as

well, but their effective data rate would be 27 Mbps due to time sharing nature of IEEE 802.11 MAC. If the second STA's communication rate was 36 Mbps, then the effective communication rate would be 21.6 Mbps.

The consistent load definition indicated in [53] is used in this work. The load $\mathfrak{l}_{a,s}$ induced by STA s on AP a is defined as the time it takes for the AP to provide the STA one unit of traffic; and the total load $\mathfrak{L}_a$ on AP a is the aggregate load of all its associated STAs. In order to generalize the AP load calculation formula to all the STAs in the communication environment, it is required to define an association index that reflects the connection of a STA to AP. It is assumed in this study that if a STA $s \in S$ is associated with AP $a \in A$ then $\mathfrak{x}_{a,s} = 1$ and the STA imposes a certain load on AP a that is inversely proportional to its connection rate, $\mathfrak{R}_{a,s}$. If it is not associated with AP a then $\mathfrak{x}_{a,s} = 0$ and it does not contribute to that AP's load. Therefore, the load of STA s on AP a and the total load of AP a can be defined as follows:

$$\forall s \in S, \forall a \in A : \mathfrak{l}_{a,s} = \frac{\mathfrak{x}_{a,s}}{\mathfrak{R}_{a,s}} \quad \text{and} \quad \mathfrak{L}_a = \sum_{s \in S} \mathfrak{l}_{a,s} \tag{5.1}$$

5.4 Balanced Association Algorithm for Extended Service Sets

In this section, the proposed association algorithm for improved resource sharing and performance in extended service sets is described. In the algorithm, it is assumed that AP performance figures are calculated in each AP with described load metric (5.1) and this information is relayed to STAs in the communication environment (*e.g.* by management frames*). Each STA joining the network associates with the AP that supplies the highest *effective data rate*. After initial association, the STA keeps track of this performance figure during its operation and triggers re-association decision when certain conditions are met. For hot-spot scenarios, contrary to the standard association algorithm (*i.e.* strongest signal first [SSF]), the proposed method prefers a less loaded AP which offers a better effective data rate and relieves possible congestion. A careful examination of (5.1) would reveal that an AP serves to all of its associated users with effective data rate that is inversely proportional to its load. The proposed algorithm is also different than *the least loaded first* (LLF) association algorithm [49]. As the name

*Management frames are dedicated packets exchanged between two interested parties carrying information regarding their behaviours in the network. Association Request, Re-association Request, Association Response, Probe Request could be named as sample management frames.

implies, with LLF algorithm, STAs choose an AP that has the least load value, ignoring the considered STA's own loading effect on the AP. For hot-spot scenarios, this type of association scheme frequently forces STAs to associate with APs located further away offering low data rates just because they have lower loads than closer APs providing better effective data rates. A particular consequence of such an association algorithm is increased average network load, therefore lowered effective data rate. Considering the fact that the proposed association algorithm *predicts* the effective data rate offers of the APs in the vicinity, it is called predictive association algorithm (PAA) in the subsequent sections of this work. The PAA is on-line, meaning that each STA not only checks the best AP (in terms of effective data rate) when it joins to network, but also dynamically reassesses available APs' effective data rate offers. In case of finding a better AP that satisfies the re-association condition, it initiates the re-association process. To alleviate the well known *ping-pong* effect for re-association decision in wireless networks [55], minimum delta effective data rate percentage threshold is defined at STAs, which is denoted as Δ^{min}. If a STA discovers an AP that would supply an effective data rate percentage at least Δ^{min} better than the rate currently it has, then it will initiate a re-association process. A formal description of the proposed association algorithm is given in (5.2) and (5.3) and illustrated in Fig.5.1. A typical STA behaviour complying with proposed association algorithm can be described as follows: When STA $s \in S$ joins the network at time T_0, it associates with an AP that grants itself the best effective data rate ($k \in A$ and $\mathfrak{x}_{k,s} = 1$):

$$
\begin{aligned}
&@\, T_0 : \\
&\overrightarrow{\mathfrak{E}_s} = \{\mathfrak{E}_{1,s}, \mathfrak{E}_{2,s} \ldots \mathfrak{E}_{m,s}\} && m = |A|,\ s \in S \\
&\mathfrak{E}_{k,s} = \underset{\{s|s\in S\}}{max}\{\overrightarrow{\mathfrak{E}_s}\} && k \in A \\
&\mathfrak{x}_{k,s} = 1 && k \in A,\ s \in S \\
&\Delta_{i,s} = \frac{(\mathfrak{E}_{i,s} - \mathfrak{E}_{k,s})\,\text{x}100}{\mathfrak{E}_{k,s}} && \{i,k\} \in A,\ i \neq k,\ s \in S \\
&\overrightarrow{\Delta_s} = \{\Delta_{1,s} \ldots \Delta_{m-1,s}\} && m = |A|,\ s \in S
\end{aligned}
\tag{5.2}
$$

As the propagation condition and the loading of APs change in a dynamic network environment, STA s recalculates the effective data rate offers of the APs in its communication range. If a STA detects an AP l that provides an effective data rate percentage more than Δ^{min} compared to current AP k (at time T_1 of 5.3) then it gives a re-association decision to AP l ($\mathfrak{x}_{k,s} = 0$ and $\mathfrak{x}_{l,s} = 1$) and updates effective data rate vector ($\overrightarrow{\mathfrak{E}'_s}$) as

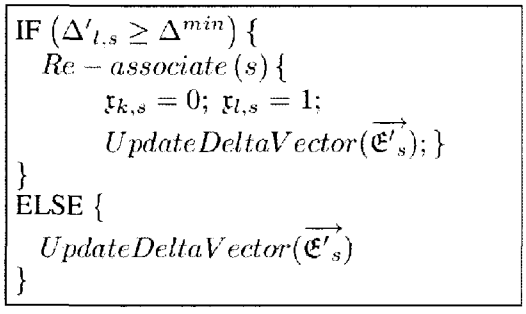

Figure 5.1: The flowchart of predictive association algorithm.

well as delta effective data rate percentage vector ($\overrightarrow{\Delta'_s}$). If the effective data rate percentage is lower than Δ^{min}, then STA s would just update its effective data rate and delta effective data rate percentage parameters without any re-association decision:

$$
\begin{aligned}
&@\,T_1: \\
&\mathfrak{E}'_{l,s} = \max_{\{s|s\in S\}} \{\overrightarrow{\mathfrak{E}'_s}\} && l \in A \\
&\overrightarrow{\mathfrak{E}'_s} = \{\mathfrak{E}'_{1,s} \ldots \mathfrak{E}'_{m,s}\} && m = |A|,\ s \in S \\
&\overrightarrow{\Delta'_s} = \{\Delta'_{1,s} \ldots \Delta'_{m-1,s}\} && m = |A|,\ s \in S \\
&\Delta'_{l,s} = \max_{\{s,l|s\in S \wedge l\in A \wedge l\neq k\}} \{\overrightarrow{\Delta'_s}\}
\end{aligned}
\tag{5.3}
$$

Minimum delta effective data rate percentage value (Δ^{min}) is a network design parameter and it introduces a trade-off between a fair effective data rate allocation among STAs and the number of re-associations. Choosing a small Δ^{min} value would fine tune the fairness among STAs at the cost of increased re-association attempts per unit time.

5.5 Interference Effect

For IEEE 802.11a PHY operating in U-NII (Unlicensed National Information Infrastructure) band, the number of non-overlapping frequencies is 12 [8]. In North America, Federal Communications Commission (FCC) allowed additional spectrum opening that increased the number of non-overlapping frequencies in U-NII band to 23 [56]. Considering the fact that IEEE 802.11b/g technologies are designed for single AP with wide

communication range targeting consumer market, it is expected to see IEEE 802.11a PHY in corporate environments where the network load is high and the networks typically spans multiple APs. A careful frequency planning along with 23 non-overlapping frequencies would suffice a pervasive connectivity and mobility with negligible interference.

However, the performance of the proposed association algorithm with limited frequency availability can still be in question, especially for networks that adopted IEEE 802.11g systems (that has 3 non-interfering operational frequencies in ISM band) rather then less interference prone IEEE 802.11a systems. Therefore, the effect of the interference with 3 frequency reuse cluster should be taken into account for complete performance analysis. Since the long term network performance is considered, an average interference calculation method taking into account the considered user and interferer location, communication rate (*i.e.* channel occupancy), transmit power level, propagation channel (pathloss and shadowing effect) and uplink & downlink communication ratio should be utilized.

A terminal (STA or AP) can cause interference to another terminal if it is using the same frequency channel and associated to a different AP (or it is a different AP) than the considered terminal. A STA causes an interference to other terminal whenever an uplink connection (*i.e.* STA⇒AP) is established and similarly an AP causes an interference to other terminal whenever it serves to its associated users (on the downlink). The main concern is to calculate the average interference on long term basis, mainly influenced by path loss and slow fading. For average interference calculation, the relative time that each individual STA or AP utilizes the channel needs to be found. The relative channel occupation times can be estimated by calculating the individual transmission duration to total AP utilization duration ratio. It is assumed that AP has no idle time and the operational frequency is used by either STAs or AP 100%. A typical interference calculation scenario is illustrated in Example 3.

5.5.1 Example 3:

Consider the communication environment illustrated in Fig. 5.2. In wireless networks, generally downlink connection dominates the overall connection. Assume that the uplink-to-total link ratio is 0.3, which means 30% of the connection durations a STA makes with its associated AP are uplink (*e.g.* request an URL [Uniform Resource Locator] like www.site.uottawa.ca) whereas 70% of the connections are downlink (*e.g.* whole website

contents with pictures and videos). Consider that with each connection a STA sends a frame of 2304 octets. In the illustrated example, STA a-1 with 6 Mbps uplink data rate would keep AP-A busy for the duration of $t^u_{a1} = 2304\,\mathbf{x}\,8(bits)/6x10^6(bps) = 3072\,\mu sec$ for each uplink packet transmission and $t^d_{a1} = 2048\,\mu sec$ for each downlink connection. Uplink and downlink connection rates are assumed to be different due to different interference levels on AP and STA. Therefore on average, for 10 random transmission opportunities, with the assumed uplink-to-total link ratio, STA a-1 would keep AP-A busy for $t^t_{a1} = 7\,\mathbf{x}\,t^d_{a1} + 3\,\mathbf{x}\,t^u_{a1} = 23552\,\mu sec$. Considering the fair transmission opportunity and the same calculation method, STA a-2 and STA a-3 channel occupation times for 10 random transmission opportunities on AP-A can be calculated as $t^t_{a2} = 1792\,\mu sec$ and $t^t_{a3} = 4608\,\mu sec$. The values presented can be normalized considering single transmission opportunity ($\overline{t^t_a}$) and single bit transmission ($|\overline{t^t_a}|$). Normalized AP-A utilization time ($|\overline{t_A}|$) then can be estimated by adding individual STA normalized uplink and downlink transmission durations as follows:

$$\begin{aligned} |\overline{t_A}| &= |\overline{t^t_{a1}}| + |\overline{t^t_{a2}}| + |\overline{t^t_{a3}}| \\ &= \left(|\overline{t^u_{a1}}| + |\overline{t^d_{a1}}|\right) + \left(|\overline{t^u_{a2}}| + |\overline{t^d_{a2}}|\right) + \left(|\overline{t^d_{a3}}| + |\overline{t^u_{a3}}|\right) \\ &= 0.1278 + 0.0458 + 0.1417 = 0.3153\,\mu sec \end{aligned} \tag{5.4}$$

Assume that AP-A and AP-B that are illustrated in Fig. 5.2 are operating in the same operational frequency. Interference effect of AP-A and its associated users on the downlink connection of STA b-1 will be illustrated in this example. Let's denote the interference power of STA $a1$ affecting the downlink connection of STA $b1$ as $I_{a1,b1}$, interference power of AP-A as $I_{A,b1}$, the average interference caused by STA a-1 uplink transmission on STA b-1 downlink connection as $\overline{I}^u_{a1,b1}$, the average interference observed on STA b-1 downlink connection due to STA a-1 downlink connection as $\overline{I}^d_{a1,b1}$, and the total interference affecting STA b-1 downlink connection due to STA a-1 data activity (transmission and reception) as $\overline{I}^t_{a1,b1}$. The total average interference power affecting the

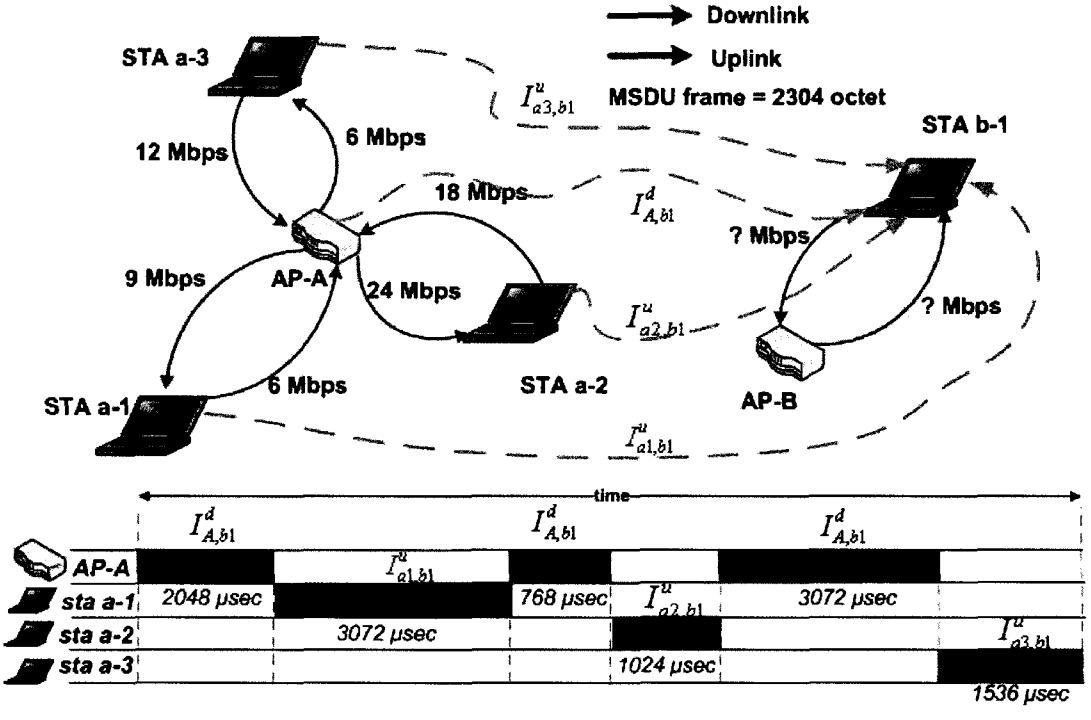

Figure 5.2: AP load calculation example with interference. AP-A and AP-B use the same operational frequency. STA b-1 is a new user to be associated with AP-B. If we consider STA b-1's downlink connection, AP-A, STA a-1, STA a-2 and STA a-3 will interfere with the STA b-1 connection and affect downlink data rate.

downlink connection of STA $b1$, $\overline{I}^{d}_{b1}$, can be found as follows:

$$\begin{aligned}
\overline{I}^{d}_{b1} &= \overline{I}^{t}_{a1,b1} + \overline{I}^{t}_{a2,b1} + \overline{I}^{t}_{a3,b1} \\
&= \left(\frac{|\overline{t^{u}_{a1}}|}{|\overline{t_A}|} I_{a1,b1} + \frac{|\overline{t^{d}_{a1}}|}{|\overline{t_A}|} I_{A,b1} \right) \cdots \\
&+ \left(\frac{|\overline{t^{u}_{a2}}|}{|\overline{t_A}|} I_{a2,b1} + \frac{|\overline{t^{d}_{a2}}|}{|\overline{t_A}|} I_{A,b1} \right) \cdots \\
&+ \left(\frac{|\overline{t^{u}_{a3}}|}{|\overline{t_A}|} I_{a3,b1} + \frac{|\overline{t^{d}_{a3}}|}{|\overline{t_A}|} I_{A,b1} \right) \\
&= \overline{I}^{u}_{a1,b1} + \overline{I}^{u}_{a2,b1} + \overline{I}^{u}_{a3,b1} + \underbrace{\overline{I}^{d}_{a1,b1} + \cdots + \overline{I}^{d}_{a3,b1}} \\
&= \overline{I}^{u}_{a1,b1} + \overline{I}^{u}_{a2,b1} + \overline{I}^{u}_{a3,b1} + \qquad \overline{I}^{d}_{A,b1}
\end{aligned} \tag{5.5}$$

On each and every downlink connection, AP-A is the interferer, which is illustrated on the sixth line of (5.5). After calculating the average interference on STA b-1, the communication rate can be found by estimating the AP-B received signal strength to total average interference and noise power ratio (SINR). The analysis can easily be extended to STA b-1 uplink connection by considering AP location as the reference point for interference calculation.

5.6 Performance Evaluation

In this section, the details of the WLAN performance evaluation process and the performance improvement of the proposed association algorithm compared to standard WLAN algorithms are presented. Simulation results are compared primarily in terms of throughput performance. Besides network and individual STA throughputs, a network fairness index is also calculated and compared. To quantify the load balancing ability of the predictive association algorithm, *the balance index* (also called The Jain's index) that is previously defined in Chapter 3 is used as a metric. Consider $\mathfrak{L}_i$ as the load of AP i in a multi-AP ($m = |A|$) communication environment, then the balance index $\mathfrak{B}$ can be defined as:

$$\mathfrak{B} = \frac{\left(\sum_{i=0}^{m} \mathfrak{L}_i\right)^2}{m \sum_{i=0}^{m} \mathfrak{L}_i^2} \tag{5.6}$$

The balance index has the property that it is equal to 1 when all APs have the same load and it gets closer to $1/m$ when the AP loads are distinctly unbalanced.

5.6.1 System Model

The simulation results are presented for multi-AP IEEE 802.11a as well as IEEE 802.11g networks to evaluate the interference effect. An exhibition hall propagation environment is used for analysis. The size of the exhibition hall is $240\,m$ x $240\,m$. Sixteen APs are regularly distributed on a grid distance of $60\,m$. The number of STAs in the network and STA locations are changed to represent different communication environments. In simulations, deciding on the modulation and coding scheme of a STA highly depends on the channel propagation model being used. ITU recommended propagation model for indoor systems at 5 GHz band given by [15] is used for path-loss calculation. Slow fading has also been considered and simulated in order to have more accurate propagation model that takes into account the environmental characteristic (indoor, outdoor) as well as the material characteristic (hard partition, soft partition) [57]. Each user is assumed to be undergoing slow fading with power levels determined with a path loss exponent and randomly distributed log-normal shadowing with a variance of $8\,dB$, which is considered to be a typical value for indoor environmet at 5 GHz frequency band [58]. This assumption is needed to determine the transmission rates available. However once the power level is determined, the channel is assumed to be perfect (*i.e.* errorless).

In the simulations AP and STA transmission power levels are assumed to be constant $200\,mW$ $(23\,dBm)$. Hot-spot cells are simulated by concentrating certain percentage of the STAs in circular areas around selected APs and considering the rest of the STAs as uniformly distributed (UD). APs are assumed to be frequency planned. The frequency planning implies 3-cell or 4-cell frequency re-use cluster for IEEE 802.11g systems and interference free environment for IEEE 802.11a systems. The communication rate of each STA varies between 6-54 Mbps and is estimated by considering the $SNIR$ level experienced at the receiver. In NS2 simulations IEEE MAC parameters (short retry limit, CWMin, CWMax, SIFS, slot duration *etc.*) as well as PHY parameters (carrier sense threshold, transmitter power, operational frequency, receiver sensitivity, PHY preamble *etc.*) are configured as defined in IEEE 802.11a specifications and illustrated in Table 3.1.

5.6.2 Numerical Results

Fig. 5.3 compares the resource sharing capability of the proposed association algorithm with standard algorithm. The figure itself is a snap-shot of a simulation scenario and illustrates user association decisions by drawing a line between STA and its serving AP.

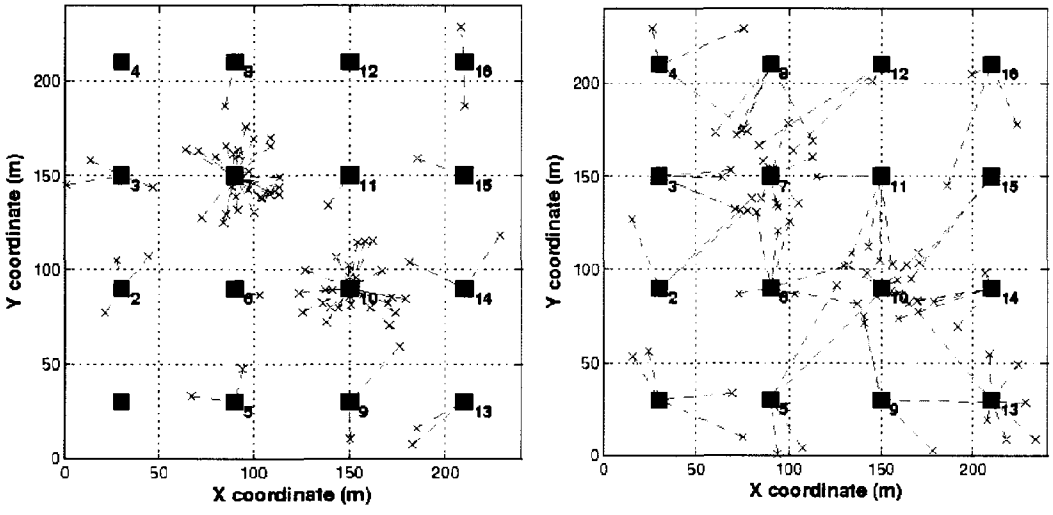

(a) Association with SSF.

(b) Association with PAA.

Figure 5.3: Illustration of different association techniques in a communication environment of 75 STAs and 16 APs. 50% of the users are located in two hot-spot cells (AP-7 and AP-10) where the other half of the users are uniformly distributed in the network. As it can be seen proposed predictive association algorithm (PAA) partially relieves the load on the hot-spots by assigning some of the hot-spot users to the neighboring APs. The environment is assumed to be interference free.

Similar STA locations and user distributions are used in the figures and the only difference is the employed association algorithms. Fig. 5.3-a illustrates the SSF algorithm, where most of the users selected AP-7 and AP-10 because of their close proximity. However, this scheme overwhelms the hot-spot APs and would result in poor average throughput, delay and load balance in the network. Fig. 5.3-b shows the load balancing ability of the proposed algorithm. The congestion in hot-spot APs are partially relieved by associating STAs to neighboring APs. The data rate improvement map of the proposed association algorithm comparison to the standard association algorithm is illustrated in Fig. 5.4. In the figure, there are 50 STAs in the communication environment. First 49 of them are utilizing the conventional association algorithm (SSF) to pick their serving AP. We were curious what data rate improvement would the last STA (50^{th} STA) get by utilizing the proposed association algorithm (PAA) instead of SSF (*i.e.* $(DataRate)^{PAA}$ - $(DataRate)^{SSF}$). To estimate per STA connection rate, 5 GHz U-NII frequency band is considered with ITU propagation model detailed in Appendix-A. All the possible locations in the network are considered for the last STA and as it can be seen from the figure, the performance improvement is mainly taking place in hot-spot areas, which proves the congestion relief ability of the proposed algorithm.

Finally the association map of the new-comer STA (50^{th} STA) to a network is illustrated in Fig. 5.5. Basically, the figure compares and illustrates how a STA joining a network with certain setup would behave in terms of association decision. The figure demonstrates the sharp contrast between proposed and standard association algorithms. Conventional association algorithm has a symmetric tile pattern, because of the distance based propagation assumption. However, if we look at the proposed algorithm, the rst thing noticed is the expansion of the lightly loaded AP coverage area and inversely, shrinkage of the loaded AP coverage area. The proposed algorithm tries to balance the network load between the neighbouring APs and improve spectral efficiency by increasing the association areas of the lightly loaded APs. In Fig. 5.5, the same simulation assumptions as Fig.5.4 are made (*i.e.* ITU propagation model, 50 STAs and 16 APs in the network, IEEE 802.11a PHY)

5.6.2.1 Impact of Interference

In IEEE 802.11a systems the interference can be negligible by judicious selection of 12 [8] (23 in North America [13]) operational frequencies. To see the effect of interference on the performance of the proposed association algorithm with IEEE 802.11g systems, which is more popular in consumer market, a set of simulations are performed. Simulation

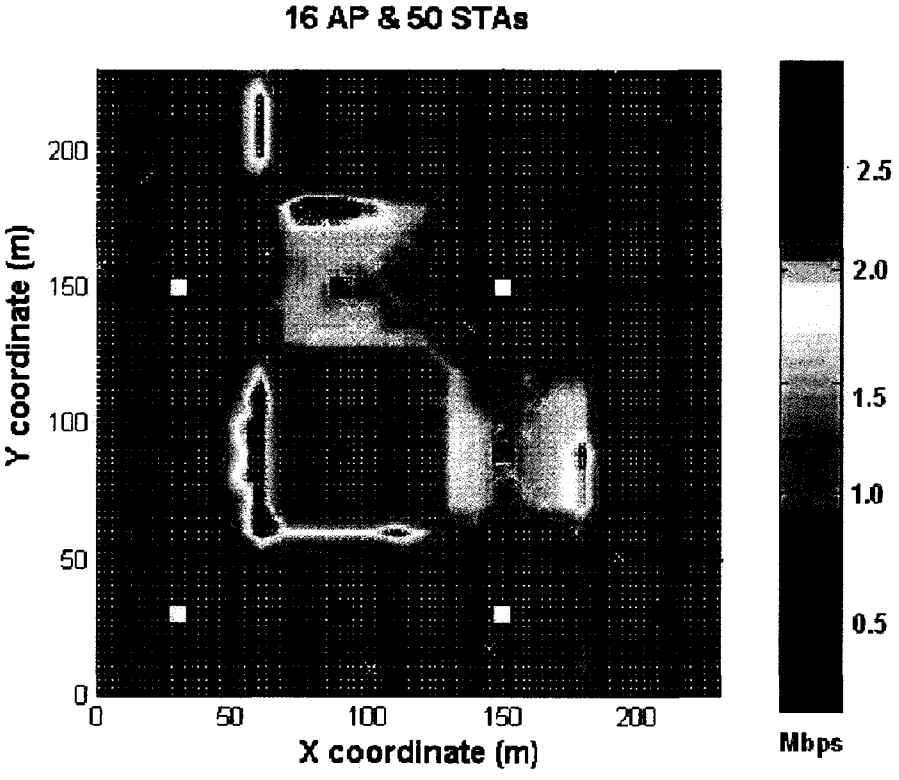

Figure 5.4: Data rate improvement map of proposed predictive association algorithm (PAA) comparison to conventional association algorithm (SSF). The figure illustrates the possible data rate improvement of the 50^{th} STA introduced in the network who chooses PAA instead of SSF. In the communication environment 4-cell frequency re-use cluster is assumed.

results illustrating the effect of interference are presented in Fig. 5.6. The Fig. 5.6 compares the median throughput performance of 50 STAs utilizing different association algorithms in separate operational bands (*i.e.* IEEE 802.11g systems in ISM band and IEEE 802.11a systems in UNII band) and user distributions. For IEEE 802.11a system, the throughput performances of both association algorithms improve as more and more users are uniformly distributed in the communication environment. For IEEE 802.11g systems, the algorithm performance behaviours are similar, but consistently lower than IEEE 802.11a systems as expected. It should be noticed that for IEEE 802.11g systems there are two reasons for low throughput performance: *i)* Congestion in hot-spots and

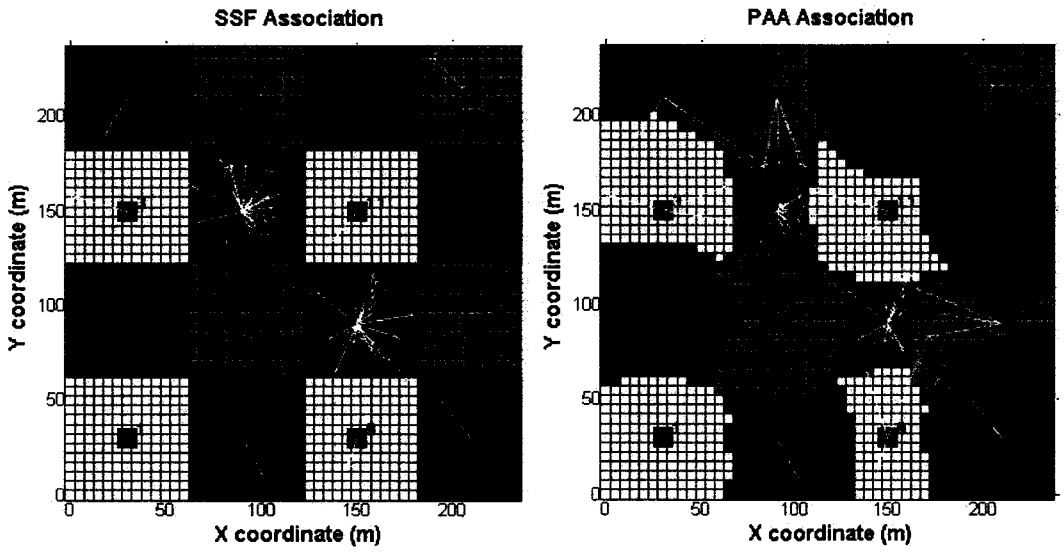

Figure 5.5: Association map of the new-comer (50^{th} STA) to an already established network. The two figures illustrates the user's spacial association preference relative to different association algorithms. In the communication environment 4-cell frequency re-use cluster is assumed.

ii) interference. Intuitively, for IEEE 802.11g systems, a similar performance increase behaviour due to increased uniform user distribution is expected. However, the more uniformly users are distributed, the more interference they would cause to each other, reducing the communication rate. Due to increased interference, we can only see a marginal performance improvement by increasing uniformly distributed users. If we focus on 10% uniformly distributed users scenario, PAA performance drops to 2.011 Mbps due to interference in IEEE 802.11g system compared to 8.844 Mbps in 802.11a system (77.3% performance drop), whereas the SSF algorithm gives 1.196 Mbps in IEEE 802.11g systems which drops from 2.32 Mbps (48% performance drop). Despite the interference, the performance of the standard association algorithm is improved 38% (from 1.1965 Mbps to 1.65173 Mbps) when the uniform distribution percentage is increased from 10% to 50%. However, the performance increase due to uniform distribution increase is barely noticeable in proposed algorithm due to always high interference nature of the algorithm (3.9% [from 2.011 Mbps to 2.0896 Mbps]). Even with the sharp performance drop due to interference (comparison to IEEE 802.11a systems), the proposed algorithm still presents a better median throughput performance compared to standard association algorithm.

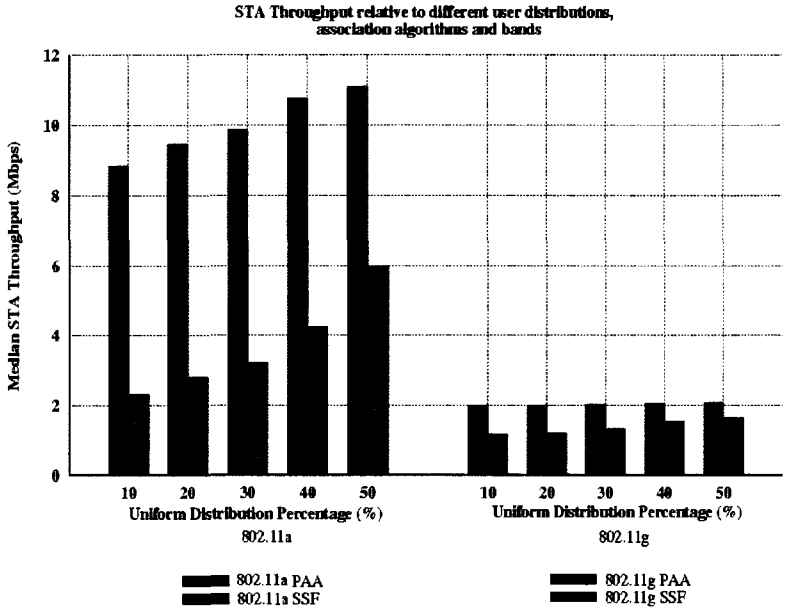

Figure 5.6: Performance of association algorithms on different technologies. For 802.11g systems 3-cell frequency reuse cluster is used in 16 AP communication environment.

5.6.2.2 Impact of Physical Layer

In this section the impact of physical layer characteristics on the AP loads is evaluated and different association algorithms are compared. The size of the considered environment is $500\,m$ x $400\,m$. Twenty APs are regularly distributed on a grid distance of $100\,m$. The number of STAs in the network changed from 100 to 250 to simulate loaded system conditions. In the simulations, the effect of IEEE 802.11g and IEEE 802.11b PHY data rates are considered. Users are assumed to be in hot-spot regions within a certain radius (120 m). AP load performance of proposed predictive association algorithm (PAA) is compared to least loaded first (LLF) association algorithm as well as default strongest signal first (SSF) association. In the LLF algorithm, the newly introduced STA in the communication environment prefers the AP that has the least load at the time.

Fig. 5.7 illustrates the performance of different association algorithms with OFDM PHY with high data rates. Users pick their data rates according to experienced SIR ratio and corresponding data rates. The attainable data rates and channel model used are given in Appendix-A. In Fig. 5.7, the most basic observation is the increase of the average AP load with increasing number of users. APs 10 and 11 experience more loading

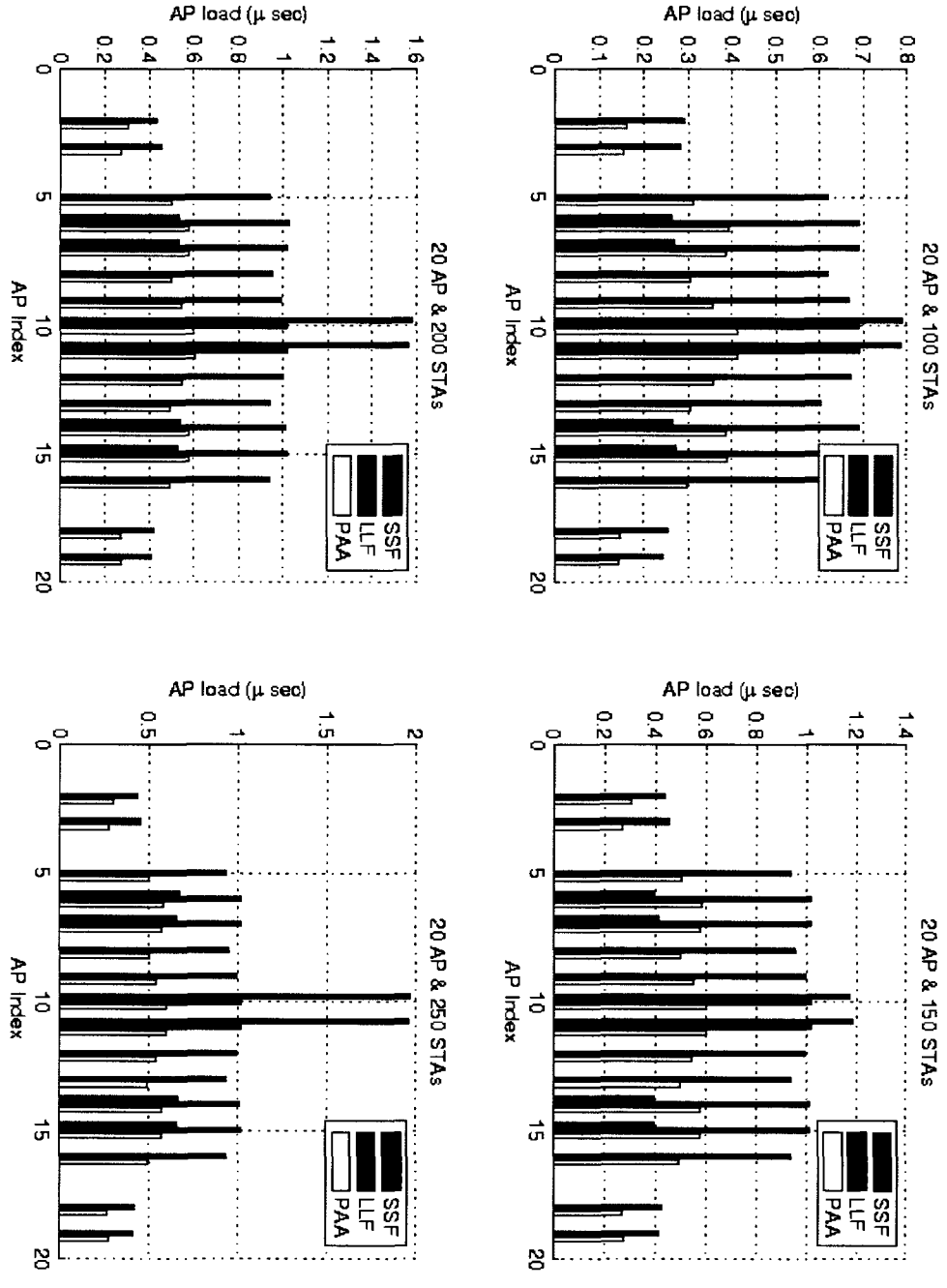

Figure 5.7: AP load comparisons with different user populations and association algorithms. Users are uniformly distributed in two hot-spot areas. OFDM PHY and attainable data rates of 6,9,12,24,36,48,54 Mbps (depending on STA-AP separation) are considered in the figure. APs 10 and 11 experience more loading due to close by hot-spot region.

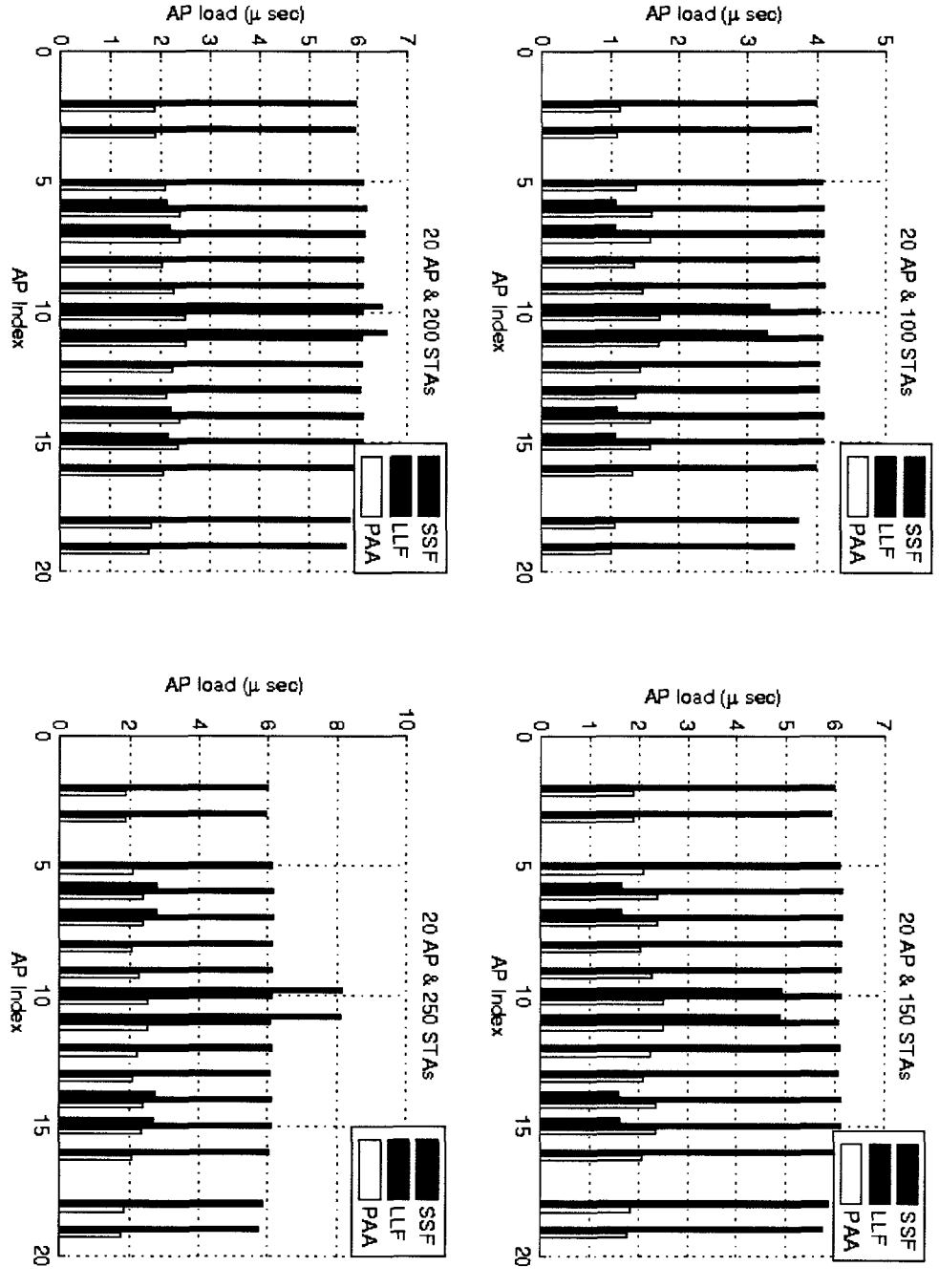

Figure 5.8: AP load comparisons with different user populations and association algorithms. Users are uniformly distributed in two hot-spot areas. IEEE 802.11b PHY and and attainable data rates of 1,2,5.5,11 Mbps (depending on STA-AP distance) are considered in the figure. APs 10 and 11 experience more loading due to close by hot-spot region.

due to close by hot-spot region. In all the figures the proposed PAA algorithm provides a balanced load across the APs. It should be noted that LLF algorithm succeeds to balance the loads among APs, however the average load per AP could be really high. In Fig. 5.8, this abnormality of LLF is more obvious, giving even higher average AP load comparison to two hot-spot APs of the SSF algorithm. The reason for such a behaviour can be explained as follows: LLF algorithm by design assigns the users to any accessible AP (*i.e.* AP that is in the coverage area of the considered STA) that has the least load value, irrespective of the offered communication rate. Such an implementation frequently leads to a scenario where the users are forced to associate to APs located further away; serving really low data rates (*e.g.* 6 Mbps for IEEE 802.11g and 1 Mbps for IEEE 802.11b systems). Since the AP load is inversely proportional to the communication rate, this causes the average AP load in the network to rise. In both performance figures (Figs. 5.7 and 5.8) the proposed association algorithm manages to strike a good balance between balanced and low average AP load.

5.6.2.3 Impact of User Distribution

In order to illustrate the effect of user distribution, for each network snap-shot simulation, total of 100 STAs are introduced in 16 AP communication environment described in Section 5.6.1. STA locations are varied at each simulation run and the median throughput values are obtained by averaging the results over 100 runs. A sample simulation snap-shot is illustrated in Fig. 5.3. STAs are distributed either in hot-spots (HS) or uniformly (UD) in communication environment. The percentage ratio of uniform and hot-spot STAs are changed for each simulation campaign. The throughput performance comparison of proposed and standard association algorithms is illustrated in Fig. 5.9. In the figure, X-axis represents different user distributions, Z-axis represents the per-STA throughput (Mbps) and the Y-axis represents the sorted STA index. STA throughputs are sorted in increasing order, meaning that throughput data value for the 99'th STA index in a 100 STA environment is the average throughput of the second best STA over all simulation iterations. If we consider the median point of the sorted STA throughputs, the predictive association algorithm (PAA) performs better than the standard association algorithm (SSF) for all user distributions. One thing we notice is the better performance of the SSF association algorithm on some STAs compared to PAA. These STAs are the ones abusing almost empty APs for communication without sharing. Nevertheless if we look at the median point, we notice almost 4 times better performance of the PAA for hot-spot user distribution and twice the performance for 50% uniformly and 50% hot-

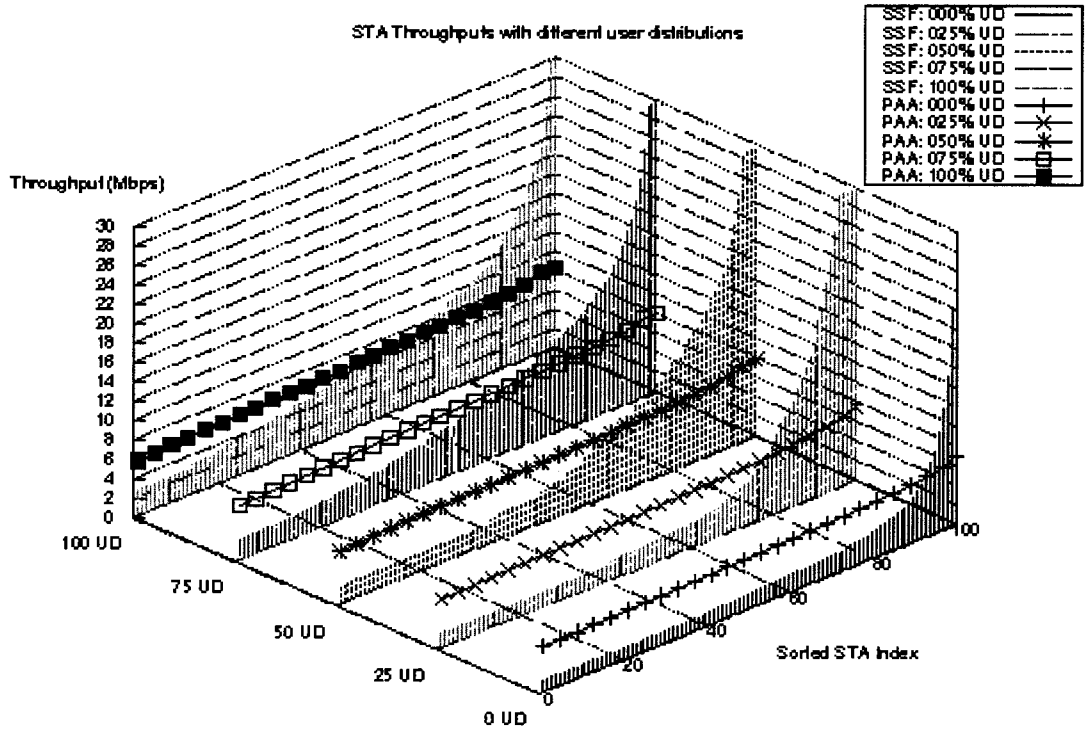

Figure 5.9: STA throughput comparisons of SSF and PAA algorithms relative to different user distributions.

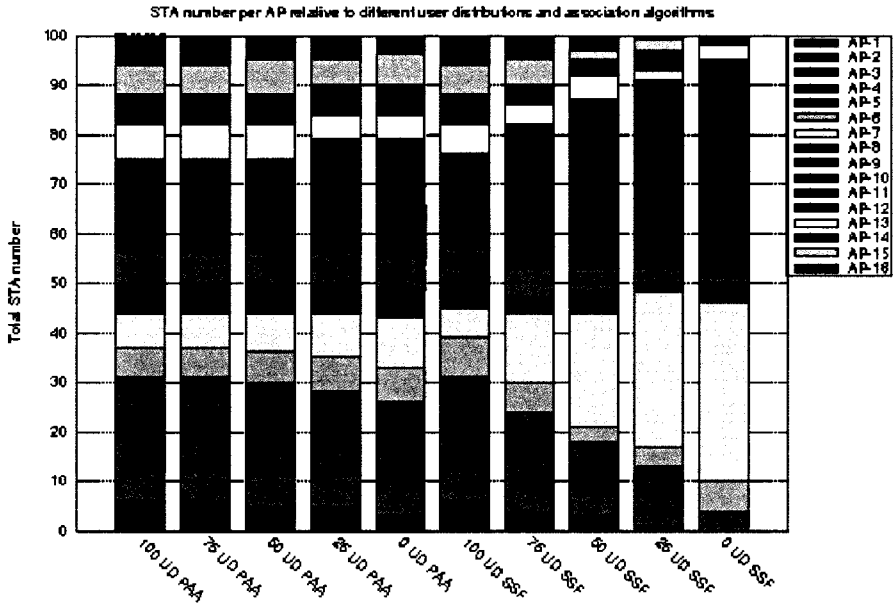

Figure 5.10: Number of STA per AP for different user distributions.

Table 5.1: Load balance indexes of different association algorithms.

	100%HS	75%HS&25%UD	50%HS&50%UD	25%HS&75%UD	100%UD
SSF	0.193	0.273	0.381	0.514	0.624
PAA	0.980	0.982	0.990	0.992	0.996

spot distributed user scenarios. The congestion in hot-spot APs is apparent for SSF. For hot-spot distribution, 88% of the users are establishing a connection with below 4 Mbps data rate with SSF, whereas there is no users in PAA that has a data rate that low. Fig. 5.10 illustrates this congestion in hot-spot APs in the communication environment. The figure plots the number of STAs associated to each AP in the network relative to different user distributions and association algorithms. As it can be seen from the figure, PAA has balanced user assignment, around 6-7 STAs per AP, independent of the user distribution. However, for SSF association algorithm, in non-uniform population scenario, hot-spot APs have around 30 STAs per AP that slashes their effective throughputs. The load balancing abilities of the association algorithms are given in Table 5.1. The Jain's index is calculated for both association algorithms with different STA distributions. As expected, as we increase the hot-spot user percentage, SSF algorithm load balance per-

formance starts falling behind. As the percentage of the hot-spot STAs increase, the index of SSF association algorithm approaches to $1/m$ (m being the number of APs in the communication environment, $m = 16$) which is the indication of highly unbalanced load distribution. Whereas, the PAA manages to keep the balance index on 0.98 level by intelligent STA associations. This load balance abnormality of the SSF algorithm for practical hot-spot scenarios can also be observed in Fig. 5.11. The figure illustrates individual AP load values in multi-AP environment. The excessive load spikes with SSF algorithm for hot-spot APs are obvious, explaining decreased throughput values for SSF algorithm.

5.6.2.4 Impact of Traffic Load

So far the performance of the proposed algorithm is presented for saturated network conditions and with greedy user assumption where channel utilization is 100%. This saturation condition can be easily satisfied if the serving AP is overloaded. For instance, if an AP is serving its associated users with maximum data rate of 54 Mbps; it can be saturated by 7 STAs transmitting 1000 bytes packets with exponential traffic having inter-arrival time of 0.001 seconds (*i.e.* the considered AP would need more than 56 Mbps to satisfy unsaturated channel condition in this case). In this section the effect of the traffic load on the proposed algorithm performance will be evaluated with NS2 simulations [33] and it will be shown that the superior performance of the proposed algorithm is valid for a large spectrum of traffic conditions.

The traffic model that is used in NS2 simulations is exponential on/off, where frames are sent at a fixed rate during on periods, and no packets are sent during off periods. In the simulation campaign, the exponential on/off generator is configured to behave as a *Poisson* process by setting the variable `burst_time_` to 0 and the variable `rate_` to a very large value, making the packet transmission time negligible and setting `idle_time_` as packet inter-arrival time. In the NS2 performance figures, the packet payload is assumed to be 1000 bytes (*i.e.* `packetSize_` 1000). The location of the STAs kept constant and STAs choose modulation and coding scheme relative to SNIR level they experience. STA traffic generator parameters are changed and they are scaled from 100% down to 1%. For a STA having a connection rate of 12 Mbps, 100% traffic would mean the considered STA generates 1000 byte frames with inter-arrival time of 0.00067 seconds (*i.e.* `idle_time_`). For this considered STA, the inter-arrival time would increase to 0.0013 seconds for 50% traffic simulation.

NS2 simulation results are presented in Fig. 5.12. The effect of user traffic on

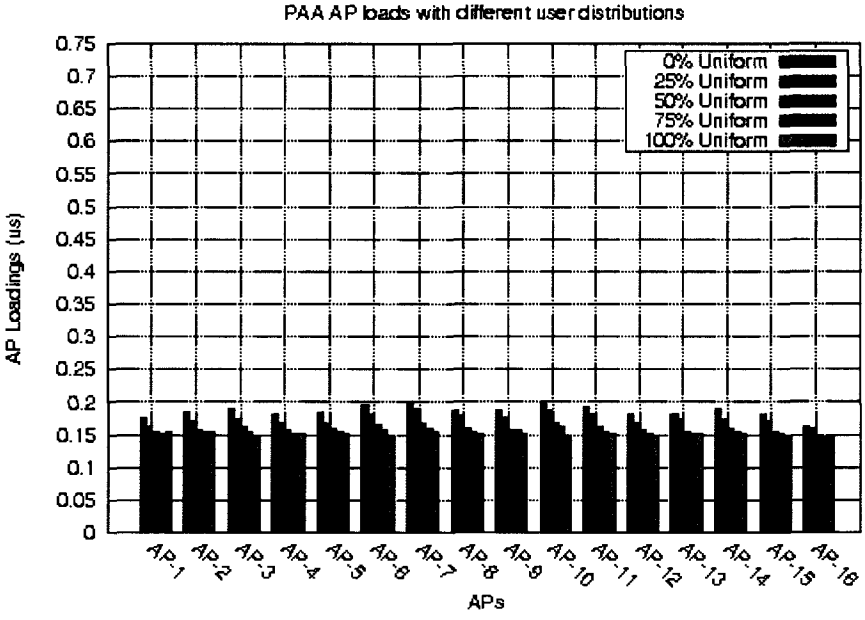

(a) Predictive association algorithm (PAA).

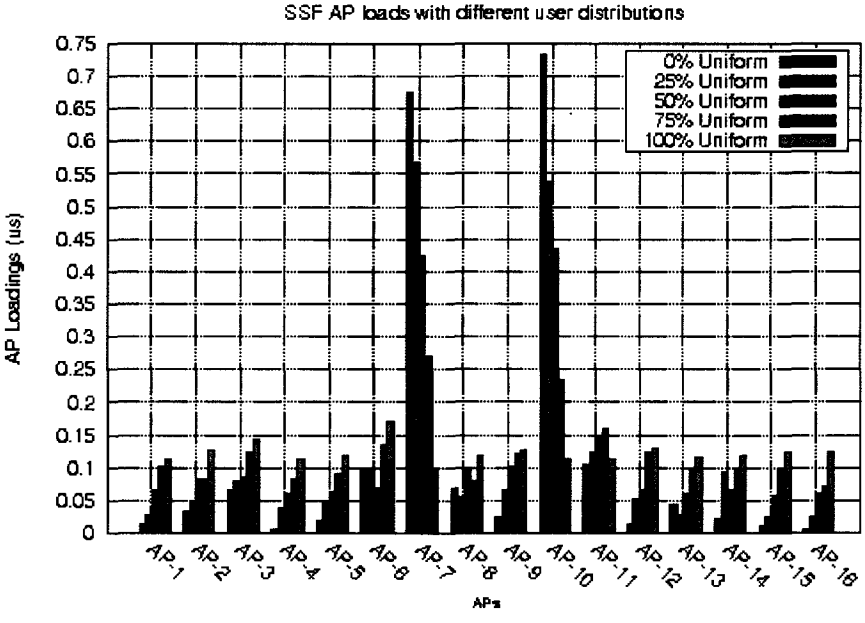

(b) Standard association algorithm (SSF).

Figure 5.11: AP loads comparison of PAA and SSF with different user distributions.

the throughput performance is illustrated in the figure by distributing 50 STAs in two hot-spots and utilizing different association algorithms. As expected, throughput is a decreasing function of traffic. With PAA the individual throughput values have a tendency to stay constant until $\backsim$ 50% traffic. This behaviour can be explained as follows. With PAA, STAs that would otherwise be associated in the hot-spot APs are distributed to neighboring APs, balancing the load, and average STA number per AP is small in comparison to SSF algorithm. Therefore, the communication environment can be unsaturated with users having a high traffic load (until $\backsim$ 50% of traffic). As the traffic level drops below $\backsim$ 50%, some idle time openings were observed where none of the STAs have a packet waiting to be transmitted. For SSF, the network is saturated until 1% STA traffic because of the hot-spot congestion (*i.e.* $\backsim$ 25 STAs per AP). Individual STA performance depends on the location of the STA (data rate) as well as how congested the AP is. Individual STA throughput performance varies between 3-8 Mbps for PAA whereas the performance drops to 0.7-3.5 Mbps for SSF algorithm.

5.7 Conclusions

A novel algorithm for associating a station to an access point is described for IEEE 802.11 extended service sets. The proposed algorithm is compared in terms of load balance index and individual station throughput considering the effects of user distribution, interference and traffic load. It has been shown that the proposed algorithm improves the average system throughput performance more than twice for practical user distributions and offers a better load distribution across the network compared to conventional association algorithm. Its adaptability feature makes it a robust solution for dynamic user environments as normally seen in practice like airports, campusses and coffee shops. The proposed algorithm equally improves the downlink and uplink throughput and channel access performances. Due to load balance nature of the novel algorithm, the number of contending STAs are far less than standard association algorithm. Considering the fact that probability of packet collision is an increasing function of contending STAs, the proposed association algorithm would have a better uplink traffic and packet access condition.

In a practical network environment, the challenges of implementing the proposed association algorithm are two folds: *i)* Calculating the performance figure (per AP load) in APs and *ii)* relaying this information to STAs in the communication environment to facilitate their association decision. In current implementation, APs are aware of the STAs

that are associated with them as well as their communication rates. Therefore APs are able to calculate their loads ($\mathfrak{L}$) with the information that is already available in current networks. A minor modification in IEEE 802.11 standards will be needed to relay this performance figure to STAs in the communication environment to assist their association decision. Management frames (beacon message, probe request, probe response *etc.*) using information elements would be perfect candidate for this functionality. Information elements included in management frames are variable-length components, contrary to fixed-length components of control frames. If we investigate this particular frame structure more closely [6], we see that most of the information elements (total of 255) are reserved for future applications. Utilization of management frames with novel information elements would be backward compatible. STAs that are able to decode such an information would detect AP load values, form their effective data rate vectors ($\overrightarrow{\mathfrak{E}'_s}$) engage proposed association algorithm and enjoy a better performance. STAs that do not have this feature would just ignore the considered information element and proceed with normal association algorithm.

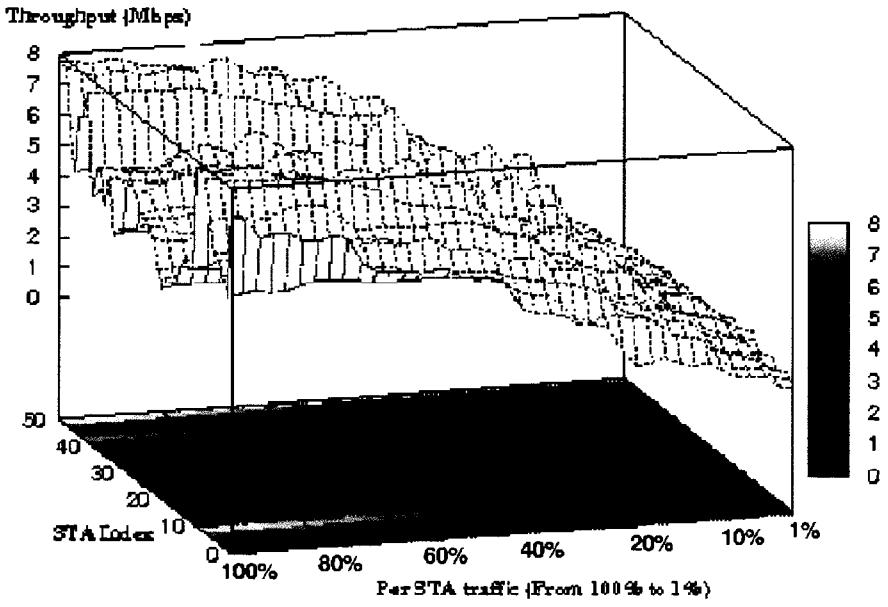

(a) Proposed association algorithm (PAA).

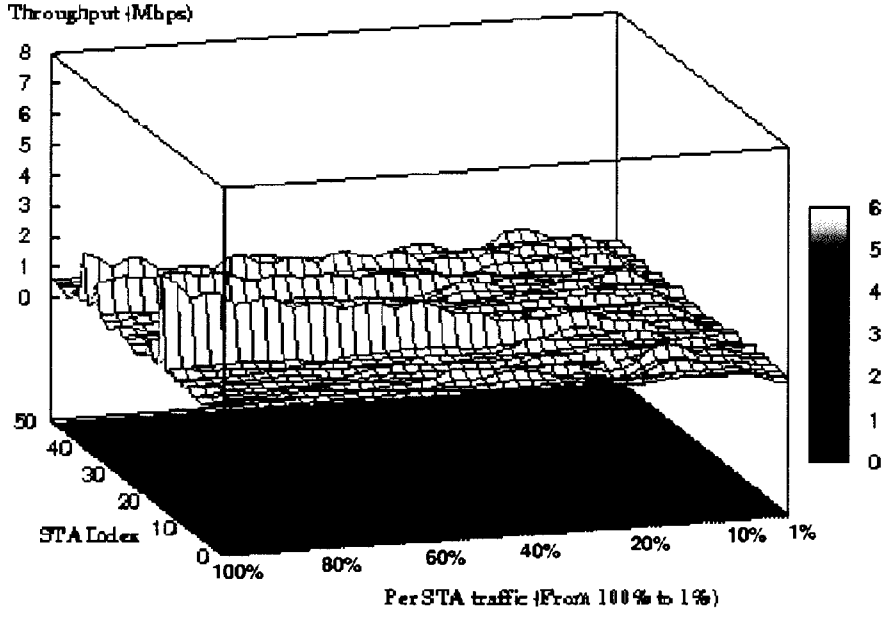

(b) Standard association algorithm (SSF).

Figure 5.12: STA throughput comparisons of SSF and PAA algorithms relative to different traffic conditions.

Chapter 6

Conclusions and Suggestions for Future Work

More and more people rely on using portable computers and internet services in their daily work. This fact is one of the major reasons that IEEE 802.11 wireless local area network market is expanding rapidly. In this dissertation, we developed an analytical method to estimate the performance of wireless local area networks in practical network conditions where hidden nodes and users with unsaturated traffic are commonplace. We have shown that the primary contention resolution algorithm of IEEE 802.11 networks faces many challenges like congestion (hot-spots), hidden nodes, excessive overhead in densely deployed corporate network environments.

In this thesis, after evaluating the performance of distributed coordination function in the presence of hidden nodes with proposed methodology and confronting the difficulties it is having, a point coordination function with novel polling indexing scheme is proposed. With such a scheme, high throughput performance is obtained by reduced overhead, no contention and proposed polling list creation method. Then the performance characterization of the primary contention resolution scheme is extended to wireless networks with multiple access points. It has been illustrated that uneven user distribution is the greatest obstacle to obtain network-wise fairness and high throughput. We proposed a novel association algorithm that significantly improves the throughput performance and fairness index in networks having multiple access points.

We have evaluated the performance of the networks in the presence of hidden nodes and unsaturated network conditions. It has been illustrated that the effect of the hidden nodes in a network with low traffic is minimal; whereas as the network load increases the

decremental effect of hidden nodes becomes more and more obvious. With the methodology developed, we have also estimated the fairness performance of the network with hidden nodes. It has been illustrated that individual STA performances highly depend on the orientation of the user in the network and its traffic load. In low traffic conditions, it has been illustrated that all the users in the network get their fair share despite the presence of hidden node. However, badly located users destined to starve upon increasing network traffic load. Comparative network performance assessments considering networks with different number of hidden node configurations are presented. Considering the fact that request-to-send/clear-to-send (RTS/CTS) channel access mechanism is designed specifically to cope with the hidden node problem, further simulation results are presented comparing RTS/CTS and DCF throughput performances in similar hidden node network environments.

We also proposed a novel association algorithm for networks comprised of multiple access points. We named this association algorithm as *predictive association algorithm.* In the designed algorithm we took into account multiple network parameters that affect the overall network functioning (*i.e.*, access point load, communication rate, interference, dynamic network structure and distributed decision making process) to predict user throughput performance before actually deciding on association. By doing so, we drastically increased the throughput performance and especially the fairness index of the networks.

6.1 Suggestions for Future Work

There are various possible future works regarding the architecture introduced in this thesis. The developed methodology can be used to evaluate the analytic throughput performance of exposed node scenarios or RTS/CTS channel access scheme. The probability calculation of hidden node occurrence in a given network setup is another interesting topic one can look at. The application of PCF to multiple access point communication environments can also be considered as an extension of the work presented in this thesis. In closing, further details of some of future research topics mentioned are given in this chapter.

6.1.1 Calculation of hidden-node and contending-node probability

As a part of this work, we developed a model to assess the performance of a network in the presence of hidden nodes. In the methodology, with given number of contending and hidden users, the network and individual user performances are calculated with great precision. However, given total number of users, expected user distribution and RF propagation model, it would be interesting to estimate the probability of a considered user to have certain number of hidden and contending users in a network configuration. For instance, considering that the user locations are selected uniformly and independently in a communication environment, *what is the probability of two users to be hidden to each other?* With any given RF propagation model and a common AP, if the link distance ($d_{STA-1,STA-2}$) between two independently created STAs ($STA-1$ and $STA-2$) is less then the carrier sense distance (d_{CS}), then these two STAs are in the carrier sense region of each-other and they are contending for the channel access; hidden otherwise (*i.e.* if $d_{CS} < d_{STA-1,STA-2}$). Therefore, given the number of users in the communication environment, user distribution and finally the RF propagation model, the propability of a considered user to have a certain hidden and/or contending user can be calculated. This calculation then can be used in the network throughput calculation for further analysis.

6.1.2 Application of PCF in multi-AP environments

Another interesting area could be to study the applicability of point coordination function in multiple access point network configurations. In such a set-up, in order to benefit PCF features (*i.e.* no interference, no hidden node), during any given time of contention free period only a set of non-interfering access points should be activated while others (possibly interfering access points) are silenced.

In PCF, if two APs poll their mobile users independently and if the polled STAs are in the carrier sense of each-other then the collision is inevitable. Considering the fact that IEEE 802.11b and g systems only have 3 non-overlapping frequencies, the implementation of PCF in multi-AP corporate environments using ISM bands is not practical. One solution to enable multiple APs to work in harmony in PCF mode is dividing the time into equal sized slots such that within each slot only a subset of APs (non-interfering) are activated, while the rest of the APs are silenced. By ensuring that the APs simultaneously activated in any slot of the time are *non-interfering*, the scheme guarantees that the system is free from interference and hidden node problems. The

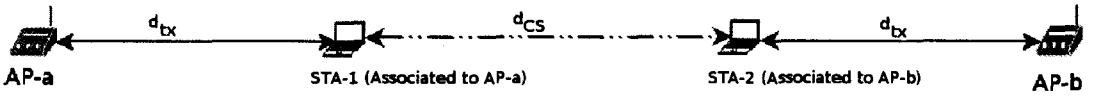

Figure 6.1: Interfering AP illustration.

peculiarity in such implementation is, in each time slot the overall system imitates the point coordination function behaviour in single access point environment. An efficient scheduling algorithm that takes into account the number of time slots allocated to each access point proportional to its load could be designed.

In implementation of PCF to multi-AP communication environment, the very first task is to find the interfering AP pairs in the multi-AP communication environment. In IEEE 802.11a networks, two thresholds are defined for terminals: *(i)* signal sensing threshold (-91.76 dBm [OFDM]) and *(ii)* minimum signal decoding threshold (-82 dBm [OFDM]) [8]. Any signal with received power below signal sensing threshold will be assumed as background noise. Similarly, a received signal needs to be at least -82 dBm level to be decoded properly. For the time being, let's consider that the path-loss is the only factor affecting the signal strength (*i.e.* no shadowing). Thus, each mobile station can be associated with two circular regions around it. The inner circle is the transmission range of the station (d_{tx}) that defines the zone in which any message sent by the station can be decoded properly; and the outer circle is the carrier sensing range (d_{CS}). Any mobile station included in this range (d_{CS}) can sense every transmission of the considered station. Two APs are assumed to be interfering when a message exchanged by one AP may prevent a proper message decoding in the vicinity of the other. Any two APs are assumed to be interfering if the distance between them are less than $2d_{tx} + d_{CS}$. This is the maximum available distance for interfering APs as illustrated in Fig. 6.1. A sample interfering AP relationship is illustrated in Fig. 6.2. Interfering APs are illustrated by drawing a straight line between them. (*i.e.* Any ongoing transmission of AP-d might interfere with AP-b, AP-c, AP-e and AP-f.) Such interfering AP relationship can be represented by the *interference graph.*

6.1.2.1 Interference Graph

The interference graph $G(A, E)$, is defined by the set of APs (A) and a set of edges (E) between any pair of APs ($a, b \in A$) that are using the same operational frequency and have the spatial separation less than $2d_{tx} + d_{CS}$, *i.e.* $d_{AP-a,AP-b} < 2d_{tx} + d_{CS}$. That is

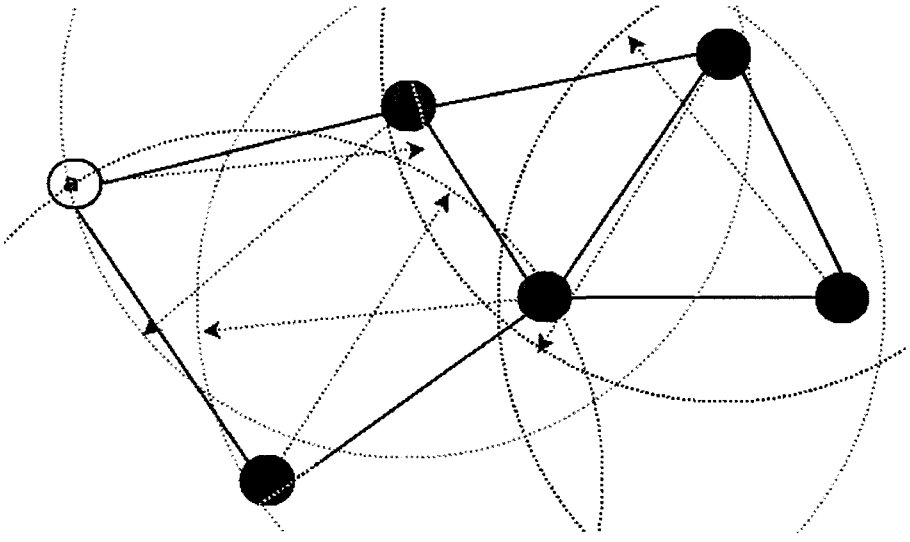

Figure 6.2: Sample interference graph.

to say if the APs are utilizing the same operational frequency and the distance between them are less than $2d_{tx} + d_{CS}$ any transmission in one AP can potentially be interference on the other AP. A sample interference graph illustrating interference distances is given in Fig. 6.2. In normal PCF applications (single AP operations), mobile users in the AP performing PCF operations are time-sharing the bandwith. The difference between single-AP PCF and multi-AP PCF applications is, for multi-AP PCF, the same time slot can be allocated to more than one APs simultaneously. However this is not possible in single AP configuration because all the mobile stations are in interfering distance of each other. Let's look at an example scenario for PCF implementation in a multi-AP environment.

6.1.2.2 Example 4:

Let's consider that the total data rate of contention free period (CFP) is 10 Mbps and each mobile user in communication environment is capable to communicate with data rate of 10 Mbps. Assume that all the APs are using the same operational frequency for the time being. Let CFP be divided into K time slots enumerated from 1 to K. We denote by SL_a the set of slots allocated to AP a in a given CFP and by k_a the number of slots in SL_a (*i.e.* $k_a = |SL_a|$). A slot assignment vector can be defined as follows: $SL = \{SL_a, SL_b, ...SL_z\}$ ($|SL| = |A|$) where each element (*i.e.* SL_a) specifies the slots

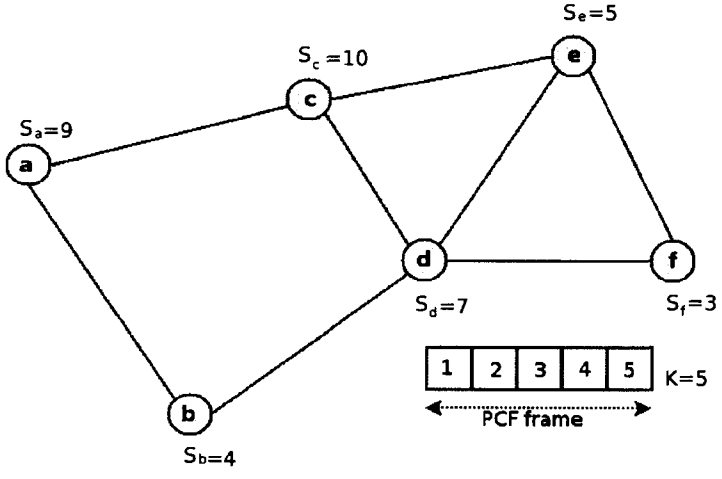

Figure 6.3: Interference graph illustration.

assigned for each AP $a \in A$. A slot assignment is feasible if for every AP a, $SL_a \subseteq [1..K]$ and any pair of adjacent nodes in the interference graph do not have any common slot. A sample figure illustrating the slot assignment is given in Fig. 6.3. In the figure this requirement means that we can not allocate more than 5 slots ($K = 5$, the maximum number of slots in CFP) to an AP and the same slot can not be assigned to APs $\{d, e, f\}$ in the given CFP, because they are interfering APs. In the figure, S_a denotes the number of mobile stations associated to AP a. Considering that total data rate of CFP is 10 Mbps, a single slot assignment to an AP will supply 2 Mbps to the considered AP and its associated users in the given CFP. The challenge is to assign the slots to the APs by taking into account APs load as well as interference characteristic and maximize the network utilization. A sample slot allocation for the considered network is illustrated in Fig. 6.4. For the example slot allocation illustrated in Fig. 6.4, slot assignment sets, average AP and per STA data rates can be calculated as follows:

- Slots assigned to AP-a $S_a = \{1, 2, 5\}$ providing total AP-a data rate of $6\,Mbps$. Considering that there are 9 STAs associated to AP-a, per-STA throughput would be $6/9\,Mbps$
- Slots assigned to AP-a $S_b = \{3, 4\}$ providing total AP-a data rate of $4\,Mbps$. Considering that there are 4 STAs associated to AP-a, per-STA throughput would

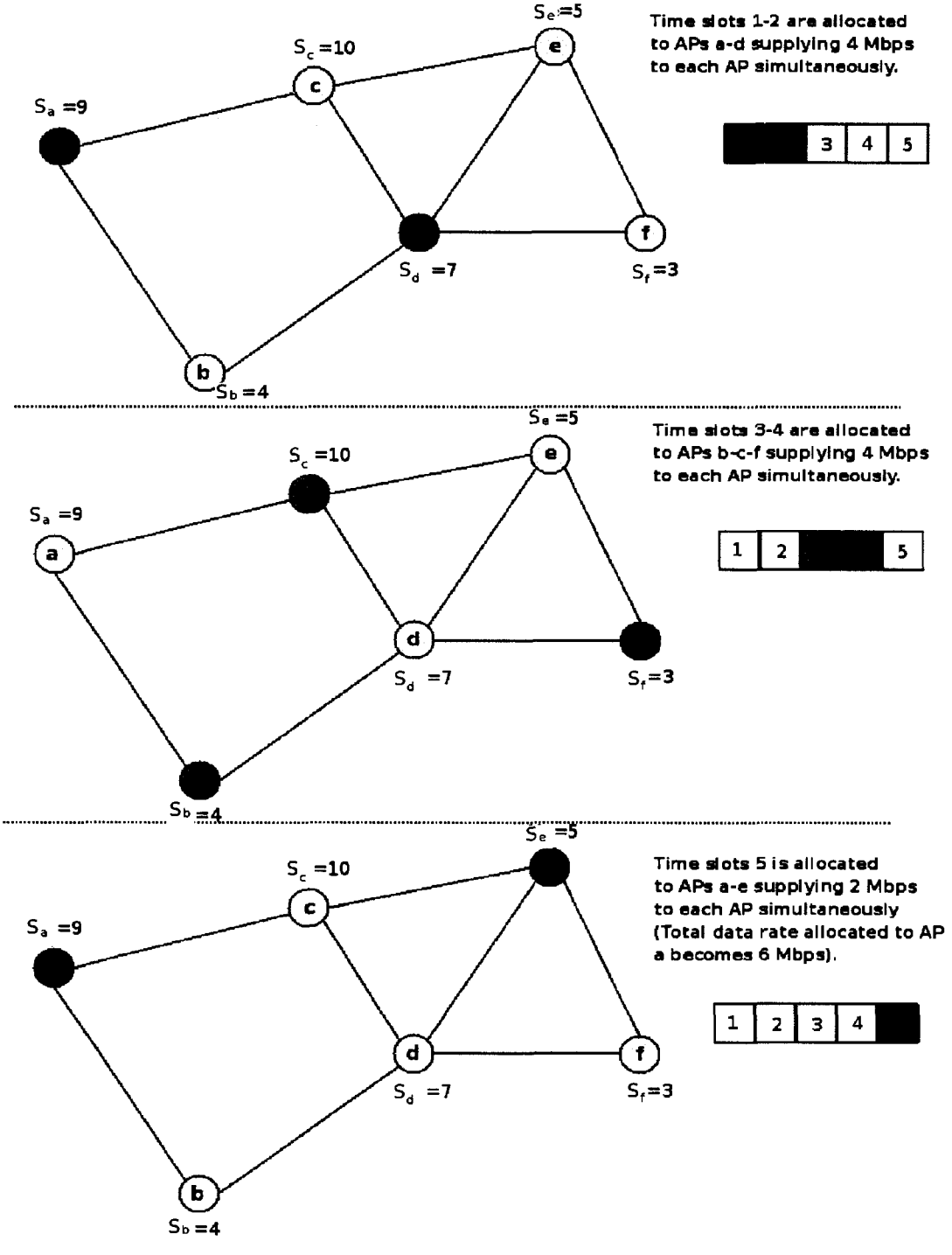

Figure 6.4: Sample slot allocation illustration.

be $4/4\,Mbps$

- Slots assigned to AP-a $S_c = \{3, 4\}$ providing total AP-a data rate of $4, Mbps$. Considering that there are 10 STAs associated to AP-a, per-STA throughput would be $4/10\,Mbps$
- Slots assigned to AP-a $S_d = \{1, 2\}$ providing total AP-a data rate of $4\,Mbps$. Considering that there are 7 STAs associated to AP-a, per-STA throughput would be $4/7\,Mbps$
- Slots assigned to AP-a $S_e = \{5\}$ providing total AP-a data rate of $2\,Mbps$. Considering that there are 5 STAs associated to AP-a, per-STA throughput would be $2/5\,Mbps$
- Slots assigned to AP-a $S_f = \{3, 4\}$ providing total AP-a data rate of $4\,Mbps$. Considering that there are 3 STAs associated to AP-a, per-STA throughput would be $4/3\,Mbps$

As it can be seen from Fig. 6.4, the achievable throughput of the system depends on the density of the interfering graph G, which is the number of edges in the graph. Generally speaking the number of slots allocated to each AP should be inversely proportional to its degree (number of edges, for instance the degree of AP-d is four, which means all four neighboring APs should be silenced when AP-d communicates) in G. Time slot assignment in a interfering graph is similar to graph colouring problem in graph theory.

Appendix A

IEEE 802.11a Propagation Model

A.1 Propagation Model

In numerical results, deciding on the modulation and coding scheme of a station depends highly on the channel propagation model used. Therefore, it is vital to have a realistic channel model to evaluate the true performance of a WLAN. The propagation model that ITU has recommended for evaluating indoor systems at 5 GHz band is given by [15]. According to this model, the received signal power at distance d can be calculated as follows:

$$P_r(d)_{dB} = P_t + G_t + G_r - 41\,\mathsf{dB} - 10\beta\mathsf{log}_{10}(d) - L_{dB} \qquad (in\ dB) \qquad \text{(A.1)}$$

where P_t is the transmitter signal power level; G_t and G_r are the antenna gains of the transmitter and the receiver respectively; $L(L \geq 1)$ is the system loss, d is the distance between transmitter and receiver in meters; 41 dB is fixed loss at 1 m and finally β is path-loss exponent that depends on the communication environment. Default path-loss exponent assumed by ITU is 3.1. Table A.1 illustrates some typical values of path-loss exponent for different propagation environments [57]. Unless noted specifically the default values for antenna gains and system loss are assumed to be $G_t = G_t = L = 0$ in (A.1). ITU propagation model given in (A.1) basically represents the communication range as a circle around the transmitter as illustrated in Chapter 4, which is a deterministic approach to calculate the received signal power level. In practice however, the surrounding environmental clutter may be significantly different at two different locations having the same transmitter-receiver separation. This leads to measured signal levels which are substantially distinct than the average predicted by (A.1). Measurements have shown that

Table A.1: Typical path-loss exponent values.

Environment		β
Outdoor	Free space	2
	Shadowed urban area	2.7 to 5
Indoor	Line-of-sight	1.6 to 1.8
	Obstructed	4 to 6

at any value of d, the received signal power at a particular location is a log-normally distributed random variable about the mean distance-dependent value [57]. In order to use more accurate propagation model that takes into account the environmental characteristic (indoor, outdoor) as well as the material characteristic (hard partition, soft partition) the shadowing propagation model is used more often in the literature. The shadowing model consists of two parts. The first part indicates the average signal strength at distance d. It is a common practice to use a close-in point as a reference point to calculate the relative received signal strength. The second part of the shadowing model reflects the variation of the received power at certain distance. It is a log-normal random variable (Gaussian distribution if measured in dB). The received signal power level (both in linear and dB scale) with shadowing model can be calculated as follows:

$$P_r(d)_{dB} = P_r(d_0)_{dB} - \left[10\beta \log\left(\frac{d}{d_0}\right)\right]_{dB} + X_{dB} \qquad (in\ dB) \qquad (A.2)$$

If we consider the reference point as the signal strength at 1 m and use equation parameter values as follows $c = 3\,\mathrm{x}\,10^8$ m/s, $P_t = 200$ mW and $f = 5$ GHz the received power level in dBm at distance d can be found as follows:

$$P_r(d) = -18 - 10\beta \log(d) + X_{dB} \qquad (A.3)$$

Deterministic path-loss signal strength calculation, random log-normal shadowing and their overall signal strength map (in dBm) are illustrated in Fig. A.1. The figure shows a communication environment with size of 256 m by 256 m and it is assumed that there is an AP in the middle of the communication environment transmitting with power of 200 mW. The very first figure illustrates the deterministic ITU propagation model and shows the received signal power in dBm. Circular communication range is evident. Second figure illustrates log-normal shadowing pattern with 0 dB mean, 8 dB standard

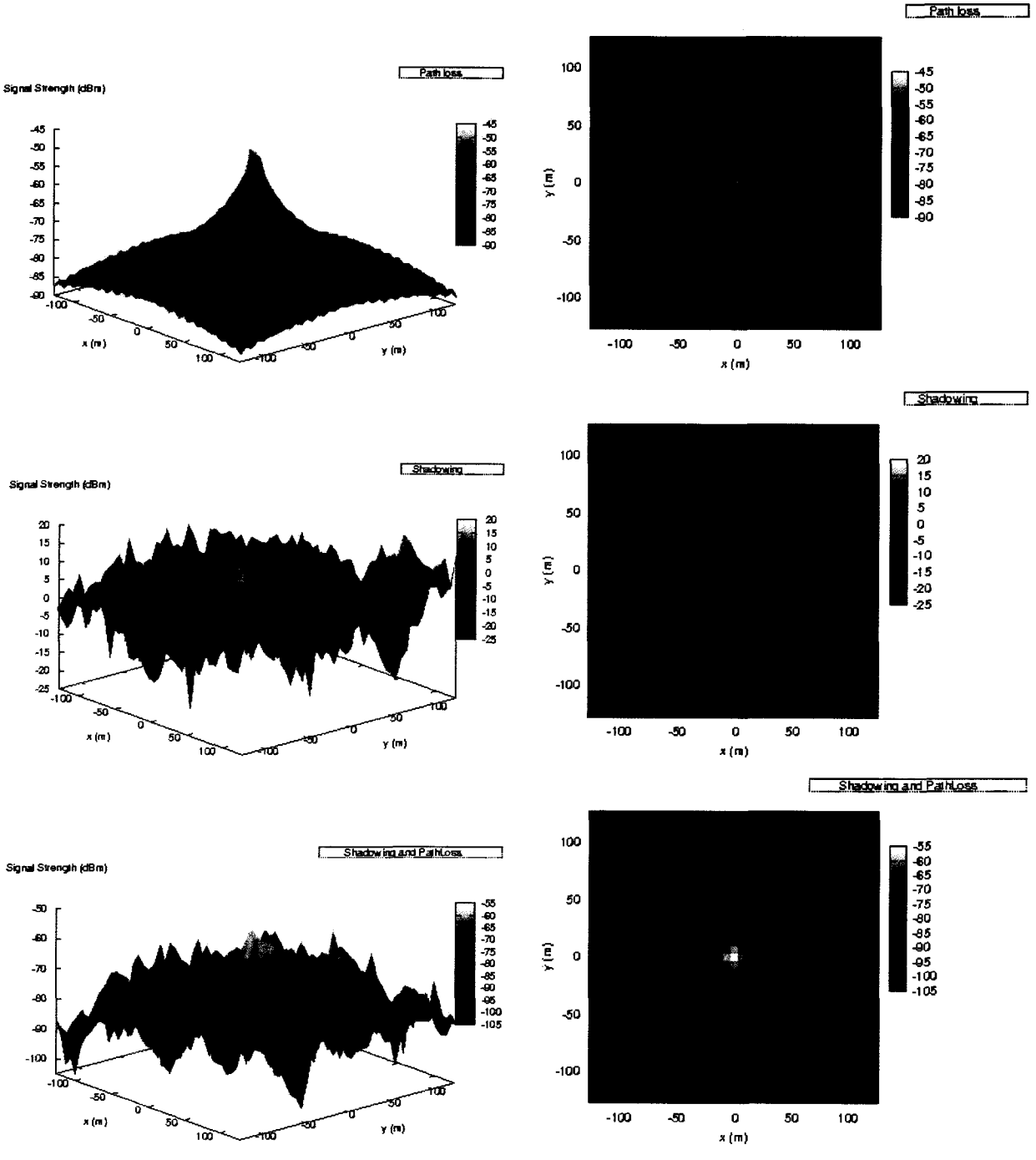

Figure A.1: The effect of shadowing and path loss together.

deviation and the correlation distance of $10\,m$ [59]. Standard deviation of the slow fading which is assumed to be $8\,dB$ depends on the environment clutter. For 5 GHz frequency band, the typical value for home environment is assumed to be $8\,dB$ [58]. However higher standard deviation values are expected for offices with hard and especially soft partition [57]. Very last figure illustrates the received signal power with shadowing mapping on the ITU propagation model. As it can be seen from Figs. A.1, the communication range of an IEEE 802.11a AP transmitting with power of $200\,mW$ is about $110\,m$.

A.2 Background Noise Calculation

The IEEE 802.11a WLAN standard recommends that receivers have a noise figure (NF) of $NF = 10\,dB$ or better [8]. On the basis of this figure, we can calculate nominal receiver noise floor value as follows:

$$
\begin{aligned}
N_0 &= (NF)\,k\,T_0 && && \text{W/Hz} \\
&= (10)\,(1.38\,\text{x}\,10^{-23}\,\text{W.s/°K})\,(290\,\text{°K}) && = 4.002\,\text{x}\,10^{-20} && \text{W/Hz} \\
&= 10\,\text{dB} - 228.6\,\text{dBW.s/°K} + 24.624\,\text{dB°K} && = -\,193.977 && \text{dBW/Hz} \\
& && = -\,163.977 && \text{dBm/Hz}
\end{aligned}
\tag{A.4}
$$

where k is Boltzman constant ($1.38\,\text{x}\,10^{-23}$ W.s/°K), T is ambient temperature ($290\,^oK$). The noise power at the receiver in a bandwidth of B ($16.6\,MHz$ [8]) can be calculated by:

$$
\begin{aligned}
N &= N_0\,B && && \text{W} \\
&= (4.002\,\text{x}\,10^{-20}\,\text{W/Hz})\,(16.6\,\text{x}\,10^{6}\text{Hz}) && = 6.64\,\text{x}\,10^{-13} && \text{W} \\
& && = -\,121.76 && \text{dBW} \\
& && = -\,91.76 && \text{dBm}
\end{aligned}
\tag{A.5}
$$

Appendix B

802.11a MAC and PHY Overview

For IEEE 802.11a WLAN throughput calculation, packet transmission (or reception) procedure of IEEE 802.11 MAC as well as the PHY services provided to MAC by the 5 GHz OFDM PHY system should be understood properly. In order to allow the IEEE 802.11 MAC to operate with minimum dependence on the physical medium dependent (PMD) sublayer, a PHY convergence sublayer is defined. The aim is to simplify the PHY service interface to the IEEE 802.11 MAC services and share a common MAC for different PHY implementations like frequency hopping, direct sequence spread spectrum and OFDM. The PMD sublayer provides a means to send and receive data between two or more stations. When a packet to send is generated in higher layers (logical link control [LLC] layer or up) MAC layer is notified to involve in the contention resolution process to transmit the packet. After taking over the packet (also called MSDU [MAC service data unit]) from higher layers, MAC header (30 or 24 bytes depending if packet goes between distribution systems or not) and the frame check sequence (FCS) (4 bytes) is added to the payload. The packet assembled (also called MPDU [MAC protocol data unit]) is then handed over to PHY layer. The overhead added by MAC layer should be taken into account for accurate throughput analysis. The detailed structure of MAC Frame format (including MAC header, LLC payload and FCS) as well as acknowledgement (ACK) frame format following every successful frame transmission are illustrated in Fig. B.1.

The two layers of 5 GHz OFDM PHY responsible for reliable packet transmission are stated as follows:

- *A PHY converge function*: This function is supported by physical layer convergence procedure (PLCP), that defines the method of mapping the payload obtained from MAC layer on frames, *e.g.* fragmentation, modulation technique determination,

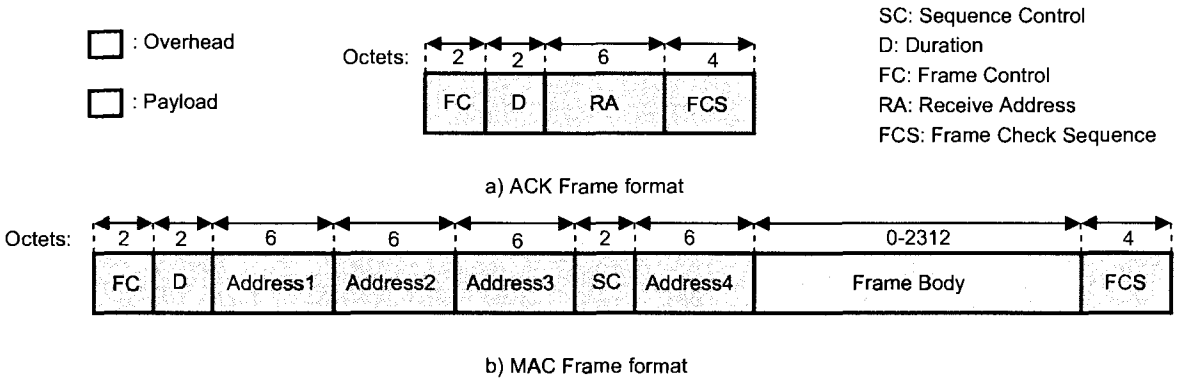

Figure B.1: IEEE 802.11 MAC frame format

coding scheme determination. This layer is defined in order to make IEEE 802.11 MAC layer independent of any PHY layer implementation.

- *A PHY medium dependent (PMD)*: PMD defines the method of transmission technique. Low level operations are executed in this layer, *e.g.* actual modulation (binary phase shift keying [BPSK], quadrature phase shift keying [QPSK]), OFDM, DSSS, FH, frequency modulation, channel estimation, energy measurement.

After obtaining the packet (also called PLCP service data unit [PSDU]) from MAC layer, PHY PLCP layer decides on the modulation and coding scheme for transmission and starts preparing the preamble. In PHY layer, PSDU with added PHY header, padding bits, tail bits and PHY preamble represents PLCP protocol data unit (PPDU). The mapping of the PHY overhead from PLCP to PMD should be defined clearly for transmission duration analysis. The mapping of PLCP header (in PHY PLCP) to PMD (in PHY PMD) field is two fold. In terms of modulation, LENGTH (defines the number of bytes in the embedded MAC frame, 12 bits), RATE (indicates the data rate, 4 bits), RESERVED bit and PARITY bit constitute a separate single OFDM symbol, denoted as SIGNAL and which is transmitted with the most robust combination of BPSK modulation and coding rate of $R = 1/2$. The SERVICE (16 bits; 6 bits to initialize the scrambler, the rest are reserved for future use) field of the PLCP header and the PSDU are transmitted at the data rate described in the RATE field and may occupy several OFDM symbols.

The throughput of a successful transmission can be found by taking into account the overhead in both PHY layer and MAC layer. It can be seen that the overhead in

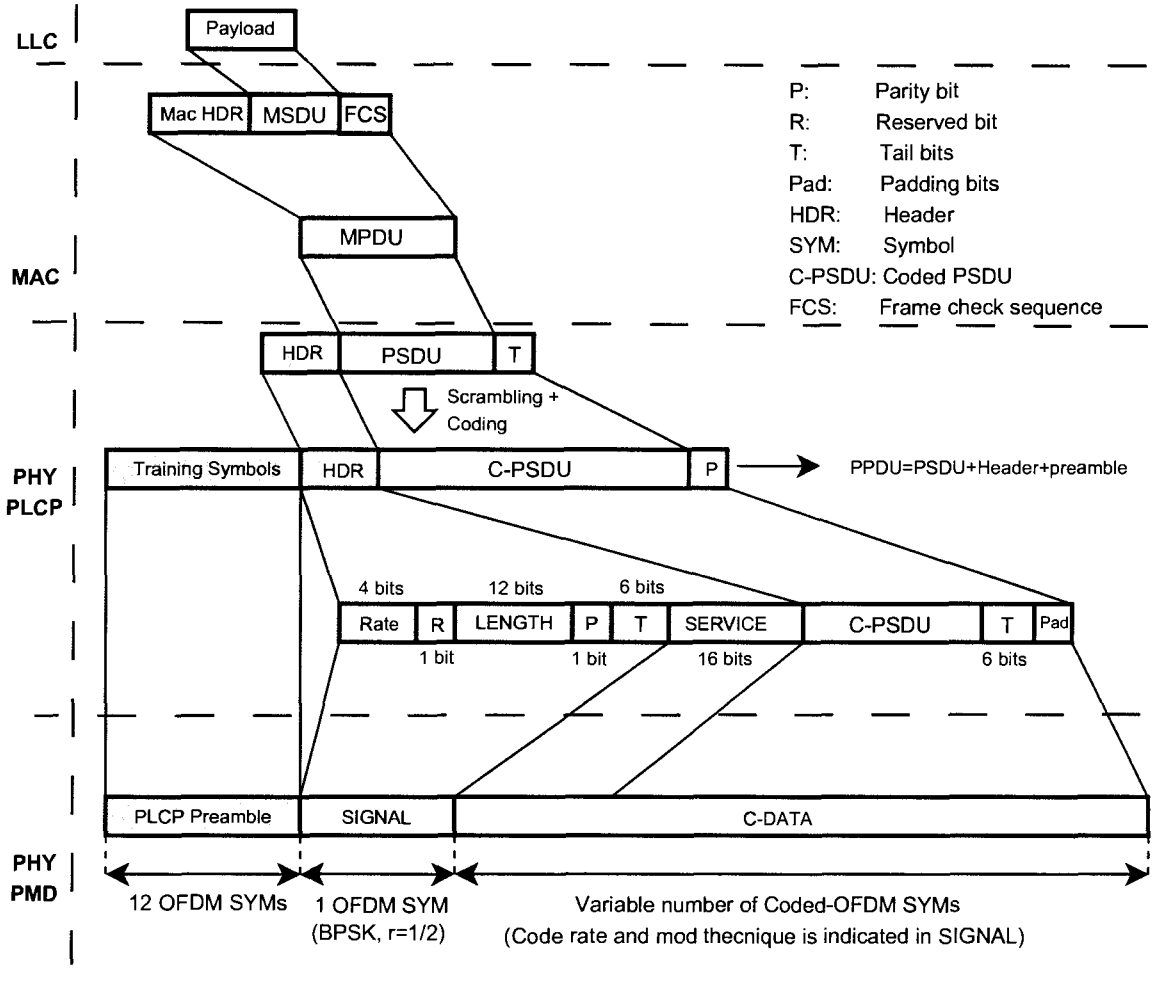

Figure B.2: IEEE 802.11a packet flow

PHY PMD is consists of PLCP Preamble (12 OFDM symbols) and the SIGNAL field (1 OFDM symbol). If we move one layer up to PHY PLCP, we notice that SERVICE field as well as tail and pad bits are a part of the overhad too. This overhead structure is illustrated in (B.2). MPDU includes MAC header and FCS. The data accepted by the MAC for delivery to another MAC on the network is called MAC Service Data Unit (MSDU) and it is pure higher layer data without any header. MSDU is indicated as *frame body* in Fig. B.1 and some researches call this as *payload*.

After considering the packet vertical flow across the layers, the throughput of the system can be found by calculating the the number of payload bits successfully transmitted in a given transmission. In IEEE MAC with DCF access mechanism, a successful frame

transmission is always followed by an ACK frame. The receiver waits T_{sifs} duration between frame reception and ACK transmission and all the mobile terminals have to wait T_{difs} duration after every single successful frame transmission. If there is a collision during the frame transmissions all the mobile terminals have to wait the collision to be over and T_{eifs} duration more after the incident to avoid repeated collisions. If we represent the duration for successful frame transmission with T_s and the duration for a collision with T_c we can find these values as follows:

$$\begin{aligned} T_s &= T_{data} + \tau + T_{sifs} + T_{ack} + \tau + T_{difs} \\ T_c &= T_{data} + \tau + T_{eifs} \end{aligned} \tag{B.1}$$

where τ is the propagation duration and T_{sifs}, T_{difs} and T_{eifs} are inter-frame spaces dependent on the PHY employed. In (B.1) all the parameters are specified in [8] except T_{data} and T_{ack} which are the data and ACK frame transmission durations. With the help of IEEE 802.11a system timing values of Table 3.1 in Chapter 3, the indicated durations can be calculated as follows:

$$\begin{aligned} T_{data} &= T_{PRE}^{PHY} + T_{H}^{PHY} + T_{H}^{MAC} + T_{Payload}^{MAC} + T_{FCS}^{MAC} + T_{TailBits}^{PHY} + T_{PadBits}^{PHY} \\ &= T_{pre} + T_{sig} + ... \\ & T_{sym} * ceil((serv + tb + 8 * (mac_h + mac_{payload} + fcs))/N_{dbps}) \\ &= 20\,\mu sec + 4\,\mu sec * \left\lceil \frac{16 + 6 + 8 * (24 + mac_{payload} + 4)}{N_{dbps}} \right\rceil \\ T_{ack} &= T_{PLCP-Pre}^{PHY} + T_{PLCP-H}^{PHY} + T_{ack} + T_{TailBits}^{PHY} + T_{PadBits}^{PHY} \\ &= T_{pre} + T_{sig} + T_{sym} + ceil((serv + tb + 8 * ack)/N_{dbps}) \\ &= 20\,\mu sec + 4\,\mu sec * \left\lceil \frac{16 + 6 + 8 * 14}{N_{dbps}} \right\rceil \end{aligned} \tag{B.2}$$

N_{dbps} is a modulation dependent parameter indicating data bits per OFDM symbol. For ACK transmission this parameter should be selected from one of the mandatory modulation modes, whereas for data transmission there is no restriction. With all given information about 5 GHz OFDM PHY an accurate system throughput for DCF medium access mechanism can be estimated by utilizing T_s, T_c, payload size ($mac_{payload}$) and probability of successful frame transmission.

Appendix C

List of Publications from this thesis

PEER REVIEWED JOURNAL PUBLICATIONS

- Ö. Ekici and A. Yongacoglu, "Balanced Association Algorithm for IEEE 802.11 Extended Service Areas", Wiley Wireless Communications and Mobile Computing, Vol.3, May 2008, pp. 1530-1545
- Ö. Ekici and A. Yongacoglu, "IEEE 802.11a Throughput Performance with Hidden Nodes", IEEE Communications Letters, vol.12, June 2008, pp.465-467
- Ö. Ekici and A. Yongacoglu, "Fairness in IEEE 802.11 Networks with Hidden Nodes", Physical Communication, Vol. 1, December 2008, pp. 255-265

INTERNATIONAL CONFERENCE PUBLICATIONS

- Ö. Ekici and A. Yongacoglu, "Novel Indexing Algorithm for Multi-rate Support in IEEE 802.11 Scheduled Access", Proc. International Symposium on Computer Networks, Istanbul, June 2008
- Ö. Ekici and A. Yongacoglu, "Modeling Hidden Terminals in IEEE 802.11 Networks", PIMRC 2008, Cannes, pp. 208-212, 2006
- Ö. Ekici and A. Yongacoglu, "Predictive Association Algorithm for IEEE 802.11 WLANs", ICTTA 2006. 2nd, Vol.2, April 2006, pp. 2394-2399
- Ö. Ekici and A. Yongacoglu, "A Novel Association Algorithm for Congestion Relief in IEEE 802.11 WLANs", Proc. of the 2006 ICWCMC, pp. 725-730, Vancouver, July 2006

Bibliography

[1] Part 11: IEEE 802.11b WG. Wireless lan medium access control (MAC) and physical layer (PHY) specification: High-speed physical layer extension in the 2.4 GHz band. Standard, IEEE, 1999.

[2] Part 11: IEEE 802.11g WG. Amendment 4: Further higher data rate extension in the 2.4 GHz band. Standard, IEEE, 2003.

[3] A. R. Prasad and N. R. Prasad. *802.11 WLANs and IP Networking security, QoS, and mobility.* Universal Personal Communications. Artech House, Boston, 1st edition, 2005.

[4] A. Hills. Large-Scale Wireless LAN Design. *IEEE Communications Magazine*, November 2001.

[5] J. Dunat, L. Eliceguiz, and C. Bonnet. Impact of Intercall Interference in a IEEE 802.11a Network with Overlapping Cells. *PIMRC 2004*, 2:825–829, September 2004.

[6] Part 11: IEEE 802.11 WG. Wireless lan medium access control (MAC) and physical layer (PHY) specification. Standard, IEEE, 2007.

[7] A. Balachandran, P. Bahl, and G. M. Voelker. Hot-spot congestion relief in public-area wireless networks. *Mobile Computing Systems and Applications*, pages 70–81, 2002.

[8] Part 11: IEEE 802.11a WG. Wireless lan medium access control (MAC) and physical layer (PHY) specification: High-speed physical layer in the 5 GHz band. Standard, IEEE, 1999.

[9] S. Choi. PCF vs. DCF: Limitations and trends. *IEEE 802.11*, 01:054, 2001.

[10] Part 11: IEEE 802.11e WG. Medium Access Control (MAC) Quality of Service (QoS) Enhancements. Standard, IEEE, 11 November 2005.

[11] IEEE P802.11n WG/D2.00:. Enhancements for Higher Throughput. Technical report, IEEE, February 2007.

[12] N. Ahmed and S. Keshav. SMARTA: a self-managing architecture for thin access points. *Proceedings of the 2006 ACM CoNEXT conference*, 2006.

[13] M. S. Gast. *802.11 wireless networks: The definitive guide.* O'Reilly Media, Inc., 2005.

[14] B. O'Hara and A. Petrick. *The IEEE 802.11 handbook: A designer's companion*, volume 2. Standards Information Network IEEE Press, New York, NY, 2nd edition, 2005.

[15] S. Haykin and M. Moher. *Modern Wireless Communications*, volume 1. Pearson Prentice Hall, Upper Saddle River, NJ, 1st edition, 2003.

[16] E. Perahia. IEEE 802.11n development: history, process, and technology. *IEEE Communications Magazine*, pages 48–55, 2008.

[17] White Paper. A detailed examination of the environmental and protocol parameters that affect 802.11g network performance. Technical report, Proxim wireless networks, 2003.

[18] Y. Xiao. IEEE 802.11 Performance Enhancement via Concatenation and Piggyback Mechanisms. *IEEE Transaction on Wireless Communications*, 4(5):2182–2192, 25 September 2005.

[19] Y. Kim, J. Yu, and S. Choi. A Novel Hidden Station Detection Mechanism in IEEE 802.11 WLAN. *IEEE Communications Letters*, 10(8):608–610, August 2006.

[20] C. K. Ho and J. M. G. Linnartz. Analysis of the RTS/CTS Multiple Access Scheme with Capture Effect. *PIMRC 2006*, pages 1–5, September 2006.

[21] P. Wang and W. Zhuang. An Improved Busy-Tone Solution for Collision Avoidance in Wireless Ad Hoc Networks. *IEEE International Conference on Communications*, 2006.

[22] G. Bianchi. Performance analysis of the IEEE 802.11 distributed coordination function. *IEEE Journal on Selected Areas in Communications*, 1:535–547, 2000.

[23] Q. Ni, I. Aad, C. Barakat, and T. Turletti. Modeling and analysis of slow CW decrease for IEEE 802.11 WLAN. *Proc. IEEE PIMRC*, 2:1717–1721, 2003.

[24] V. Vitsas and A. C. Boucouvalas. Performance analysis of the advanced infrared (AIr) CSMA/CA MAC protocol for wireless LANs. *ACM Wireless Networks*, 9:495–507, September 2003.

[25] E. Ziouva and T. Antonakopoulos. CSMA/CA performance under high traffic conditions: throughput and delay analysis. *Computer Communications*, 25:313–321, February 2002.

[26] H. Wu, Y. Peng, K. Long, S. Cheng, and J. Ma. Performance of reliable transport protocol over IEEE 802.11 wireless LANs: analysis and enhancement. *INFOCOM 2002*, 2:599–607, 2002.

[27] Y. Xiao. A simple and effective priority scheme for IEEE 802.11. *IEEE Communication Letters*, 2003.

[28] V. M. Vishnevsky and A. I. Lyakhov. 802.11 LANs: saturation throughput in the presence of noise. *Proc. IFIP Networking 2002*, pages 1008–1019, 2002.

[29] D. Malone, K. Duffy, and D. J. Leith. Modeling the 802.11 distributed coordination function in non-saturated heterogeneous conditions. *IEEE/ACM Transactions on Networking*, pages 159–172, 2007.

[30] J. Sangiamwong and T. Sugiyama. Hidden Node Problem Aware Routing Metric for Wireless LAN mesh networks. *PIMRC 2007*, pages 1–5, September 2007.

[31] H. Khalife and N. Malouch. Interaction Between Hidden Node Collisions and Congestions in Multihop Wireless Ad-hoc Networks. *ICC 2006*, 9:3947–3952, June 2006.

[32] J. Anderson et al. *Wireless Communications Systems and NEtworks.* Information Technology: Transmission, Processing, and Storage. Kluwer Academic Publishers, Nwe York, 2004.

[33] *The Network Simulator- ns2,.* http://www.isi.edu/nsnam/ns/, 2006.

[34] D. Chiu and R. Jain. Analysis of the increase and decrease algorithms for congestion avoidance in computer networks. *Journal of Computer Networks and ISDN Systems*, 17(1):1–14, 1989.

[35] Y. Xiao and J. Rosdahl. Performance analysis and enhancement for the current and future IEEE 802.11 MAC protocols. *ACM SIGMOBILE Mobile Computing and Communications Review (MC2R), special issue on Wireless Home Networks*, 7:6–19, 2003.

[36] T. Kawata, S. Shin, and A. G. Forte. Using Dynamic PCF to Improve the Capacity for VoIP Traffic in IEEE 802.11 Networks. *IEEE Wireless Communications and Networking Conference*, 3:1589–1595, March 2005.

[37] A. Wei and S. Boumerdassi. A New PCF Scheme for Multimedia Traffic in IEEE 802.11 Wireless-LAN. *International Conference on Computer Science and Technology*, May 2003.

[38] Y. J. Kim and Y. J. Suh. Adaptive polling MAC schemes for IEEE 802.11 wireless LANs supporting voice-over-IP (VoIP) services. *Wiley Wireless Communication and Mobile Computing*, 4(8):903–916, October 2004.

[39] B. Kim, S. W. Kim, Y. Fang, and T. F. Wong. Two-Step Multipolling MAC Protocol for Wireless LANs. *IEEE Journal on Selected Areas in Communications*, 23(6):1276–1286, June 2005.

[40] A. Kaiijanavapastit and B. Landfeldt. An Analysis of a Modified Point Coordination Function in IEEE 802.11. *PIMRC 2003*, pages 1732–1736, September 2003.

[41] B. P. Crow, I. Widjaja, J. G. Kim, and S. T. Prescott. IEEE 802.11 wireless local area networks. *IEEE Communications Magazine*, 9:116–126, 1997.

[42] A. Kamerman and L. Monteban. WLAN-ii: A high-performance wireless LAN for the unlicenced band. *Bell Labs Journal*, 2:118–133, 1997.

[43] G. Holland, N. Vaidya, and B. Paramvir. A rate-adaptive MAC protocol for wireless networks. Technical Report 0, Department of Computer Science Texas A and M University, 2000.

[44] D. Qiao, S. Choi, A. Soomro, and G. S. Kang. Energy-efficient PCF operation of IEEE 802.11a WLANs via transmit power control. *Computer Networks*, 42:39–54, 2003.

[45] A. Otyakmaz, U. Fornefeld, J. Mirkovic, D. C. Schultz, and E. Weiss. Performance evaluation for IEEE 802.11G hot spot coverage using sectorised antennas. *PIMRC 2004*, 2:1460–1465, September 2004.

[46] White Paper. Atheros eXtended Range Technology Going the Distance. Technical report, Atheros, April 2004.

[47] A. Lyakhov and V. Vishnevsky. Unfair Access Problem in Wi-Fi Hot-spots. *PIMRC 2007*, pages 1–5, September 2007.

[48] I. Papanikos and M. Logothetis. A study on dynamic load balance for IEEE 802.11b wireless LAN. *Proc. COMCON*, 2001.

[49] Cisco Systems Inc. Data sheet for cisco aironet 1200 series. Technical report, 2004.

[50] T. Korakis, O. Ercetin, and S.Tripathi. Link quality based association mechanism in IEEE 802.11h compliant wireless lans. In *1st workshop on Resource Allocation in Wireless NETworks*, Boston, MA, 2005. RAWNET 2006.

[51] S. T. Sheu and C. C. Wu. Dynamic Load Balance Algorithm (DLBA) for IEEE 802.11 Wireless LAN. *Tamkang Journal of Science and Engineering*, 2(1):45–52, 1999.

[52] H. Velayos, V. Aleo, and G. Karlsson. Load balancing in overlapping wireless LAN cells. *IEEE International Conference on Communications*, 7:3833–3836, 2004.

[53] Y. Bejerano, S. Han, and L. Li. Fairness and load balancing in wireless LANs using association control. *Proc. ACM MobiCom*, 1:315–329, 2004.

[54] A. Kumar and V. Kumar. Optimal association of STAs and APs in an IEEE 802.11 WLAN. *Proc. National Communications Conference*, 1:1–5, 2005.

[55] E. Seurre, P. Savelli, and P. J. Pietri. *EDGE for Mobile Internet.* Artech House Publishers, 2003.

[56] Federal Comm. Commission (FCC). http://hraunfoss.fcc.gov/edocs_public/attachmatch/fcc-03-287a1.pdf., 2008.

[57] T. S. Rappaport. *Wireless Communications Principles and Practice.* Prentice Hall, 1996.

[58] G. Durgin, T. S. Rappaport, and H. Xu. Measurements and models for radio path loss and penetration loss in and around homes and trees at 5.85 GHz. *IEEE Tran. on Communications*, 46(11):1484–1496, 1998.

[59] European Telecommunications Standards Institude. Umts; selection procedures for the choice of radio transmission technologies of the umts. Technical report, ETSI, April 1998.